

Diagnostyka

Diagnosics and Structural Health Monitoring

Rok założenia 1990

ISSN 1641-6414



Nr 3(59)/2011

RADA PROGRAMOWA / PROGRAM COUNCIL

PRZEWODNICZĄCY / CHAIRMAN:

prof. dr hab. dr h.c. mult. **Czesław CEMPEL** *Politechnika Poznańska*

REDAKTOR NACZELNY / CHIEF EDITOR:

prof. dr hab. inż. **Ryszard MICHAŁSKI** *UWM w Olsztynie*

CZŁONKOWIE / MEMBERS:

prof. dr hab. inż. **Jan ADAMCZYK**

AGH w Krakowie

prof. **Francesco AYMERICH**

University of Cagliari – Italy

prof. **Jérôme ANTONI**

University of Technology of Compiègne – France

prof. dr. **Ioannis ANTONIADIS**

National Technical University Of Athens – Greece

dr inż. **Roman BARCZEWSKI**

Politechnika Poznańska

prof. dr hab. inż. **Walter BARTELMUS**

Politechnika Wroclawska

prof. dr hab. inż. **Wojciech BATKO**

AGH w Krakowie

prof. dr hab. inż. **Adam CHARCHALIS**

Akademia Morska w Gdyni

prof. **Li CHENG**

The Hong Kong Polytechnic University – China

prof. dr hab. inż. **Wojciech CHOLEWA**

Politechnika Śląska

prof. dr hab. inż. **Zbigniew DĄBROWSKI**

Politechnika Warszawska

Prof. **Charles FARRAR**

Los Alamos National Laboratory – USA

prof. **Wiktor FRID**

Royal Institute of Technology in Stockholm – Sweden

dr inż. **Tomasz GAŁKA**

Instytut Energetyki w Warszawie

prof. **Len GELMAN**

Cranfield University – England

prof. **Mohamed HADDAR**

National School of Engineers of Sfax – Tunisia

prof. dr hab. inż. **Jan KICIŃSKI**

IMP w Gdańsku

prof. dr hab. inż. **Daniel KUJAWSKI**

Western Michigan University – USA

prof. **Graeme MANSON**

University of Sheffield – UK

prof. dr hab. **Wojciech MOCZULSKI**

Politechnika Śląska

prof. dr hab. inż. **Stanisław RADKOWSKI**

Politechnika Warszawska

prof. **Bob RANDALL**

University of South Wales – Australia

prof. dr **Raj B. K. N. RAO**

President COMADEM International – England

prof. **Massimo RUZZENE**

Georgia Institute of Technology – USA

prof. **Vasily S. SHEVCHENKO**

BSSR Academy of Sciences Mińsk – Belarus

prof. **Menad SIDAHMED**

University of Technology Compiègne – France

Prof. **Tadeusz STEPINSKI**

Uppsala University - Sweden

prof. **Wiesław TRĄMPCZYŃSKI**

Politechnika Świętokrzyska

prof. dr hab. inż. **Tadeusz UHL**

AGH w Krakowie

prof. **Vitalijus VOLKOVAS**

Kaunas University of Technology – Lithuania

prof. **Keith WORDEN**

University of Sheffield – UK

prof. dr hab. inż. **Andrzej WILK**

Politechnika Śląska

dr **Gajraj Singh YADAVA**

Indian Institute of Technology – India

prof. dr hab. inż. **Bogdan ŻÓŁTOWSKI**

UTP w Bydgoszczy

WYDAWCA:

Polskie Towarzystwo Diagnostyki Technicznej
ul. Narbutta 84
02-524 Warszawa

REDAKTOR NACZELNY:

prof. dr hab. inż. **Ryszard MICHAŁSKI**

SEKRETARZ REDAKCJI:

dr inż. **Sławomir WIERZBICKI**

CZŁONKOWIE KOMITETU REDAKCYJNEGO:

dr inż. **Krzysztof LIGIER**

dr inż. **Paweł MIKOŁAJCZAK**

ADRES REDAKCJI:

Redakcja Diagnostyki
Katedra Budowy, Eksploatacji Pojazdów i Maszyn
UWM w Olsztynie
ul. Oczapowskiego 11, 10-736 Olsztyn, Poland
tel.: 89-523-48-11, fax: 89-523-34-63
www.diagnostyka.net.pl
e-mail: redakcja@diagnostyka.net.pl

KONTO PTD:

Bank PEKAO SA O/Warszawa
nr konta: 33 1240 5963 1111 0000 4796 8376

NAKLAD: 500 egzemplarzy

Spis treści / Contents

Adam MARTOWICZ, Mateusz ROSIEK, Tadeusz UHL – AGH University of Science and Technology in Kraków	3
SHM system based on impedance measurements <i>System monitorowania stanu konstrukcji działający w oparciu o pomiary impedancji</i>	
Grzegorz SŁUŻAŁEK, Piotr DUDA, Henryk WISTUBA – Uniwersytet Śląski	9
Tribological characteristics of AOC modified with carbon particles and nano-pipes <i>Właściwości tribologiczne anodowych warstw tlenkowych modyfikowanych cząstkami węgla i nanorurkami</i>	
Józef GACEK, Jacek JANISZEWSKI – Military University of Technology	13
Experimental investigation of mechanical properties of copper at high-strain-rate loading conditions <i>Badania doświadczalne właściwości mechanicznych miedzi w warunkach dynamicznego odkształcenia</i>	
Marek SKŁODOWSKI – Institute of Fundamental Technological Research, Joanna PINIŃSKA, Paweł ŁUKASZEWSKI, Alicja BOBROWSKA – Faculty of Geology University of Warsaw	19
Application of Rayleigh wave to diagnostics of degradation of historic construction materials <i>Zastosowanie fali Rayleigha do diagnostyki degradacji historycznych materiałów konstrukcyjnych</i>	
Mirosław WITOŚ, Mariusz ZIEJA – Air Force Institute of Technology	25
High sensitive methods for fatigue detection <i>Wysokoczułe metody detekcji zmęczenia</i>	
Sławomir WIERZBICKI – University of Warmia and Mazury in Olsztyn	35
Evaluation of on-board diagnostic systems in contemporary vehicles <i>Ocena funkcjonowania systemu diagnostyki pokładowej współczesnych pojazdów samochodowych</i>	
Andrzej GRZĄDZIELA – Akademia Marynarki Wojennej w Gdyni	41
Diagnostics gas turbine rotors in non stationary states <i>Diagnostowanie układów wirnikowych silników turbinowych w stanach nieustalonych</i>	
Eliza JARYSZ-KAMIŃSKA – West Pomeranian University of Technology in Szczecin	47
Selection of measuring equipment in assembly process - analysis of selected elements <i>Dobór wyposażenia pomiarowego w procesach montażowych - analiza wybranych elementów</i>	
Tomasz BARSZCZ – AGH University of Science and Technology in Kraków, Nader SAWALHI – Prince Mohammad Bin Fahd University	53
Wind turbines' rolling element bearings fault detection enhancement using minimum entropy deconvolution <i>Poprawa wykrywania uszkodzeń łożysk tocznych w turbinach wiatrowych przy użyciu metody minimum entropy deconvolution</i>	
Grzegorz SŁUŻAŁEK, Henryk WISTUBA, Marek KUBICA – Uniwersytet Śląski	61
3D Model Of Anodic Oxide Coating Modified With Carbon Particles <i>Model 3D warstwy tlenkowej modyfikowanej cząstkami grafitu</i>	
Maciej TABASZEWSKI, Czesław CEMPEL – Politechnika Poznańska	65
Zastosowanie ewolucji wartości szczególnych w wielosymptomowej diagnostyce maszyn <i>Application of evolution of singular values in multisymptom diagnostics of machines</i>	
Warto przeczytać / Worth to read	74

SHM SYSTEM BASED ON IMPEDANCE MEASUREMENTS

Adam MARTOWICZ, Mateusz ROSIEK, Tadeusz UHL

AGH University of Science and Technology, Department of Robotics and Mechatronics
al. A. Mickiewicza 30, 30-059 Krakow, Poland
tel. +48 126173640, fax. +48 126343505, adam.martowicz@agh.edu.pl

Summary

The paper presents the results of laboratory testing procedure applied for the SHM system developed at AGH-UST Department of Robotics and Mechatronics, Poland. Experimental setup has allowed for the measurement of electromechanical impedance with piezoelectric transducers bonded on an aluminum panel. In the paper there are presented the principle of nondestructive testing based on the impedance measurement, the description of developed SHM system and the results of performed experiments. It is shown how local changes introduced into the panel properties influence measured electromechanical impedance.

Keywords: SHM, piezoelectric transducer, electromechanical impedance.

SYSTEM MONITOROWANIA STANU KONSTRUKCJI DZIAŁAJĄCY W OPARCIU O POMIARY IMPEDANCJI

Streszczenie

Artykuł przedstawia wyniki testów laboratoryjnych przeprowadzonych dla systemu monitorowania stanu technicznego konstrukcji opracowanego w Katedrze Robotyki i Mechatroniki AGH w Krakowie. Zbudowane stanowisko pomiarowe umożliwiło pomiar impedancji elektromechanicznej za pomocą przetworników piezoelektrycznych przytwierdzonych do aluminiowej płyty. W artykule opisano metodę realizacji nieniszczących testów bazujących na pomiarach impedancji, przedstawiono opracowany system monitorowania oraz wyniki uzyskane w przeprowadzonych eksperymentach. Przedstawiono wpływ lokalnych zaburzeń własności płyty na zmierzone wartości impedancji elektromechanicznej.

Słowa kluczowe: monitorowanie stanu konstrukcji, przetwornik piezoelektryczny, impedancja elektromechaniczna.

1. INTRODUCTION

Structural Health Monitoring (SHM) systems stand for a class of applications of non destructive testing (NDT) dedicated for continuous monitoring of the condition of mechanical constructions [1-3]. SHM is usually carried out with the results of measurements performed in arrays of sensors which are permanently installed on monitored construction, first of all in critical localizations. SHM applications characterize the integration of sensors and actuators, the use of smart materials and the ability of data processing inside monitored structures. SHM has been proposed and developed in order to reduce the costs of maintenance activities by swapping from scheduled to health based inspections. Moreover procedures of data processing applied in SHM help to predict remaining life time for monitored structure.

Applications of SHM can be divided into two groups. First group is defined as global SHM and allows for damage detection with the assessment of characteristics measured for a whole structure, e.g.

acceleration of vibrations. Local SHM, in turn, is based on the measurement of structure properties performed for a certain region only, e.g. with local excitations done with piezoelectric transducers (PZT). One of the most known technique used to monitor the condition of mechanical properties is SHM based on the measurements of electromechanical impedance. It takes the advantage of electromechanical coupling utilized in PZT and therefore allows for both excitation of the vibration in the PZT vicinity and structural response measurement performed for the frequency range from 10 kHz up to 500 kHz. Measured frequency characteristics of impedance are used to track local perturbations of mechanical properties resulting from incipient and then growing damage.

Emerging application areas of SHM determines the necessity of continuous development of monitoring systems including both hardware and software contribution. The effort is put to increase the quality of monitoring process by improving the sensitivity to incipient damages as well as to prevent from false alarms. On the other hand the reduction

of energy consumption, installation and maintenance costs may be a key issue when designing a new SHM system.

The paper is organized in the following sections: section 2 describes SHM based on impedance measurements, section 3 presents developed SHM system, the experimental setup and obtained results of laboratory tests are presented in sections 4 and 5 respectively, final section 6 covers summary and concluding remarks.

2. IMPEDANCE BASED SHM

Impedance based SHM stands for the assessment of condition of mechanical structure performed with the measurements of electromechanical impedance. Frequency characteristics of impedances are determined with PZT bonded on monitored structure. Due to introduced electromechanical coupling there is possibility of both activating the mechanical vibrations in a structure and then the measurement of its response. The inference on presence of damage is carried out by the comparison between yielded frequency characteristics. There are possible two configurations applicable for the measurements of electromechanical impedance:

- Point Frequency Response configuration (shown in Fig. 1); It assumes that only one PZT is used which simultaneously acts as both actuator and sensor. The drawback of the application is however reduced emission of vibration power and sensitivity of the measurement because of the compromise on the electromechanical characteristics of PZT which is expected to be both effective actuator of vibration and sensitive sensor. The electromechanical impedance is determined with the voltage and current measured directly for PZT, i.e. as in the case when common electric impedance is determined, and can be found by the following equation:

$$\underline{Z} = \frac{V_{IN} - V_{OUT}}{\frac{V_{OUT}}{R}} \quad (1)$$

- Transfer Frequency Response configuration (shown in Fig. 2); The configuration determines the use of two PZT for separate excitation and measurement. The advantages of described approach are: the increase of measurement sensitivity and vibration energy transmitted into structure resulting from the fact that each of used PZT can be separately chosen accordingly to the task it accomplishes. The main drawback is however the increase of number of bonded PZT and more complex control electronic circuit which must contain additional systems including charge amplifiers. Electromechanical impedance is calculated as follows:

$$\underline{Z} = \frac{V_{IN}}{\frac{V_{OUT}}{R}} \quad (2)$$

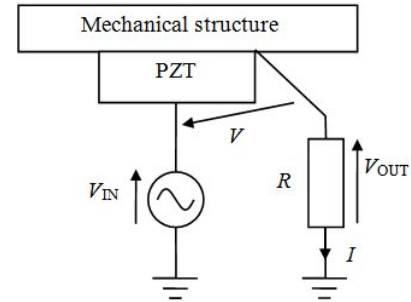


Fig. 1. Point Frequency Response configuration

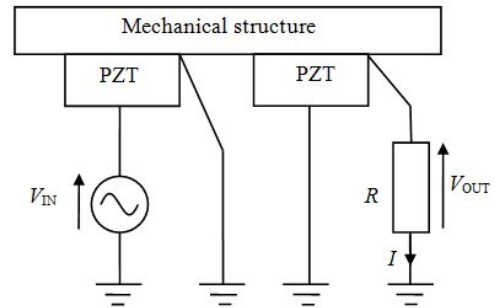


Fig. 2. Transfer Frequency Response configuration

For both configurations during measurement the structure is excited to locally vibrate for the range of high frequencies. Therefore it is feasible the inference on damage presence even though its size is small. High frequency measurement characterizes significant sensitivity to local changes in mechanical properties of monitored structure. It results from the fact that this changes mostly interfere with high frequency normal modes characterizing small wavelengths, i.e. of damage size. There must be noted however that impedance based SHM may be effectively performed only within the vicinity of mounted PZT, i.e. with distances of millimeters and centimeters rather than meters [4].

For the quantitative assessment of the differences between baseline and current impedance characteristics the following exemplary damage indexes (DI) may be applied [1,5]:

$$DI1 = \sum_{i=1}^n |(\text{Re}(Z_{0,i}) - \text{Re}(Z_i))(\text{Re}(Z_{0,i}))^{-1}| \quad (3)$$

$$DI2 = \left(\sum_{i=1}^n ((\text{Re}(Z_{0,i}) - \text{Re}(Z_i))(\text{Re}(Z_{0,i}))^{-1})^2 \right)^{1/2} \quad (4)$$

$$DI3 = \sum_{i=1}^n \left((\text{Re}(Z_{0,i}) - \text{Re}(Z_i))(\text{Re}(Z_{0,i}))^{-1} \right)^{1/2} \quad (5)$$

$$DI4 = 1 - \left((n-1)s_0s \right)^{-1} \cdot \sum_{i=1}^n \left(\left(\operatorname{Re}(Z_{0,i}) - \operatorname{Re}(Z_0) \right) \left(\operatorname{Re}(Z_i) - \operatorname{Re}(Z) \right) \right) \quad (6)$$

where: $Z_{0,i}$ and Z_i are respectively referential and current values of impedance for i -th frequency step, Z_0 , s_0 and Z , s are mean values and standard deviations of referential and current impedances, n stands for the number of considered frequencies.

Impedance based SHM characterizes application versatility dealing with both the type of monitored mechanical structure and the construction material. Most known applications of described type of SHM are [6-11]: bolted and screw joints, welded and spot-welded joints, glued joints, pipelines and railroad tracks, performed for metallic and composite materials, concrete and reinforced concrete.

3. DESCRIPTION OF DEVELOPED MONITORING SYSTEM

Impedance based SHM has been applied in developed monitoring system. The overall structure of the system is presented in Fig. 3.

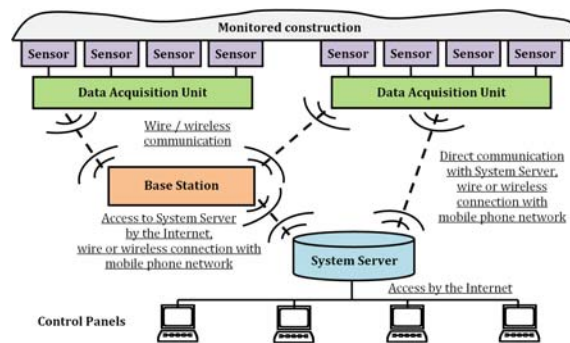


Fig. 3. Structure of developed SHM system

The system consists of Data Acquisition Units (DAU), Base Stations and System Server which enables for the connection with Control Panels. DAU and Base Stations are localized in the area of monitored structure. The main task of DAU is to check the condition of the construction by the impedance measurements performed with mounted PZT. DAU also allows for data processing and can calculate DI accordingly to implemented algorithms. Used DAU is presented in Fig. 4. It is possible to connect up to 16 sensors to each DAU considering that both Point and Transfer Frequency Response configurations are possible. For the measurement of impedance in Transfer Frequency Response configuration it is possible to choose any pair of actuator-sensor amongst all connected PZT. The data which is gathered in DAU is sent to Base Station or directly to System Server by either wire or wireless connection. All the information is stored in

System Server and can be acquired at any time with Control Panels. Control Panels are mobile or desktop computers which have access to the Internet and already installed SHM system software. The configuration settings of the whole system can be reprogrammed remotely. The measurements can be triggered automatically according to programmed time intervals or manually with Control Panels.

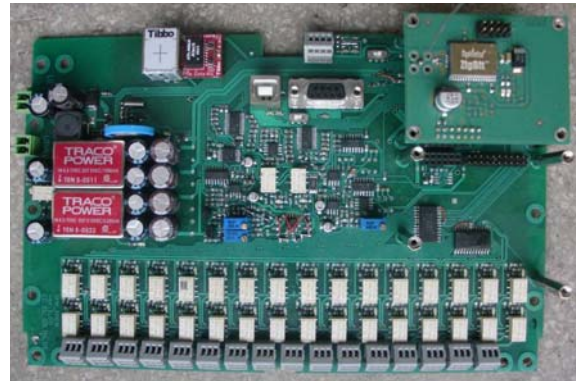


Fig. 4. Data Acquisition Unit

Applied analog electronic path enables for the impedance measurements up to 100kHz. The environmental conditions can be assessed with additional temperature and humidity sensors. The variation of mentioned above two parameters should be assessed as it significantly influences the frequency characteristics determined for electromechanical impedance [12].

In the system there are possible several communication techniques to enable for the data transfer between all system components. Between DAU and Base Station there have been implemented the following communication technologies: wireless (ZigBee and WiFi) and wire connection with the Ethernet protocol. The data connection between Base Station and System Server can also be possible either as wire, i.e. by the Internet, or by using mobile phone network infrastructure (GSM technology). For applications where there is a direct communication between DAU and System Server, i.e. applications which do not require Base Stations, applicable communication techniques are the same as previously mentioned for the connection between Base Station and System Server. DAU may work either independently or create a network.

Elaborated system may work properly for wide ranges of parameters describing the environmental conditions: at the temperature from -40°C up to $+85^{\circ}\text{C}$ (from -20°C up to $+50^{\circ}\text{C}$ for the system equipped with additional high capacity accumulators) with humidity up to 100%. Used housings allow for industrial applications and ensure the protection compliant with IP66 protection level [13]. All wire outlets from housing boxes are insulated.

DAU is supplied with accumulators optionally equipped with photovoltaic panels used to extend the operating period without any maintenance activity.

The other system components are powered by external voltage 230V/50Hz. Base Station is equipped with uninterruptible power supply.

4. EXPERIMENTAL SETUP

To verify the properties of developed monitoring system a series of experiments have been performed on a freely suspended aluminum plate panel. Examined object has been equipped with four piezoelectric patches made of PIC151 material (PI Ceramic) permanently bonded using epoxy glue. Dimensions of used PZT are 10 mm, 10 mm, and 0.3 mm.

Two locations of the damage introduced to the structure have been considered. In the first case the damage has been placed in the equal distances between the transducers. In the second case in turn it has been moved towards PZT number 4. Damage has been simulated as an additional mass and stiffness. Thick steel washers in two different sizes have been attached to the panel using wax to induce local changes in the dynamical properties of the structure. Dimensions of the tested object and damage localizations are presented in Fig. 5, the experimental setup is shown in Fig. 6.

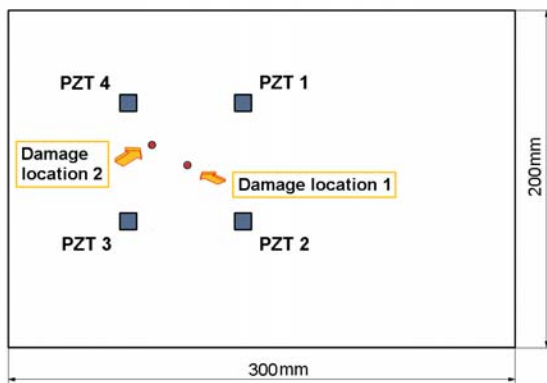


Fig. 5. Dimensions of monitored structure and damage location

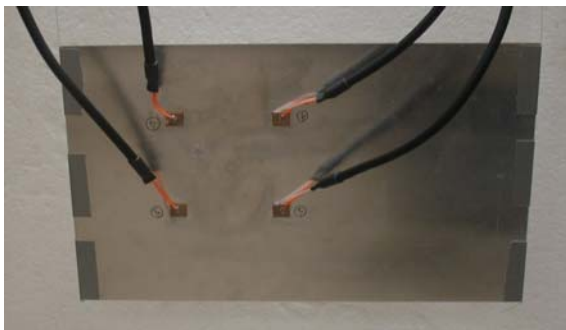


Fig. 6. Experimental setup

Two sets of baseline measurements have been performed for the undamaged structure to check the repeatability of experiments and to determine initial values of damage metrics. Next, damage has been introduced and the measurements have been repeated for the same frequency ranges.

5. RESULTS OF EXPERIMENTS

As an outcome of experiments a set of electromechanical impedance plots has been obtained. Both Point and Transfer Frequency Response functions have been evaluated for all piezoelectric transducers working as actuators and sensors. The measurements have been performed for the frequency range from 24 kHz up to 28 kHz with a frequency step equal 10 Hz. Relatively small frequency step has been chosen to ensure sufficient resolution of the measurements due to high modal density of the structure for chosen high-frequency range.

The exemplary results obtained for Point Frequency Response configuration for PZT no. 1 and no. 3 are shown in Fig. 7 and 8 respectively. It can be seen that appearance of the damage causes shifts of the resonance peaks and changes of their amplitude. Shown impedance modules have been directly calculated with raw values received from impedance analyzer data registers without any data scaling. Therefore no unit is added in plots.

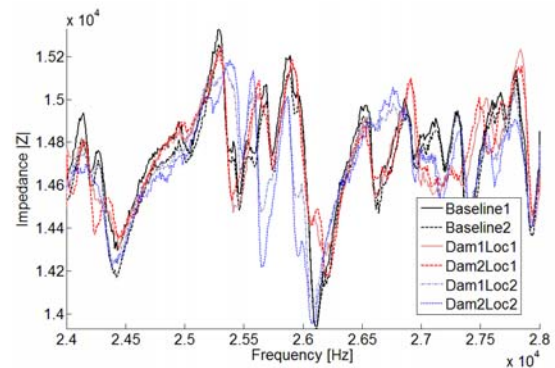


Fig. 7. Impedance plots obtained for transducer no. 1 – Point FRF

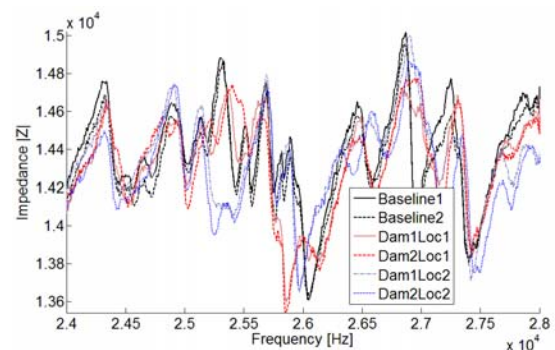


Fig. 8. Impedance plots obtained for transducer no. 3 – Point FRF

The values of damage metrics calculated on the basis of recorded impedance data for the failure placed in location 1 are presented in Fig. 9. For all PZT monotonic relationships between damage size and the value of DI have been obtained. In case of second damage location the proportions between metrics calculated for different damage sizes remained similar.

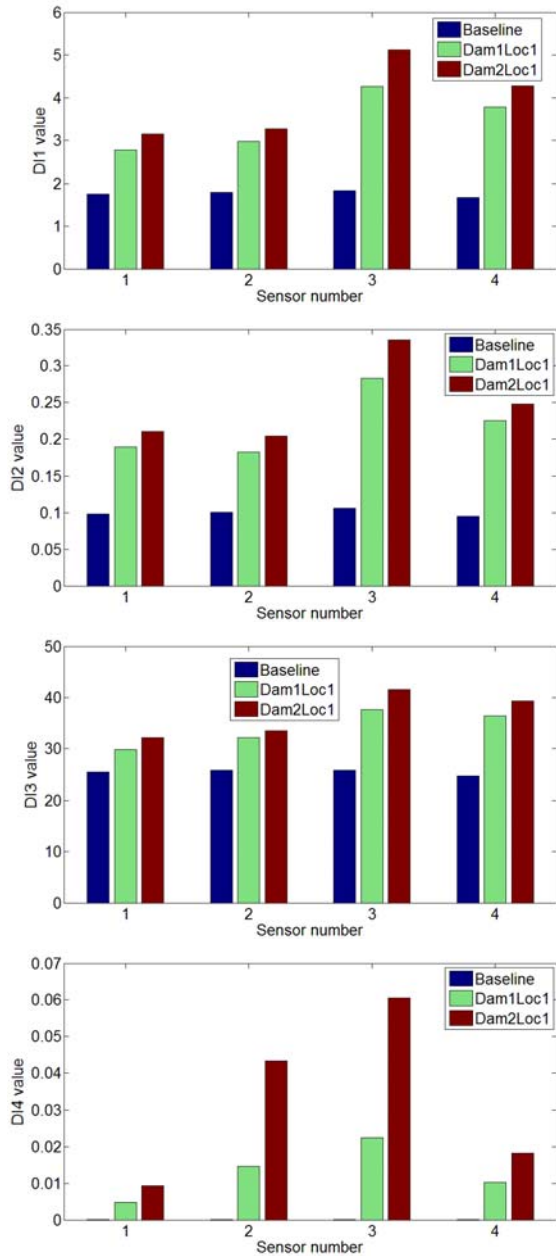


Fig. 9. Damage indexes calculated for Point FRF of the electromechanical impedance – damage location 1

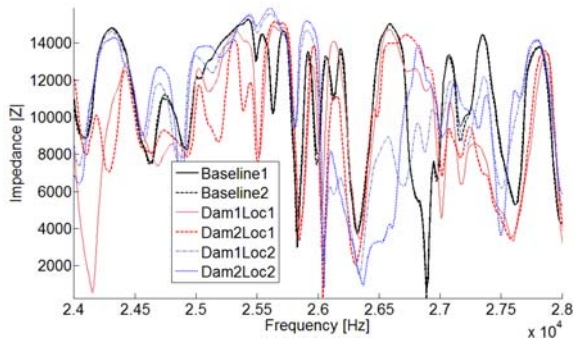


Fig. 10. Impedance plots obtained for transducer no. 2 – Transfer FRF

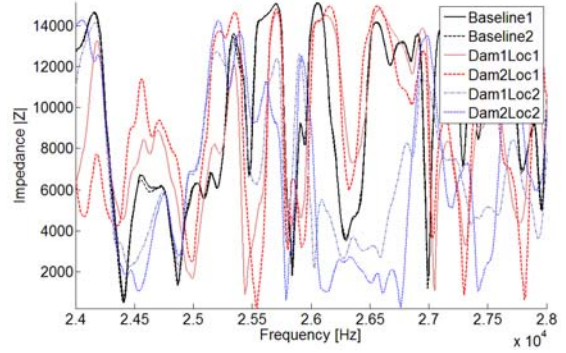


Fig. 11. Impedance plots obtained for transducer no. 4 – Transfer FRF

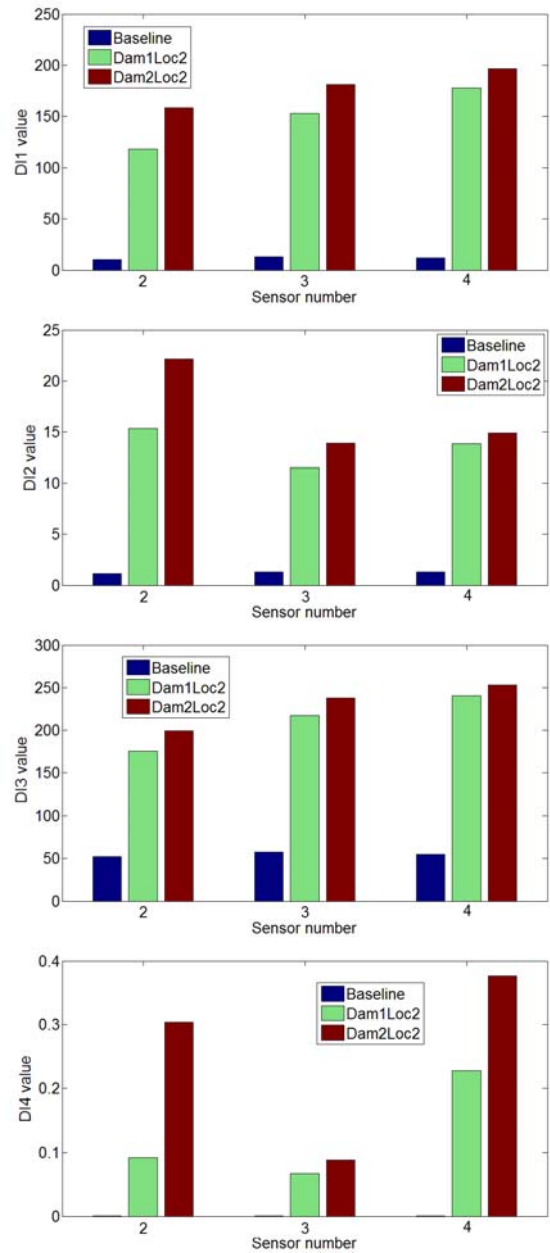


Fig. 12. Damage indexes calculated for Transfer FRF of the electromechanical impedance – damage location 2

Selected impedance plots evaluated for Transfer Frequency Response configuration are shown in Fig. 10-11 for PZT no. 1 acting as an actuator and transducers no. 2 and 4 working as sensors. Corresponding DI for exemplary damage location 2 are presented in Fig. 12. In all considered cases the greatest differences between particular failure sizes were observed for the statistical metric DI4. Moreover better repeatability for impedance baseline signals has been found for Transfer FRF case.

In accordance with obtained experimental results a conclusion can be made that tested application of impedance based SHM allows to detect a presence of the damage in mechanical structure and track its growth.

6. SUMMARY, CONCLUDING REMARKS

In this paper a conception of SHM system based on electromechanical impedance measurements is presented. The results of experiments performed using developed hardware show that described measurement method is sensitive to incipient and growing damage. Due to found its properties impedance based SHM is a promising technique for local monitoring of mechanical constructions.

ACKNOWLEDGEMENTS

The work was supported by the Polish Grant POIG.01.01.02-00-013/08-00 Monitoring of Technical State of Construction and Evaluation of its Lifespan- MONIT.

BIBLIOGRAFY

- [1] Park G., Inman D.J.: *Structural health monitoring using piezoelectric impedance measurements*. Phil. Trans. R. Soc. A, 365, pp. 373-392, 2007.
- [2] Giurgiutiu V.: *Structural Health Monitoring with Piezoelectric Wafer Active Sensors*. Elsevier Academic Press, Amsterdam; Boston, 2008.
- [3] Klepka A., Ambroziński Ł.: *Selection of piezoceramic sensor parameters for damage detection and localization system*. Diagnostyka, 4, 56, 2010.
- [4] Sun F.P., Chaudhry Z., Liang C., Rogers C.A.: *Truss structure integrity identification using PZT sensor-actuator*. Journal of Intelligent Material Systems and Structures, 6, pp. 134-139, 1995.
- [5] Rosiek M., Martowicz A., Uhl T., Stępiński T., Łukowski T.: *Electromechanical impedance method for damage detection on mechanical structures*. Proceedings of 11th IMEKO TC 10 workshop on Smart diagnostics of structures, Krakow, October 18-20, 2010.
- [6] Ayres J.W., Lalande F., Chaudhry Z., Rogers C.A.: *Qualitative impedance-based health monitoring of civil infrastructures*. Smart Materials and Structures, 7, pp. 599-605, 1998.

- [7] Chiu W.K., Koh Y.L., Galea S.C., Rajic N.: *Smart structure application in bonded repairs*. Composite Structures, 50, pp. 433-444, 2000.
- [8] Fasel T.R., Sohn H., Park G., Farrar C.R.: *Active Sensing using Impedance-based ARX Models and Extreme Value Statistics to Damage Detection*. Earthquake Engineering & Structural Dynamics Journal, 34, 7, pp. 763-785, 2005.
- [9] Park S., Inman D. J., Yun Ch-B.: *An outlier analysis of MFC-based impedance sensing data for wireless structural health monitoring of railroad tracks*. Engineering Structures, 30, pp. 2792-2799, 2008.
- [10] Tseng K.K., Wang L.: *Smart piezoelectric transducers for in situ health monitoring of concrete*, Smart Materials and Structures, 13, pp. 1017-1024, 2004.
- [11] Wait J.R., Park G., Farrar Ch.R.: *Integrated Structural Health Assessment using Piezoelectric Active Sensors*, Shock and Vibration, 12, 6, pp. 389-405, 2005.
- [12] Park G., Kabeya K., Cudney H.H., Inman D.J.: *Impedance-based Structural Health Monitoring for temperature varying applications*. JSME International Journal, Series A, 42, 2, 1999.
- [13] The international standard IEC 60529 Degrees of protection provided by enclosures (IP Code)



Adam MARTOWICZ Ph.D. is scientific assistant at the Department of Robotics and Mechatronics, AGH-UST. His scientific interests focus on SHM, uncertainty and sensitivity analysis and structural dynamics.



Mateusz ROSIEK M.Sc. is a Ph.D. student at the Faculty of Mechanical Engineering, AGH-UST. His scientific interests focus on utilization of piezoelectric transducers for SHM and structural dynamics applications.



Tadeusz UHL Prof. is a head of the Department of Robotics and Mechatronics, AGH-UST. His main research areas cover SHM, modal analysis, active vibration reduction, control systems and mechatronics.

TRIBOLOGICAL CHARACTERISTICS OF AOC MODIFIED WITH CARBON PARTICLES AND NANO-PIPES

Grzegorz SŁUŻALEK, Piotr DUDA, Henryk WISTUBA

Wydział Informatyki i Nauki o Materiałach, Wydział Nauk o Ziemi
41-200 Sosnowiec; ul. Śnieżna 2, sluzalek@us.edu.pl, piotr.duda@us.edu.pl,
henryk.wistuba@us.edu.pl

Summary

The paper represents the results of investigations conducted on the tribological tester T-01 on pin-on-disk pair for the conditions of the friction of technically dry. Analysis stereological counter-specimen was subjected from AOC and AOC modified with carbon particles and nano-pipes, that is composites coats. The values of the coefficient of the friction and the parameters of the roughness are presented, to four groups of samples.

Keywords: anodic hards layer, nanomaterials, friction, wear, tribological properties.

WŁAŚCIWOŚCI TRIBOLOGICZNE ANODOWYCH WARSTW TLENKOWYCH MODYFIKOWANYCH CZĄSTKAMI WĘGLA I NANORURKAMI

Streszczenie

Artykuł przedstawia wyniki badań przeprowadzone na stanowisku tribologicznym T-01 w skojarzeniu trzpień-tarcza w warunkach tarcia technicznie suchego. Poddano analizie stereologicznej przeciwpółki wykonane z czystego APT i APT modyfikowanej cząstkami węgla i nanorurkami czyli powłokami kompozytowymi. Zestawiono wartości współczynnika tarcia oraz parametry chropowatości, dla czterech grup próbek.

Słowa kluczowe: anodowa warstwa tlenkowa, nanomateriały, tarcie, zużycie, właściwości tribologiczne.

1. OXIDE CERAMIC LAYER

Modifications of an oxide coating maintain all its advantages and improve operating properties of a composite material formed in such a way (e.g. a decrease in the friction coefficient or intensity of wear of co-partners). Anodic oxide coatings (AOC), which were obtained on the EN AW-5251 aluminum alloy in the ternary electrolyte, were examined in the work. The following types of the oxide coating modifications were used: in a form of an addition of graphite powder into the electrolyte during production; by vacuum sublimation by a graphite electrode and modifying the base coating with nanoparticles. For comparison purposes a non-modified oxide coating was used as a reference.

The ternary electrolyte composition consisted of a water solution of the sulfuric acid, oxalic acid and phthalic acid (SFS), being an organic addition to protect the aluminum oxide formed against an aggressive influence of the electrolyte (dissolution of the oxide coating) [1]. This electrolyte composition was used to anodize four groups of specimens, additionally while hard anodizing counter-specimens modified by a simplex method there was a graphite powder with a grain diameter of <1 micrometer in the amount of 20 g/l (PE) in the

electrolyte. Other two groups of specimens were modified by duplex methods.

The anodic oxide surface was made by a direct current method at the same current and temperature conditions. Anodizing time for all counter-specimens was the same and was 60 min (Fig. 1). The current intensity was 3 A/dm², the electrolyte temperature was 20 °C (PB). Then, the oxide coatings formed in such a way were modified [2,3]:

1. Method 1 – the counter-specimen marked as PG –the carbon was injected into pores and on the surface of the pure oxide by vacuum sublimation,

2. Method 2 – the counter-specimen marked as PN –carbon nano-pipes were formed in the pores of the aluminum oxide.

The oxide coatings formed as a result of anodic oxidation are often subjected to removing of electrolyte residues, humidity and other impurities in the vacuum sprayer.

A Jeol IEE-4B vacuum sprayer was used for this purpose (Fig. 1). The carbon nano-pipes obtained by the α -CNT method were added to the oxide coating.

A mandrel made of the PEEK/BG high grade polymer composite was a tribological partner [4]. The material used is a thermo-material medium-crystalline linear aromatic polymer. The PEEK/BG composite PEEK- based contains dispersions of

additions in a form of PTFE, graphite and short carbon fibers.



Fig. 1. Place for anodizing and Jeol IEE-4B vacuum evaporator

2. EXPERIMENTAL STUDIES

The tribological tests were performed for all types of specimens with coupling with the PEEK/BG material in the conditions of the technically dry friction on the T-01 M tribological test apparatus (Fig. 2 and 3) [5,6]. Other parameters of tribological tests:

- Friction path - 1500 m
- Load - 10 N
- Linear velocity - 0,2 m/s
- Friction diameter - Ø 25 mm
- Pin diameter - Ø 5mm
- Ambient temp - 21±1 °C
- Air humidity - 40%±5%

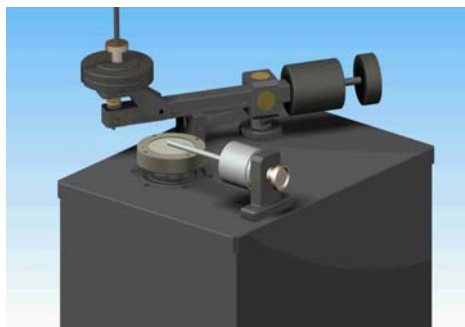


Fig. 2. 3D visualization model of tester T-01M



Fig. 3. Tribological pair pin on disk

Measurement results of the friction coefficient, linear displacements and the stabilized temperature of co-operation are showed in Fig. 4,5,6.

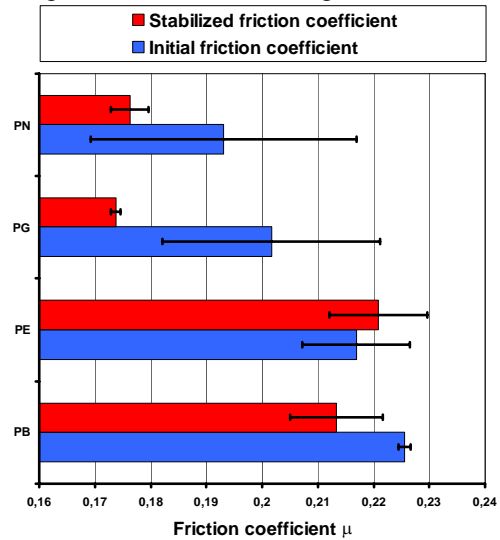


Fig. 4. Presentation of the initial and stabilized friction coefficient

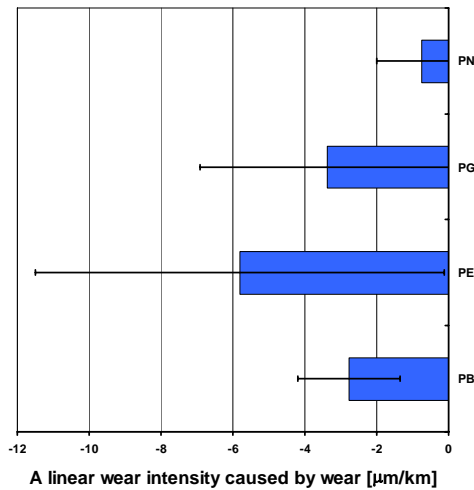


Fig. 5. A linear wear intensity caused by wear

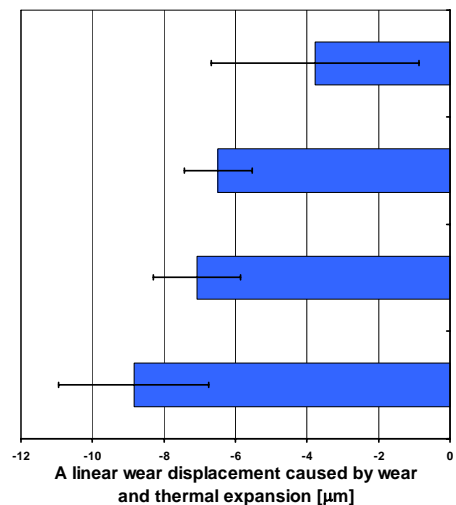


Fig. 6. A linear wear displacement caused by wear and thermal expansion

Measurement results of the friction coefficient, linear displacements and the stabilized temperature of co-operation are presented in table 1, 2.

Table 1. Initial and stabilized friction coefficient

	Initial friction coefficient	Stabilized friction coefficient
PN	0,193 ± 0,024	0,176 ± 0,003
PG	0,202 ± 0,020	0,174 ± 0,001
PE	0,217 ± 0,010	0,221 ± 0,009
PB	0,226 ± 0,001	0,213 ± 0,008

Table 2. Intensity of linear wear

	PN	PG	PE	PB
Intensity of linear wear	-0,748 ± 1,242	-3,362 ± 3,542	-5,804 ± 5,679	-2,775 ± 1,419

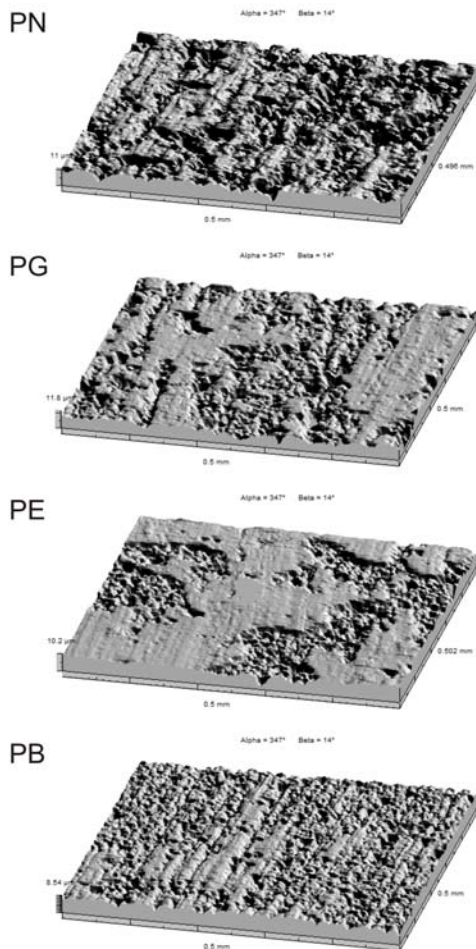


Fig. 7. The geometrical surface structure obtained as the result of profilometer measurements by a contact method

The geometrical surface structure obtained as the result of profilometer measurements by a contact method (TALYSURF 3D Taylor Hobson) is presented in figures 7. Results Abbott curve were introduced together with the graphic interpretation of functional parameters showed on figure 8. Amplitude parameters (S_a , S_q , S_p , S_t), spatial parameter (S_d) and functional parameter (S_{ci}) are presented in table 3.

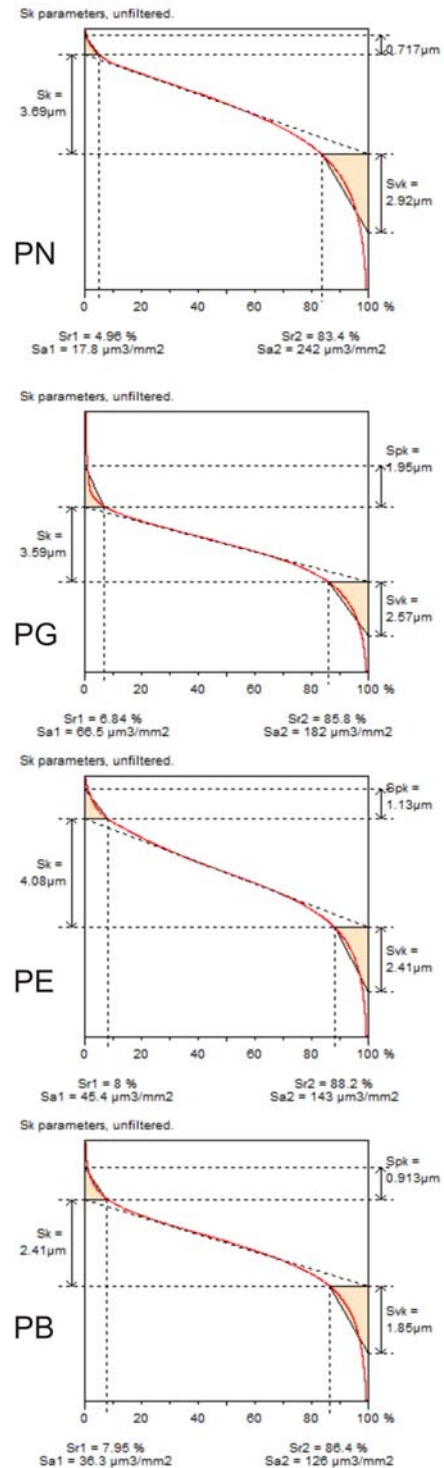


Fig. 8. Graphical study of Sk parameters

Table 3. Parameters calculated on the surface PN, PG, PE, PB

	PN	PG	PE	PB
Sa [μm]	1,32	1,23	1,21	0,84
Sq [μm]	1,73	1,78	1,58	1,14
Sp [μm]	3,22	18,6	3,76	7,66
St [μm]	11,5	26,1	11,6	13,4
Ssk	-1,27	0,82	-0,86	-0,76
Sku	5,27	16,1	4,91	7,05
Sds [pk/mm^2]	48,92	5550	58,82	7727
Sci	1,03	1,01	1,29	1,15

Analysing the parameters of the roughness of the surface from the amplitude group significant differences of the influence on profiles tribological were not affirmed. Decrease of the value coefficient friction is the most probably connected with the morphology of the surface layer.

3. SUMMARY

The AOC base modifications regardless of a way of their realization have an advantageous influence on the tribological characteristic in coupling with the PEEK/BG material. The lowest values of the initial and stabilized friction coefficient were obtained for couplings where the oxide coatings were modified by the vacuum sublimation of the PG carbon and the PN nanomaterial. It is also confirmed by the 3D surface topography of the variants analyzed.

During the tests a continuous slip film from the PEEK/BG material was formed and after setting it up led to the PEEK/BG material-PEEK-BG cooperation. In spite of such a system the substrate on which such a layer was formed, has a significant influence on the temperatures recorded near the friction zone and on a change of the linear dimensions of the specimen. Further stereometric, tribological examinations and numerical experiments will be performed for the coating modified with nanomaterials and obtained by sublimation.

4. REFERENCES

- [1] W. Skoneczny: „Kształtowanie wybranych właściwości warstw powierzchniowych na bazie tlenku aluminium”. Wydawnictwo Akademii Techniczno-Humanistycznej, Bielsko-Biała 2009 r.
- [2] G. Służałek, H. Wistuba: „Sposób wytwarzania powłok kompozytowych na aluminium i jego stopach”. Zgłoszenie patentowe P 390876 2010 r.
- [3] H. Wistuba, G. Służałek: „Sposób wytwarzania powłok kompozytowych na aluminium i jego stopach”. Zgłoszenie patentowe P 390877 2010 r.

- [4] Z. P. Lu, K. Friedrich: „On slipping friction and wear of PEEK and its composites”. *Wear*, 181-183 (1995), 624-631.
- [5] G. Służałek, M. Kubica, H. Bąkowski: „Rozkład naprężeń i odkształceń wybranych węzłów tarcia w badaniu warstwy typu duplex”. *Mechanik* 2010r. nr 1.
- [6] M. Kubica, G. Służałek, M. Wrazidło: „Trójwymiarowy, animowany model Testera T-11 wykorzystywanego do badań tribologicznych węzłów tarcia trzpień-tarcza i kulka-tarcza”. *Mechanik* 2011r. nr 2.



Grzegorz SŁUŻAŁEK Ph.D. is an assistant professor in Department of Materials Science of University of Silesia. His scientific interests focus on CAx, FEA, nanomaterials, tribology.



Piotr DUDA Ph. D. (Eng.) is an assistant professor in Department of Materials Science of University of Silesia. His scientific interests focus on CAx, FEA, biomaterials, tribology.



Henryk WISTUBA Ph.D. is senior research in Interdepartmental Laboratory of Structural Research University of Silesia His scientific interests focus on nanomaterials, tribology.

EXPERIMENTAL INVESTIGATION OF MECHANICAL PROPERTIES OF COPPER AT HIGH-STRAIN-RATE LOADING CONDITIONS

Józef GACEK, Jacek JANISZEWSKI

Department of Mechatronics, Military University of Technology
ul. Sylwestra Kaliskiego 2, 00-908 Warszawa 49
jacek.janiszewski@wat.edu.pl

Summary

Experimental studies on mechanical properties of Cu-ETP copper under strain rates above $2.6 \times 10^3 \text{ s}^{-1}$ are presented in this work. The electromagnetic expanding ring experiment and impact Taylor test were used as the tools for examining the dynamic behaviour of selected copper. Experimental study by using above-mentioned techniques was performed to assess a methodological correctness of experiments in which laboratory apparatuses developed at Military University of Technology were used.

Keywords: expanding ring test, Taylor impact test, high-strain-rate deformation.

BADANIA DOŚWIADCZALNE WŁAŚCIWOŚCI MECHANICZNYCH MIEDZI W WARUNKACH DYNAMICZNEGO ODKSZTAŁCENIA

Streszczenie

W artykule przedstawiono badania doświadczalne właściwości mechanicznych miedzi Cu-ETP w warunkach dynamicznego obciążenia. Badania dynamiczne wykonano za pomocą elektromagnetycznego testu pierścieniowego i zderzeniowego testu Taylora. Celem badań była ocena poprawności metodycznej przeprowadzonych badań, podczas których zastosowano aparaturę laboratoryjną, opracowaną w Wojskowej Akademii Technicznej.

Słowa kluczowe: test pierścieniowy, uderzeniowy test Taylora, deformacja dynamiczna.

1. INTRODUCTION

Many engineering applications, such as metal forming, armour penetration, shaped charge jet generation, crash absorbers deformation in cars etc., may benefit from an understanding of the influence of deformation velocity on mechanical materials properties. For over the past six decades many investigators have made an effort to reveal factors influencing on strength and ductility under dynamic plastic deformation [1]. For this purpose, many different experimental techniques have been developed, among which split Hopkinson pressure bar (SHPB) method is the most common [2, 3]. However, the method of Hopkinson has many limitations, so many other experimental methods were used to examine the behaviour of materials under dynamic deformation. For these methods among others may include impact Taylor test [4] and the electromagnetic expanding ring test [5].

The impact Taylor test was developed for determining, in simple way, the yield stress of materials under dynamic compression. The method involves impacting a rigid circular cylinder (material sample) against a rigid target and making post-impact measurement of the deformed shape of specimen (Fig. 1). On the basis of measuring the

impact velocity and the degree of deformation of cylindrical samples can be calculated the value of dynamic yield stress using the equation, which was derived by Taylor [4] (Fig. 1).

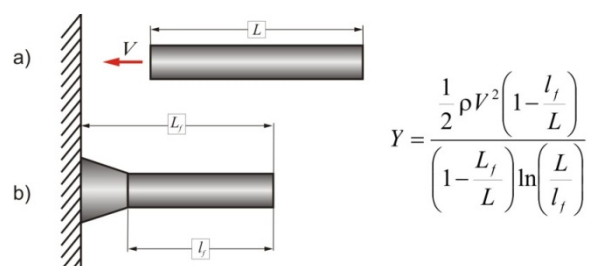


Fig. 1. Schematic illustration impact Taylor experiment and equation for estimating the dynamic yield point Y , where: ρ - density of sample material cylinder, V - velocity of impact; L - length of the sample before the impact; L_f - total length of the sample after the collision, l_f - the length of undeformed part of the sample

An electromagnetic expanding ring technique is more complex and demanding application of advanced test equipment and measurement systems,

such as a velocity interferometer system for any reflector (VISAR) or a high-speed camera. Generally, this method is based on recording of the motion of the thin-walled ring made from the tested material, which was launching due to electromagnetic forces induced during discharging of capacitors through solenoid coil (Fig. 2).

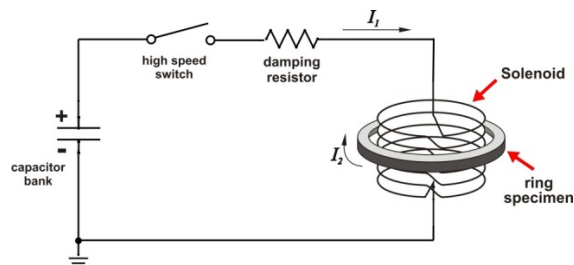


Fig. 2. Diagram of the arrangement for electromagnetic ring expansion

By measuring the radial displacement $r(t)$ or velocity history $v(t)$ of the ring specimen for inertial stage of expansion, the circumferential stress σ_θ and true strain ϵ_θ for ring material under high-strain rate tension conditions can be determined at the imposed strain rate using relationships presented below:

$$\sigma_\theta = -\rho r \frac{\partial^2 r}{\partial t^2}, \quad \epsilon_\theta = \int_{r_0}^r \frac{dr}{r} = \frac{\ln r}{r_0} \quad (1)$$

where: ρ - density of sample material cylinder, r_0 and r - initial and current radius of ring specimen, respectively.

In the paper, the experimental study for Cu-ETP copper was carried out with the use of the above mentioned techniques to assess a methodological correctness of experiments, in which laboratory apparatuses developed at Military University of Technology were used.

2. EXPERIMENTAL PROCEDURE

The studies on mechanical properties of Cu-ETP copper under strain rates of the order of $5 \times 10^3 \text{ s}^{-1}$ were performed by using apparatuses presented in Fig. 3. The laboratory arrangement for impact Taylor test (Fig. 3a) consists of pyrotechnic launching system, the maraging steel target plate with polished surfaces, and recording system, which is composed of high-speed camera and illumination system. On the other hand, an experimental setup for expanding ring test presented in Fig. 3b, principally, consists of three main components; *pulse power system* containing 240 μF capacitors bank and two impulse thyristors, *loading assembly*, and finally *charging system* (invisible in Fig 3b). The solenoid with the ring sample is inserted into a loading assembly. It consists of two 20 mm polycarbonate

plates with cavities, which support the solenoid with the copper ring and a wax ring at the outside of the cavity. The wax ring plays a role of a capture medium for fragments generated during fracture of the ring sample.

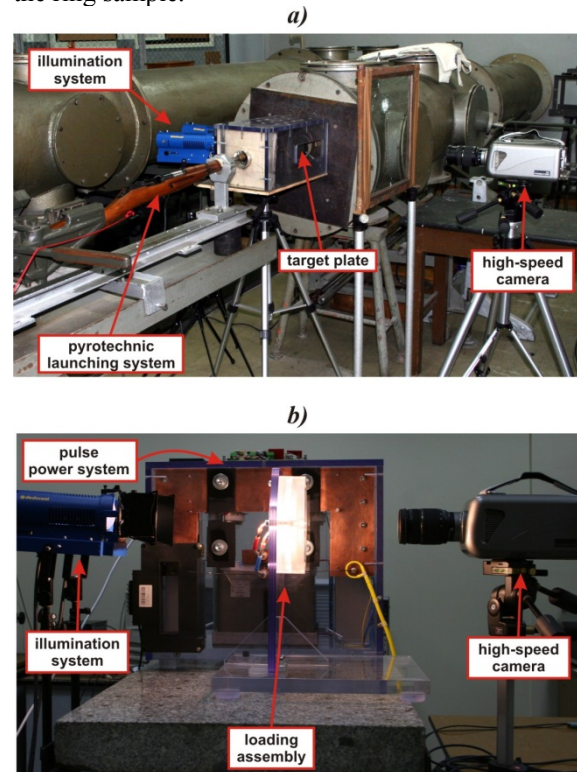


Fig. 3. View of the arrangement for impact Taylor test and electromagnetic ring experiment

As is the case of experimental setup for Impact Taylor test, displacement of the ring during expansion process was recorded with the high-speed camera (Fig. 3), whereas the ring velocity history was calculated from the high-speed images using the TEMA Automotive software. To obtain good accuracy of the ring expansion velocity with the use of available equipment, the observation field of high-speed camera was limited to a small area, in which there was visible only a moving ring segment and two scaled points (Fig. 4).

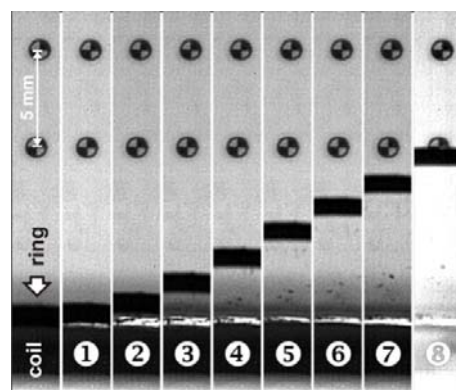


Fig. 4. The sequence of images showing the copper ring segment motion

Cylinder and ring samples were machined from the cold-rolled Cu-ETP copper bar with 40-mm diameter. The engineer properties of tested copper are presented in Table 1. The dimensions of cylindrical samples were 8 mm x 40 mm, whereas the rings had the mean diameter of 32 mm, and the cross-sectional area of 1.5 mm x 1.5 mm.

Table 1. Mechanical properties of the cold-rolled Cu-ETP copper

Ultimate tensile strength R_m	[MPa]	263
Yield strength $R_{0,2}$	[MPa]	239
Elongation A_5	[-]	0.30
Hardness	HV1	90
Average grain size	[μm]	55

3. RESULTS AND DISCUSSION

In Figure 5, the selected images recorded by using digital high-speed camera and photographs of samples after tests are arranged to illustrate the process of plastic deformation of the sample material in both Taylor test and ring experiment conditions.

As it is seen in Fig. 5, the Taylor specimen made of Cu-ETP copper was ‘mushroomed’ by the impact,

and its geometric profile is typical for metals with good ductility and high strain-hardening exponent. Good ductility of the studied Cu-ETP copper is also confirmed by the expanding ring test. The copper ring seen in Fig. 5 expands radially for a relatively long time and deforms plastically without disturbing the integrity of material structure (fracture strain $\approx 39\%$), and next the ring breaks into small fragments.

Quantitative results of the dynamic tests were collected in Table 2 and 3, where, moreover, there are included calculation data on the basis of which the dynamic yield stress \bar{Y} and circumferential stress σ_{θ} were determined. It should be noted that, in the case of Taylor's test, the dynamic yield stress was determined in accordance with the classical methodology proposed in [4] (exact analysis), while the plastic flow stress at the ring experiment were calculated using the equation (1) and for strain equal to 0.25 (it is strain for which a ring sample deforms only due to inertia forces).

For the Taylor impact test, the average value of dynamic yield stress for the tested copper is 342 MPa, while the plastic flow stress at 0.25 strain extracted from ring test is equal to 341 MPa. Generally, these results show that the dynamic plastic flow stress of copper increased significantly compared to the corresponding static stress yield.

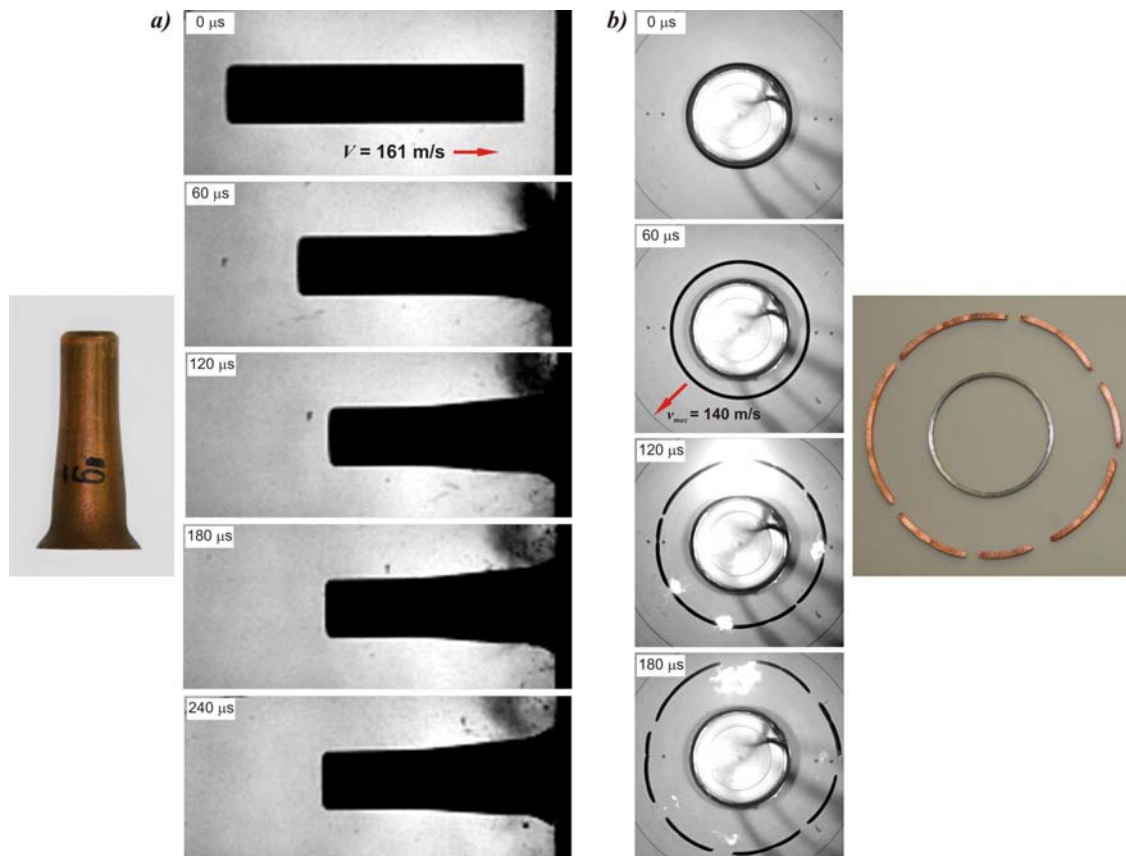


Fig. 5. The sequence of images showing the deformation of copper cylinder (a) and ring specimen (b) under high-strain-rate loading conditions

Table 2. Experimental and calculated data extracted from impact Taylor for the cold-rolled Cu-ETP copper

Test no.	Original length [mm]	Velocity V [m/s]	Overall length of the sample after test L_f [mm]	Undeformed sample length l_f [mm]	Strain rate [s ⁻¹]	Dynamic yield stress Y [MPa]
07	40.017	162.7	30.969	12.15	2,92 x 10 ³	348
08	40.023	150.7	31.964	12.15	2,70 x 10 ³	337
09	39.915	161.2	30.931	10.95	2,78 x 10 ³	332
10	40.014	185.5	29.121	9.07	3,00 x 10 ³	338
11	40.050	141.8	32.692	13.46	2,67 x 10 ³	342
12	39.869	132.5	33.399	14.76	2,64 x 10 ³	352
Average value						342

Table 3. Experimental and calculated data extracted from electromagnetic ring test for the cold-rolled Cu-ETP copper

Test no.	Max. expansion velocity [m/s]	Deceleration $\frac{\partial^2 r}{\partial t^2}$ [m/s ²]	Strain rate for $\epsilon_\theta = 0,25$ [s ⁻¹]	Plastic flow stress σ_θ for $\epsilon_\theta = 0,25$ [MPa]
07	139.4	1744803	5,74 x 10 ³	323
08	142.9	1890156	5,93 x 10 ³	350
09	140.4	1892992	5,88 x 10 ³	350
10	141.0	1833737	5,83 x 10 ³	339
Average value				341

This behaviour of copper under dynamic loading is typical and confirmed in numerous scientific publications [e.g. 3, 4]. Moreover, the level of plastic flow stress received for Cu-ETP is similar to flow stress obtained for resembling types of copper. For example, the obtained stress value extracted from Taylor impact test for Cu-ETP copper is very consistent with the analogous value for hardened OFE copper ($Y = 335$ MPa) presented in [6] (test conditions; the specimen is initially 7.6 mm in diameter and 57.1 mm long, the impact velocity was 189 m/s). Similarly, the good agreement between the obtained results and the data found in the literature was achieved for electromagnetic ring test. For example, in the work [7], flow stress for OFE copper determined by using electromagnetic ring experiment was approximately 345 MPa at 0.25 strain (Fig. 1, page 2339 in [7]), whereas in the present work, flow stress for Cu-ETP is 341 MPa at the analogous deformation level.

Based on the above-mentioned comparative analysis, generally, it can be concluded that the

developed apparatus can deliver reliable results of experimental materials studied under high strain rate loading conditions. Results presented here also prove the methodological correctness of applied measurement techniques and calculation procedures.

4. SUMMARY

The impact Taylor test and electromagnetic expanding ring experiment were presented in this paper. The main goal of our studies presented in this paper was assessment of methodological correctness of above-mentioned experiments in which the laboratory apparatuses developed at Military University of Technology were used. Tests were performed on Cu-ETP, for which dynamic properties are available in the literature. It was found very good agreement of the results of our experiments with similar results presented in the literature. Based on this observation, it can generally be stated that the developed apparatus and applied measuring

procedures ensure methodological correctness and the reliability of the experimental data obtained during high strain rate testing.

REFERENCES

- [1] Zukas J.Z., Nicholas T., Swift H.F.: Greszczuk L.B., Curran D.R., *Impact Dynamics*, A Wiley-Interscience Publication, John Wiley&Sons, New York-Chichester-Brisbane-Toronto-Singapore (1982).
- [2] Meyers M.A.: *Dynamic behaviour of materials*. John Wiley and Sons, INC, New York-Chichester-Brisbane-Toronto-Singapore, (1994).
- [3] Gray III G.T.: *ASM Handbook: Mechanical Testing and Evaluation, vol. 8*. In: Kuhn H, Medlin D, editors.. Materials Park, OH: ASM International; (2000), p. 939÷1270.
- [4] Taylor G.: *The use of flat-ended projectiles for determining dynamic yield stress I. Theoretical considerations*. Proc.Roy. Soc. London Series A. 1948, 194, 289.
- [5] Gourdin W.H.: *Analysis and assessment of electromagnetic ring expansion as a high-strain-rate test*, J. Appl. Phys., 65, 2, (1989), 411÷422.
- [6] House J.W.: Aref B., Foster Jr J.C., Gillis P.P., *Film data reduction from Taylor impact test*, Journal of Strain Analysis VOL 34 NO 5, 1999, p. 337-345.
- [7] Gourdin W.H.: Lassila D.H., *Flow Stress of OFE Copper at Strain Rates from 10^{-3} to 10^4 s⁻¹: Grain-size Effects and Comparison to the Mechanical Thresholds Stress Model*, Acta metal mater. Vol. 39, No. 10, (1991).



Prof. D.Sc. Eng Józef GACEK – director of the Institute of Armament Technology at the Military University of Technology. He is outstanding specialist in the field of ballistics and weapon construction. Author of many papers and books on exterior ballistics and armament technology.



Ph.D. Jacek JANISZEWSKI, is a scientific - educational employee at Institute of Armament Technology at the Military University of Technology. Main areas of researches are armament technology (especially shaped charged technology) and high strain rate deformation of materials.

APPLICATION OF RAYLEIGH WAVE TO DIAGNOSTICS OF DEGRADATION OF HISTORIC CONSTRUCTION MATERIALS

Marek SKŁODOWSKI*, Joanna. PINIŃSKA**, Paweł. ŁUKASZEWSKI**, Alicja BOBROWSKA**

*Institute of Fundamental Technological Research, Polish Academy of Sciences
ul Pawińskiego 5 B, 02-106 Warsaw, POLAND, msklod@ippt.gov.pl

**Faculty of Geology University of Warsaw
Al. Żwirki i Wigury 93, 02-089 Warsaw, POLAND

Summary

Paper presents results of degradation modelling of historical construction materials based on Rayleigh surface wave velocity (CR) measurement for two marbles widely used as the structural and decorative material in historical constructions. Environmental loading is modelled by freezing and thawing cycles performed in laboratory. Rayleigh wave measurement method does not need any coupling medium between the stone and ultrasonic probe and is 100% non-destructive. It is shown that exponential law can be used to model the proces of degradation of elastic properties of the tested materials.

Keywords: degradtion modelling, material integrity, Rayleigh wave, edge probes, historical materials.

ZASTOSOWANIE FALI RAYLEGHA DO DIAGNOSTYKI DEGRADACJI HISTORYCZNYCH MATERIAŁÓW KONSTRUKCYJNYCH

Streszczenie

Praca przedstawia wyniki modelowania degradacji historycznych materiałów konstrukcyjnych na podstawie pomiarów prędkości fali Rayleigha dla dwóch marmurów szeroko stosowanych w zabytkowych budowlach jako materiał konstrukcyjny i dekoracyjny. Obciążenia środowiskowe modelowane są cyklami zamrażania i rozmrażania przeprowadzonymi w laboratorium. Metoda pomiaru fali Rayleigha nie wymaga żadnego ośrodka sprzęgającego pomiędzy materiałem a sondą ultradźwiękową i jest w 100% nieniszcząca. Wykazano, że proces degradacji właściwości sprężystych badanych materiałów dobrze modeluje prawo wykładnicze.

Słowa kluczowe: modelowanie degradacji, integralność materiału, fala Rayleigha, sondy ostrzowe, zabytkowe materiały.

1. INTRODUCTION

Diagnostics of historical construction materials includes, among the others, assessment of their nowadays physical na mechanical properties. This is done mainly in a non-destructive way because of the great cultural value of historical constructions. However evaluation of the degradation processes and their dynamics cannot be done by measuring actual properties only.

It is necessary to compare the actual data with the properties of original non-degraded materials and the same properties at several levels of degradation to descibe a susceptibility of the material to environmental loads like day and night thermal cycles, freezing and thawing in winter times etc.

In the case of stones used as a construction material it is possible to obtain fresh-from-quarry samples of the material to perform laboratory investigation of the degradation evolution. Reference measurements are done for fresh, intact

matrial and then the same measurements are done after prescribed number of cycles of experimentally medeled environmental loads.

In the present work two stones - Marble Cervairole (MC) from Buca quarry in Seravezza (Italy) and Marble Gioia (MG) from Gioia quarry near Carrara (Italy) -were tested. Independent variable of an artificial ageing process was the number of freezing and thawing cycles. The number of cycles was correlated with the changes of ultrasonic Rayleigh surface wave [1] velocity.

Degaradation analysis is based on the non-destructive evaluation of the rate of the loss of material integrity under assumption of proportionality between surface wave velocity and dynamic shear modulus of elasticity [2].

Collected data were used to evaluate the degradation process of the marbles using the mathematical model based on phenomenological description of the loss of meterial integrity [3].

2. DIAGNOSTIC METHOD

Rayleigh wave [1] was primarily used in stone testing for measurement of elastic constants of stones [4]. This comes from the fact that elastic constants can be expressed by means of longitudinal, (compressive) and transversal (shear) wave velocities [2].

Let us denote the measured velocities of shear and longitudinal waves as V_S and V_L respectively. Then the material constants called “dynamic material constants” can be expressed by the equations:

$$v_d = \frac{0.5 - (V_s/V_l)^2}{1 - (V_s/V_l)^2} \quad (1)$$

$$E_d = \rho V_l^2 \frac{(1+v_d)(1-2v_d)}{(1-v_d)} \quad (2)$$

$$G_d = \rho V_s^2, \quad (3)$$

where v_d is the Poisson's ratio, E_d is the Young's modulus, G_d is the shear modulus and ρ is the material density. Theory [2] confirmed by experiments e.g. [4] shows that surface wave can be used to approximate the value of shear wave velocity, $V_R \approx 0.9V_s$, and hence used to calculate dynamic shear modulus of elasticity as:

$$G_d \approx V_R^2 \quad (4)$$

This formula serves as a basis for evaluation and modeling of the process of marbles degradation.

2.1. Rayleigh surface wave measurements

The measurement procedure does not need any energy transmitting medium between the specimen and ultrasonic probe and is 100% non-destructive [5]. Apparatus consists of a pulse generator, a set of two edge probes, signal processing and sampling unit and a PC. The probes consist of steel edges and piezoelectric transmitting/receiving transducers [6].

The edges are configured to ensure the contact nibs of both probes being parallel to each other and their geometry being suitable to generate and sense the surface Rayleigh wave in a stone outer skin layer.

The idea of the measurement method is sketched in Figure 1 and the edge probes are shown in Figure 2. The surface wave velocity is calculated on a basis of the recorded travel time of the ultrasonic pulse over a distance between the edges' nibs. The distance between both nibs is measured with digital slide caliper or alternatively can be fixed in advance to the measurements to the required value by using the calibrating plate inserted between the nibs.

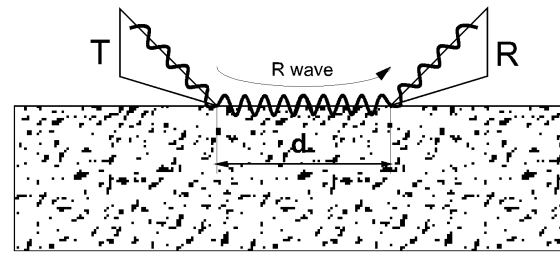


Fig. 1. Surface Wave measurement principle

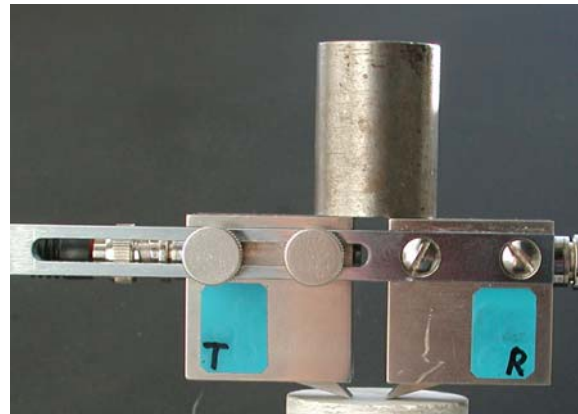


Fig. 2. Edge probe used for the Surface Wave velocity measurements

A computer was used as an oscilloscope screen and for software manipulation which allowed signal recording and pulse travel time measurement. Travel time measurements were corrected for apparatus characteristic delay time of the pulse travelling through the both probes. Rated frequencies of the probes were 1000-2000kHz, with the lower one used for the MG specimens showing greater attenuation of surface waves [7].

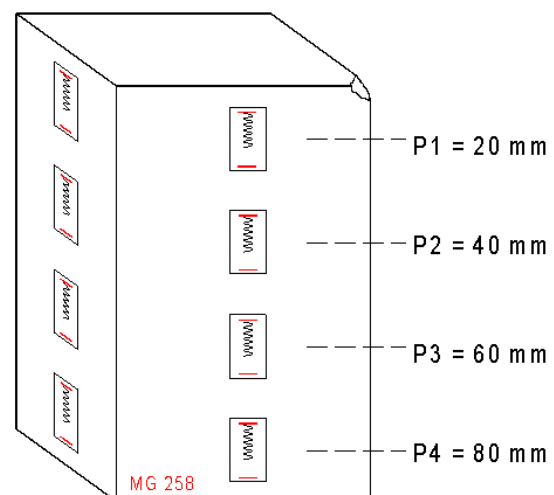


Fig. 3. Locations of Surface Wave velocity measurements

The specimens of 10 cm height were used and four equally spaced locations were chosen on two perpendicular specimens surfaces. This is schematically shown in Figure 3.

During experiments the probes were placed on a specimen surface to span the desired location symmetrically with the both contact nibs. The distance of the nibs was varying from 8 mm to 16 mm depending on the wave attenuation within a specimen.

2.2. Modeling of environmental loading

The artificial aging events were Freeze and Thaw (F-T) cycles. Each cycle consisted of 4 hours freezing to -10°C and then 4 hours thawing at 21°C [7]. The cycles were carried out in series of 20 F-T events which made one weathering cycle step. The specimens were dried in an oven after each cycle step in 40°C to the constant mass and ultrasonic pulse travel time was measured as described above.

Thermal effect of the drying process was evaluated before the beginning of systematic artificial ageing in order to establish the proper drying temperature at the end of the prescribed number of F-T cycles. It was shown that applied drying temperature of 40°C does not introduce the change in measured surface wave velocities. During freezing phase of the cycle and during drying of the specimens temperature measurements inside a reference specimens were performed. The reference specimens were drilled to a depth of 5 cm parallel to their longer axis and a thermocouple was used to measure the temperature inside the specimen. Three specimens of Cervairole Marble (MC) and Gioia Marble (MG) were used for measurements in each cycle step except the step zero were reference values of surface wave velocities were measured for fresh, from quarry stones. In this case five specimens of each marble were used. The recorded data were used in further marble degradation analysis based on the observed mean values of surface wave velocity.

3. EXPERIMENTAL RESULTS

Measurements of ultrasonic surface waves were performed according to the above described procedure [7]. Five specimens of MC and MG marbles were tested before weathering and three others each time new specimens after 20-100 F-T cycles. The specimens tested after 100 F-T cycles were additionally weathered and tested in step after 120 cycles.

Values of surface wave velocities which has been used to analyse RC and MG stones decay are collected in Table 1. There are presented mean values for each cycle step calculated for X and Y planes of Cervairole and Gioia Marbles specimens. Mean data are accompanied by standard deviations based on 36 the measurements for each data in general, except of two cases for Gioia Marble where only 30 measurements were successful due to greater wave attenuation.

Table 1. V_R [m/s] measurements with edge probes

marble & side	MC X		MC Y	
	Velocity	St.dev.	Velocity	St.dev.
0	2740	24	2720	43
20	2580	84	2590	23
40	2880	138	2850	92
60	2580	29	2620	106
80	2670	67	2630	71
100	2560	98	2500	37
120	2580	61	2530	42
marble & side	MG X		MG Y	
	Velocity	St.dev.	Velocity	St.dev.
0	1900	187	1900	142
20	1500	173	1450	201
40	1600	235	1700	290
60	1500	134	1500	186
80	1450	85	1500	94
100	1300	172	1300	110
120	1500	164	1400	107

Scattering of the results is usually greater for MG marble which is of granoblastic (homoblastic) microstructure and is less homogeneous than the xenoblastic RC marble. It is also seen that MG marble has lower average surface wave velocity and more distinct weathering trend then RC marble. Both weathering trends seem to be non-monotonic while looking at average values.

To describe the real weathering tendency the measured velocity values were compared with phenomenological mathematical model of weathering decay of stones which has been done in the next section.

4. ANALYSIS

Dynamic elastic properties of the marble were assessed on a basis of measured surface Rayleigh wave propagation velocity. It can be seen from the formulae (2 - 4) that the square of the elastic wave velocity is proportional to elastic moduli of the tested material. Thus one can introduce Material Elasticity Index (MEI) as a square measure of a ratio of actual and reference wave velocity according to equation:

$$MEI_{VR} = \left(\frac{V_R}{V_{R0}} \right)^2 \tag{5}$$

where actual V_R velocity was measured after F-T artificial weathering and reference V_{R0} velocity is that measured for intact marble (fresh, from quarry). Freezing and thawing increases stone surface deterioration which decreases dynamic elastic properties of the stone thus lowering the surface

wave velocity. Hence observed elasticity index MEI_{VR} is a decreasing function of stone degradation with value of 1 for the intact marble.

Mathematical model assuming a loss of stone integrity Ψ proportional to the integrity at the beginning of each cycle [3] was used to evaluate the material degradation.

This assumption can be expressed in a form of differential equation as follows:

$$-\frac{d\Psi}{dN} = \lambda\Psi \quad (6)$$

where $d\Psi/dN$ is the disintegration rate, minus sign indicates that the integrity is decreasing, λ is the decay constant, and N is the number of cycles.

The solution of (6) is the exponential material degradation law of the form:

$$\Psi = e^{-\lambda N} \quad (7)$$

The MEI_{VR} indexes were calculated separately for Cervaiolo and Gioia Marbles for X and Y specimen wall on a basis of V_R velocities of 36 measurements recorded for each specimen wall after each artificial ageing cycle. These 36 indexes were averaged and standard deviation errors were calculated. The results were analysed individually for each wall of MC and MG marble categories.

Primary analysis, with all the results included into analysis, showed poor correlations with physically sound fit functions. The correlation R^2 parameter was as low as 0.235 in one case and prediction bounds of 95% probability were very broad. This showed that some of calculated MEI_{VR} were influenced by other experimental factors than material degradation only. Further analysis showed that discarding the indexes calculated for the cycle No 20 for both marbles improves the fit to the great extent. Three other index values were also removed from the analysis giving all together 7 out of 28 calculated indexes which were unacceptable. After this modification the exponential curves, based on the mathematical model assuming a loss of stone integrity proportionally to the integrity at the beginning of each cycle, were fitted to the calculated indexes. The actual R^2 correlation and 95% prediction bounds were substantially tightened.

Summarized MEI_{VR} indexes are given in Table 2. The index values which were excluded from the further analysis are shadowed.

Graphical illustration of the calculated MEI and fit functions are drawn in Figures 4 and 5 for MC and MG marbles respectively. There are also shown prediction bounds and statistical information about the given exponential fit. It is also seen that discarded index values fall apart from prediction bounds of the well-correlated, physically sound fits justifying that some unpredicted experimental errors were introduced during the cycle No 20 of F-T

weathering of both marbles and in three other cases as well.

Table 2. Material Elasticity Index based on Surface Wave Velocity measurements

marble & side	MC X		MC Y	
	$(v_R/v_{R0})^2$	St.dev	$(v_R/v_{R0})^2$	St.dev
0	1	0.02	1	0.03
20	0.88	0.06	0.91	0.02
40	1.10	0.10	1.10	0.07
60	0.88	0.02	0.93	0.08
80	0.94	0.05	0.93	0.05
100	0.87	0.07	0.84	0.02
120	0.88	0.04	0.86	0.03
marble & side	MG X		MG Y	
	$(v_R/v_{R0})^2$	St.dev	$(v_R/v_{R0})^2$	St.dev
0	1	0.20	1	0.16
20	0.59	0.14	0.61	0.19
40	0.75	0.22	0.84	0.29
60	0.60	0.11	0.68	0.18
80	0.58	0.07	0.66	0.08
100	0.50	0.14	0.46	0.08
120	0.66	0.14	0.59	0.09

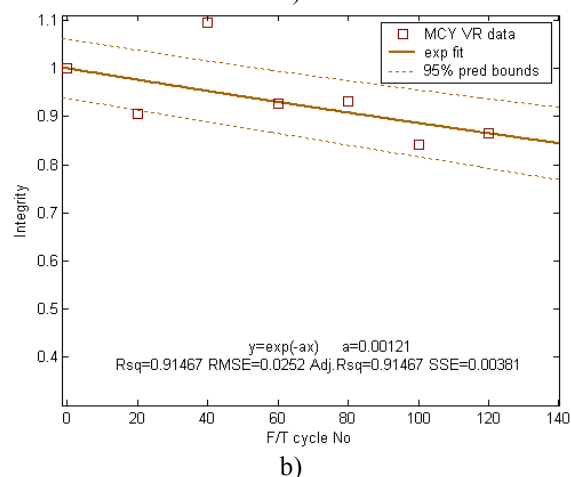
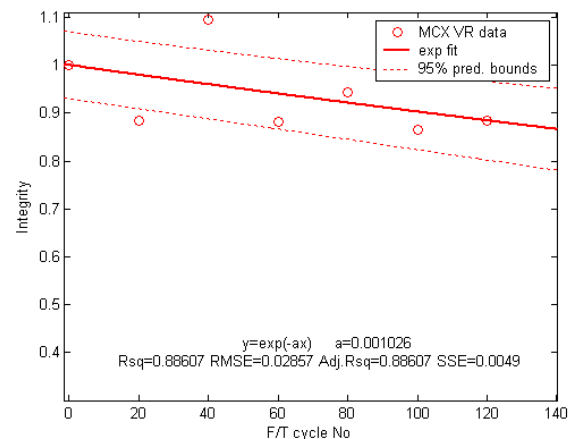


Fig 4. Integrity of Cervaiolo Marble after F-T ageing treatment: a) X-plane, b) Y-plane

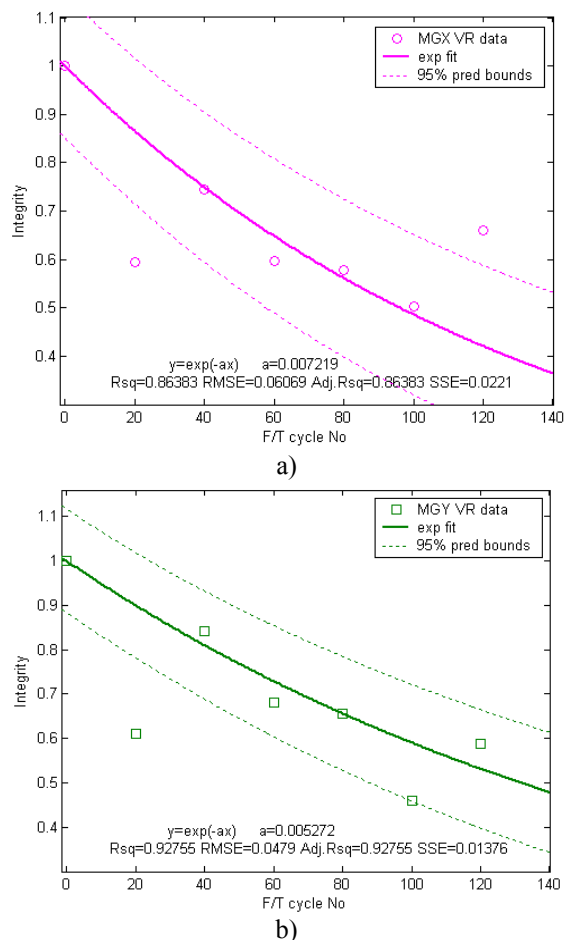


Fig. 5. Integrity of Gioia Marble after F-T ageing treatment:
 a) X-plane, b) Y-plane

5. CONCLUSIONS

Research confirmed that Rayleigh surface waves can be efficiently used for diagnostic of surface degradation of historical construction materials. Application of edge probes to the measurements of surface wave velocity is especially suitable for testing of monuments because it does not need any coupling medium which may degrade surface of the heritage object. The apparatus is portable and can be used in laboratory and for on-site testings as well.

By virtue of the method only thin surface layer is analysed and many local measurements allow statistical analysis.

Assumed exponential degradation model fits well to the experimental data. Resulting exponential curves were fitted to the calculated experimental indexes with R^2 correlation factor equal to 0.8368 in the worst case.

Data collected for Gioia and Cervaiolo Marbles shows that Gioia Marble is much less resistant to Freezing and Thawing ageing factors than Cervaiolo Marble.

RTF. Prosimy również o przysłanie na adres redakcji artykułu w formacie PDF, co ułatwi ostateczną jego redakcję.

LITERATURE

- [1] Strutt, J.W., (Third Baron Rayleigh): *On Waves Propagated Along the Plane Surface of an Elastic Solid*. Proceedings of the London Mathematical Society, 17 (1885), str. 4–1.
- [2] Landau, L.D., Lifszyc, E.M.: *Teoria sprężystości*. IV ed., PWN, Warszawa 1993, str. 125-128, (in Polish).
- [3] Mutlutürk, M., Altindag, R., Türk, G.: *A decay function model for the integrity loss of rock when subjected to recurrent cycles of freezing–thawing and heating–cooling*. International Journal of Mechanics & Mining Sciences 2004, 41, str. 237–244.
- [4] Pinińska, J.: *Surface wave velocity as a laboratory non-destructive control of the rock properties*. in “Proc. 5th Int. IAEG Congress”, Buenos Aires, 20-25 October 1986, str. 59-65, Rotterdam, Boston: Balkema.
- [5] Pęski, Z.: *Nowa metoda generowania fali powierzchniowej*. „13 Krajowa Konferencja Badań Nieniszczących”, Kozubnik, str. 25-27 October 1984 (in Polish).
- [6] Pęski Z., Ranachowski, J.: Patent Pending 142739, Poland 1988.
- [7] Skłodowski, M., Pinińska, J., Łukaszewski, P., Bobrowska, A. and Gutkiewicz, P.: *Report on ultrasonic surface wave velocity measurements: MCDUR-ACUTHERM EC 6FP, Project, McDUR - G6RD-2000-00266, ACUTHERM - GRD3-2001-60001 (unpublished) 2005.*



Dr. Marek SKŁODOWSKI
 Graduated in 1974 in mechatronics at Warsaw University of Technology. In 1980 he completed his doctoral thesis in Institute of Fundamental Technological Research, Polish Academy of Sciences in Warsaw. Currently he is Main

Specialist in Smart Technology Centre there. Main research activities are experimental stress analysis, development of measurement methods, sensors and equipment for material testing and in situ measurements in the field of historical constructions.



Dr Paweł ŁUKASZEWSKI

Graduated in 1986 in geology at Warsaw University. In 1997 he completed his doctoral thesis in Faculty of Geology at Warsaw University. Currently he is on position of academic teacher in Geomechanics Department at Warsaw University. Main research activities are design

methodology for rock engineering, in situ and laboratory testing of rock properties, non-destructive and destructive testing of rock elasticity properties specific and regional geomechanical characterization of rocks and rock massifs and acoustic emission measurements.



mgr Alicja BOBROWSKA

She studied at the Institute of Hydrogeology and Engineering Geology at Department of Geology, University of Warsaw and graduated in 1997 there. She is currently an employee at the Institute of Hydrogeology and Engineering Geology, Department of Geomechanics.

The main activities include the use of ultrasonic non-destructive testing of rock materials, deterioration processes, analysis of the deterioration factors, methods of their evaluation, simulation and interpretation of geomechanical research in historical architecture.

HIGH SENSITIVE METHODS FOR FATIGUE DETECTION

Mirosław WITOŚ, Mariusz ZIEJA

Instytut Techniczny Wojsk Lotniczych (Air Force Institute of Technology, AFIT)
01-494 Warszawa ul. Księcia. Bolesława 6, Poland, fax. +4822 851105, e-mail: miroslaw.witos@itwl.pl

Summary

The diagnostic and research aspects of compressor blade fatigue detection are investigated in the paper. The authors review the characteristic of different modes of metal blade fatigue (LCF, HCF, VHCF). The polycrystalline defects and impurities influencing the fatigue, along with their related surface finish techniques, are taken into account. The experimental methods of structural health assessment are considered. The Tip Timing (TTM), Experimental Modal Analysis (EMA) and Metal Magnetic Memory (MMM) provide information on the damage of diagnosed object (compressor blade). It has been proven that the shape of resonance characteristic gives an ability to determinate if fatigue or a blade crack is concerned. Early damage symptoms, i.e. modal properties of material strengthening and weakening phases (structural and magnetic anisotropy) have been described.

Keywords: compressor blade, damage, fatigue, modal analysis, lattice-spin coupling.

WYSOKOCZUŁE METODY DETEKCJI ZMĘCZENIA

Streszczenie

W artykule przedstawiono doświadczenia z badań stoiskowych i diagnozowania zmęczenia łopatek sprężarki. Wskazano typowe przypadki zmęczenia metalowych łopatek (LCF, HCF i VHCF). W rozważaniach uwzględniono cechy rzeczywistego materiału konstrukcyjnego, w tym wpływ domieszek, defektów struktury polikrystalicznej i obróbki wykańczającej na zmęczenie materiału. Przedstawiono metody badawcze stosowane do monitorowania stanu technicznego. Wykazano, że metoda tip timing (TTM), eksperymentalna analiza modalna (EMA) i magnetyczna pamięć metalu (MMM) udostępniają informację o narastającym zmęczeniu diagnozowanego obiektu (łopatki sprężarki). M.in. wykazano, że kształt krzywej rezonansowej jest związany z poziomem zmęczenia struktury i pęknięciem pióra. Opisano wczesne symptomy zmęczenia, m.in. właściwości modalne fazy umocnienia i osłabienia (strukturalnej i magnetycznej anizotropii).

Słowa kluczowe: łopaska sprężarki, degradacja, zmęczenie analiza modalna, sprzężenie siatka krystaliczna-spin.

1. INTRODUCTION

Many different fatigue failures (LCF, HCF and VHCF) could occur throughout the turbine engine's life, Figure 1.

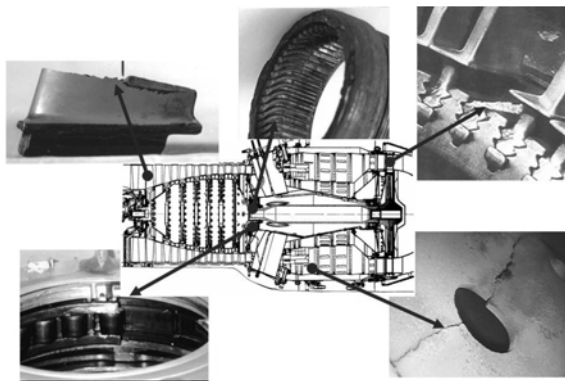


Fig. 1. Structural fatigue problems of turbine engines

Fatigue cracks propagating in rotor blades, the incorrect control of the engine's fuel system and the lack of knowledge on the loads affecting the bearing

system generally cause a formidable hazard to flight safety, as well as to engine life and reliability. Therefore, the AFIT keeps looking for new methods of recognizing stochastic loads during the engine's running, and the effects thereof upon the engine's structural reliability. The paper presents three methods:

- A non-contact blade-vibration measuring technique (tip timing method) [1-10], which is one of the most interesting methods of complex diagnosing of jet engines and a powerful tool to investigate dynamic phenomena in the running engine. The method has been used in the Polish Air Force since 1993 with the SNDL-1b/SPL-2b diagnosing system developed for the SO-3 engines. Since 1997, this method has been also used in the post-repair/post-overhaul acceptance tests.
- An experimental modal analysis, which has been used as a sensitive NDT method during overhaul blade tests since 2008 [11].

c) A metal magnetic memory, which has been used as a sensitive observer of residual and applied stress, and continuous material damage [12-18]. These methods are source of information about blade quality (of design, production and overhaul) and real dynamics of phenomena (correlation by modal proper-ties), which have an effect on blades damage and fatigue differentiation. This information has been used to actively control fatigue of compressor blade and verify FEM model.

2. MOTIVATION

In the years 1975-91 as many as 25 first-stage compressor blades of ten SO-3 engines suffered fatigue-attributable break-offs, which caused two accidents. The metallographic examination of damaged blades made out of the 18H2N4WA steel has proved that the crack initiation centres were located either on the leading edges (55%) or on the blade-back surfaces (45%), in the areas of nodal lines of the first mode vibration. Crack propagation occurred at low-level stresses (HCF problem) or high-level stresses (LCF problem), Figure 2. Fatigue fracture covering as much as 95% of the blade's cross section was found in one of the blades. Furthermore, it has also been found that erosion and corrosion, both occurring on the blade's face surface, as well as fine mechanical damages on the leading edge are stress concentrators [2]. Fatigue problem was also observed in titanium blades (Ti5.8Al-3.7Mo) in the TW3-117 engines in the years 2005-2007.

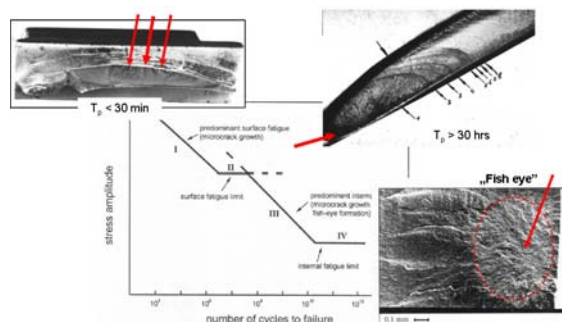


Fig. 2. Fatigue problems (LCF, HCF, VHCF) of compressor blades

The gigacycle fatigue problem (VHCF with “fish eye” symptoms) of compressor blade has been observed at foreign users, e.g. in Russia [19,20], Figure 2. Compressor blades run a risk of VHCF problem because they count more than $3 \cdot 10^9$ cycles for 1st flexible mode and more than $1 \cdot 10^{10}$ cycles for 1st torsional mode during time between overhaul (TBO). High risk of VHCF problem, with crack nucleation under the blade surface and stresses level below fatigue life stresses, concerns of high resistant material and blades made with surface finish techniques [21-23].

Uncontrolled blade over fatigue:

- is a threat for service safety;
- limits aero-engine life time;
- increases maintenance costs.

It is also a great challenge for a diagnostics engineer.

If blade fatigue is found, who is responsible for the problem?

Classical NDT (eddy current, ultrasound, magnetic and fluorescent methods) are very low effective to diagnose blade crack before damage, because of:

- crack gap closing during engine standstill (about 50% of crack area after 12 hrs);
- lack of reliable information about real operating conditions;
- lack of knowledge about early cracking symptoms and mechanisms;
- difficult access to tested blades (because of inlet stator vane).

An other disadvantage of the NDT methods in use (during overhaul and service) is no possibility of fatigue prognosis. This disadvantage is very important for the 1st compressor blades of the SO-3 engine. The blades have design errors - too low the first-mode mistuning form the 2nd rotational harmonic excitation. There for, too high stress and fast fatigue crack initiation can occur during operation. These conditions take place during the take-off phase when there is a foreign object lying in the inlet or the inlet icing occurs. Under such conditions time between crack initiation and blade damage can be shorter than time of a single flight.

An intuitive diagnostic symptom of a blade crack is a change its modes frequency. The cracking propagation and blade break off occur at limiting decrease in frequency, the value of which depends on the crack centre's position and the loading. Blades' frequency check offers too short prognosis horizon. It is sufficient in the system monitoring only; for example, in the tip-timing method.

3. THE TIP TIMING METHOD

The tip timing idea consists in observing displacement of loaded component part. In our case, it will be a rotating and vibrating blade. The observer is built onto a fixed part of machinery. The measured signal contains:

- Aperiodic part $A(t)$ – average instantaneous rotational speed of perfect stiff rotor.
- Oscillating part $P(t)$ – resultant from: pitch errors, blade, rotor and disk vibration and instantaneous rotational speed perturbations (from the engine control system, flow, g-force, clearance in a kinematic system, and torsional vibration).
- Noise and weak oscillating components $I(t)$

$$S(t) = A(t) + P(t) + I(t) \quad (1)$$

so it is possible to design a general-purpose observer for real operating conditions of rotating parts and have a complex view on:

- Disadvantageous dynamic phenomena (flutter, stall, surge, resonance, load coupling);
- The influence of production, overhaul and maintenance real conditions on the level of malfunctioning and fatigue prognosis.

Blade vibration and deflection are a source of a time-interval (measured) change between flexible key phases. Time period signal would be measured with a frequency method [10].

Analyzed data (discrete time of signal $S(k)$) – a number of pulses $Code_i$ with clock frequency counting between key phases includes three groups of variables to be identified in effect of further numerical signal analysis

$$S(k) = Code_i = K_{i,i+1} Trunc \left(\frac{\Delta T_{i,i+1}}{t_{clock}} \right) = \left(\frac{(1 + \zeta_B) 2\pi / N_B}{(1 + \zeta_R) \omega} \right)_{i,i+1} \quad i \in \langle 1, 2, \dots, N_B \rangle \quad (2)$$

where, k – discrete time, N_B – number of blades, $\Delta T_{i,i+1}$ – time interval between two blade passes; t_{clock} – time period of generator pulses; $K_{i,i+1}$ – error and disturbance factor ($K_{i,i+1} = 1$ for data without error), ζ_B – jitter of blades group components, ζ_R – jitter of rotor group components, ω – angular velo-city of ideal rotor.

Every component of $S(k)$ is used to diagnose. An oscillating part $P(k)$ is a main carrier of diagnostic information about blades damage and danger dynamics phenomena. An aperiodic part $A(k)$ and part $I(k)$ give the capability to compare new diagnostic symptoms to the health of machinery. The scope of interest of TTM data processing includes [1-10]:

- Vibration level of all blades at the same time.
- Disadvantageous dynamic phenomena.
- Blade stress and health.
- Disk health.
- Engine health.

The tip timing method is not intended to direct measure: load, local displacement (strain) and local stresses in the blade. This can be estimated by using TTM data and other numerical methods (GPA – Gas Path Analysis; FEM – Finite Element Method; CFD – Computational Fluid Dynamics, statistical ones) and knowledge about blade modal properties. Characteristic features of the TTM are:

- getting information about vibration and quasi-static blade deflection only once during 360 degrees rotation;
- irregular signal sampling rate, affected by vibration parameters (like amplitude, frequency and phase). The Nyquist-Landau law describes discrete-time information;

- periodic measurement data structure – data can be illustrated with matrix with N_B columns (number of blades) and rows that represent each full 360 degrees cycle of a rotor;
- the inherent in a signal oscillating parts that are not connected with blade vibration. There are two groups of oscillating parts of a signal: synchronized and non-synchronized with rotor rotational frequency;
- observation of effects of coincident amplitude modulation (AM), frequency modulation (FM) and phase modulation (PM) if there are oscillating parts in a signal.

To develop the expert analysis on compressor blade and engine health, the qualitative evaluation of applicability of the tip timing method was done in 1987-1993. The possibility of estimating the blade health (crack initiation and propagation) on a running engine was taken into consideration [2]. Signal components are obtained with the narrow-band filtering and AM/FM demodulation. They are very useful to expert analysis of health of the engine itself and to the 1st stage compressor blades, the engine fuel system and the bearing system [6].

Blade vibrations are shown in the form of phase distributions as points of phase trajectory crossing the phase plane [2], Figures 3 i 4. A characteristic feature of the method is information that lasts about a total number of modal frequency periods between two subsequent points of phase trajectory crossing the phase plane, with basic modal parameters of the blades preserved. This phenomenon enables detection of the LCF and HCF crack initiation and propagation in the blade during the engine operation.

3.1. Examples

The object under scrutiny has been the 1st stage compressor blade (28 blades made out of the 18H2N4WA steel, each 100 mm long, chord 37 mm, twisted by the angle of 38°). Frequencies of three subsequent modes of blade vibration were as follows (average values): 350 Hz and 1380 Hz (bending vibration), 1890 Hz (torsional vibration).

Synchronous resonance

During examination with a strain gauge no evident symptoms of interrelationships between the disk and blade vibrations were observed – compressor stages are of compact design. However, it was observed that within the take-off range of the SO-3 engine operation ($n = 15600$ rpm), synchronization of blade vibration with forces from the 2nd harmonic of the rotational speed ($f_{1mode} = 520$ Hz) may occur, Figure 3. Such phenomena observed, e.g. after some foreign object (bird, ice) has been deposited on the stator blade-ring, induce blade vibration up to some dangerous level where the material yield point is reached and exceeded, and quick initiation and propagation of the LCF and HCF crack occurs. Under such conditions of blade

operation, time of safe operation of any turbojet engine may be much shorter than one flight/mission of an aircraft.

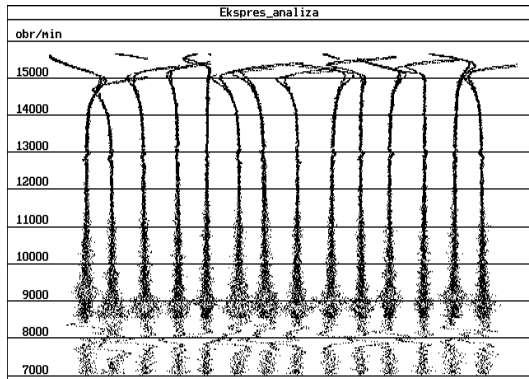


Fig. 3. How foreign-matter depositions may affect the level of stress in the SO-3's 1st stage compressor blades - effect of foreign matter in compressor inlet [2]

The blade cracking

After an analysis of destructive testing results (controlled propagation of blade cracking under normal conditions of operating the SO-3 engine) it was found that:

- during the blade cracking initiation (no open crack visible on the blade surface) only change in the B factor of dynamic increment of blade vibration frequency is seen, Figure 4.a) – frequency of the blade's free vibration $f_B(0)$ is constant

$$f_B(n) \approx \sqrt{f_B(0)^2 + B n^2} \quad (3)$$

- the occurrence of a blade crack decrease in the range of excitations from the rotational-speed II harmonic by 1000 rpm ($\Delta f = 16.6$ Hz), Figure 4.b). At the moment, frequency (the 1st mode) of the blade's free vibration changed by less than 3 Hz;
- when the crack reaches about 30% of the blade profile evident reduction in frequency of free vibration and decrease in the range of excitations from the rotational-speed III harmonic ($n \cong 8000$ rpm) was observed;
- just before the blade break-off (about 65% of profile for the crack from the leading edge, 95% of profile for the crack from the back of the blade), an evident effect of stiffening due to centrifugal forces was observed, Figure 4.c). Changes in the dynamic scale inflicted by the broken blade are comparable with those in other dynamic scales (the influence of the engine's rotational speed).

The representative one-hour profile of the engine mission used for the bench test has comprised:

- starting of the engine,
- engine warm-up,
- ground idle running (3x 4.5 min),

- running the engine within take-off range of speed (4.5 min)
- running the engine within cruising range of speed (4.5 min)
- eleven full acceleration/deceleration cycles (ground idle - take-off range of speeds – ground idle),
- half-way accelerations/decelerations within the range: idle - 12000 rpm (3x4.5min, 5 cycles/min),
- half-way accelerations/decelerations within the range: 12000 rpm - take-off range (3x4.5min, 5 cycles/min),
- engine cooling,
- stopping the engine.

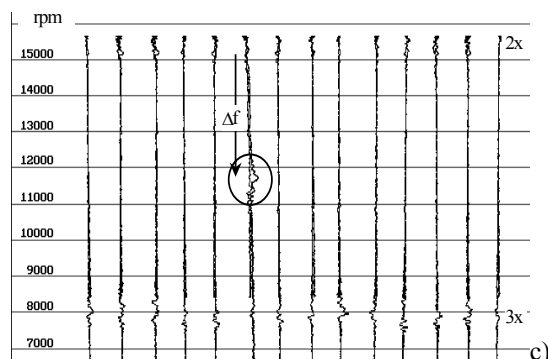
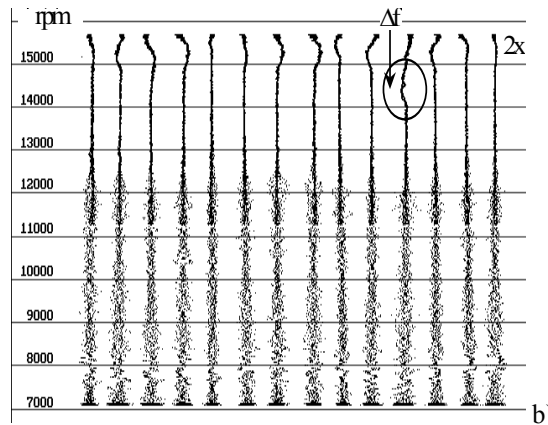
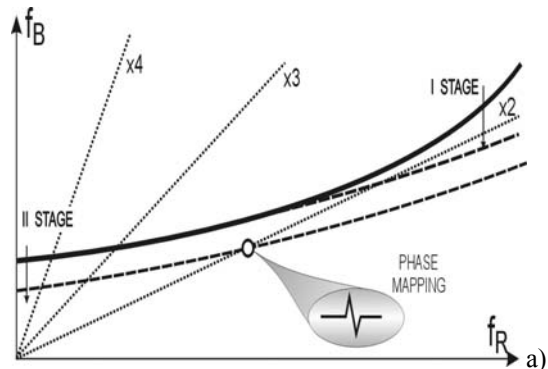


Fig. 4. The effect of blade cracking as phase representation of blade vibration [2]: a) blade frequency plotted in the Campbell diagram; b) the first stage of blade cracking – changes only B ; c) final stage of blade cracking – 5 minutes before break (LPF)

In such a mission profile, the blade crack propagation from the crack initiation down to the blade break-off took more than 30 hrs for the normal level of excitations. On the other hand, it didn't take more than 20 minutes (about $6,2 \cdot 10^3$ blade cycles with the 1st mode frequency) of the engine running within the take-off range of speed and at high level of stress (deposition of some foreign object in the inlet). It has been proven that the TTM gives credible prognosis for 50 engine work hours (over $9 \cdot 10^7$ HCF and 100 LCF cycles, 1/8 TBO). It has been also proven [11] that TTM symptoms of the cracking are closely related to:

- the strengthening phase – the quality factor of the resonance system increases together with the friction mode frequency;
- the weakening phase – growth in the resonance curve asymmetry and growth in nonlinearity.

Nowadays, these symptoms are not used in the SNDL-1b/SPL-2b system. They provide a capability of broadening prognosis horizon.

4. THE EXPERIMENTAL MODAL ANALYSIS METHOD

Experimental modal analysis is an effective aid in solving blades' fatigue problems. It allows of finding an answer to the question: "Why does a blade crack?", not only: "Is it cracked?". The modal parameters of all the analysis modes (within the frequency range of interest) constitute a complete dynamic description of the blade structure [11,24]:

- ✎ blade material,
- ✎ blade geometry,
- ✎ the influence of surface treatment and adding protection coating;
- ✎ technical health (structural heterogeneity, crack and fatigue).

The characteristic feature of blade vibration measurement on a modal excitation system is knowledge of both a force level and a blade response on it. That's why it is possible to identify blade modal properties for following modes.

The broadband identification (up to 20 kHz) of modal properties of a compressor blade made of 18H2N4WA steel and Ti5.8Al-3.7Mo titanium alloy, has been made on the PSV-400 Polytec scanning vibrometer and low power PZT exciter.

The identification of early fatigue and cracking symptoms of these blades has been made on the B&K electro-dynamic exciter 4802T. The experimental stand, used during the SO-3 and TW3-117 engine overhauls, included:

- the MTI Instrument laser measurement system MicroTrack™II with CMOS measurement head LTC-120-40 [25];
- the Vibration Research Corporation VR-8500 controller that includes 24 bit A/D and D/A converters, and RISC processor [26];

- the Vibration Research Corporation Vibration View software to control the exciter, data acquisition and analysis [26].

The sensitivity of measurement system is 100 mV/mm.

Experiments have been performed in four stages in which:

- the measurement method has been verified,
- blade cracking symptoms have been identified,
- early symptoms of fatigue have been identified,
- new diagnostic symptoms have been verified for titanium blade.

It has been proven that used measurement technique (MTI laser head) guarantees reliable modal results when vibration amplitude is higher 2 μ m. Reliable resonance curve shape during sine test has been got for force frequency: 2.5 Hz/min for 1st flexible mode (1F, $Q_s > 350$) and 1.0 Hz/min for 1st torsion mode (1T, $Q_s > 1000$). Such a stand gives an ability to make precise measurements with an exact test profile and frequency step. The measurement system gives almost laboratory accuracy. That's why it let [11]:

- Precise identification of blade modal properties in measured frequency range.
- Metrological factors influence analysis on recorded resonance characteristics.
- Modal parameters trends analysis observed during fatigue tests.

The modal properties identification (sine test) was based on the transition function

$$G(\omega) = \frac{Y(\omega)}{X(\omega)} \begin{bmatrix} m \\ m \end{bmatrix} \quad (4)$$

where $X(\omega)$ – displacement of an exciter head (blade root); $Y(\omega)$ – displacement of a blade tip.

4.1. Modal properties of a defect-free (non-cracked) blade

In the case of a defect-free blade (health) resonance characteristics of particular modes were gained, ones that could be well described with a model of a single-degree-of-freedom linear system (SDOF) – of mass m suspended on a spring with spring rate K and viscous damping C [27]. For sine test SDOF model describe

$$m \frac{d^2 y(t)}{dt^2} + C \frac{dy(t)}{dt} + Ky(t) = F(t)$$

$$F(t) = A(\omega) \sin(\omega t) \quad (5)$$

$$y(t) = B(\omega) \sin[\omega t + \phi(\omega)]$$

Characteristics of subsequent modes remain continuous under resonance conditions and exhibit good symmetry around the resonance frequency (within the band-width of 3 dB), Figure 6. The blade displacement at the measuring point can be described with:

- vibration amplitude

$$b(\omega) = \frac{y_{st}}{\sqrt{\left[1 - \left(\frac{\omega}{\omega_o}\right)^2\right]^2 + \left(\frac{\delta}{\pi} \frac{\omega}{\omega_o}\right)^2}} \quad (6)$$

- vibration phase angle

$$\varphi(\omega) = \arctan \left(\frac{\frac{\delta}{\pi} \frac{\omega}{\omega_o}}{1 - \left(\frac{\omega}{\omega_o}\right)^2} \right) \quad (7)$$

where, ω_o – a free vibration frequency, δ – a logarithmic damping decrement.

4.2. Diagnostic symptoms of a cracked blade

When analyzing resonance curve shape we can observe how different it is for cracked blade. The blade has all nonlinear properties [11,29] which describe a nonlinear 2DOF model, Figure 5.

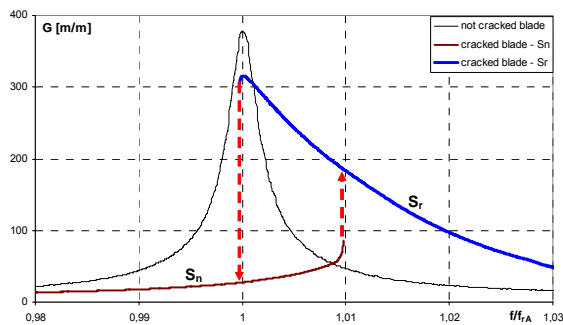


Fig. 5. The effect of a crack on the 1st mode characteristics shape (steel blade, $a = 19.62$ m/s^2 , f_{rA} – frequency of amplitude resonance)

Close to the resonance frequency it is possible to observe two branches of characteristics: resonance attractor – S_r , and non-resonance attractor - S_n , and jumps between them. The shape of a cracked-blade's resonant curve is affected by the blade's material and conditions existing on the edge of the crack gap. The characteristic curve is sloped to the left (towards lower frequencies) for the crack with material weakening. On the other hand, for the gap with material hardening, the curve is sloped to the right (towards higher frequencies). The knowledge of resonant curve inclination is essential for correct interpretation of measurements, including correct identification of the resonant and non-resonant branches. During one-sided test we observe "asymmetry" resonance curve with seeming quality factor decreases. Resonance frequency and characteristics are functions a blade amplitude. They were not asymmetry symptom for:

- small loads that don't develop an open crack. Asymmetry is growing with a load increase;

- a notch on a blade, which was used as a simplified crack model (no friction at a notch hole). No friction in notch modeled blade is a source of other differences in modal properties, Table 1, and fatigue (JCF phenomena).

Table 1. Blade with 11 mm length damage (*starting from TE*) placed 20 mm from lock

Blade	Frequency change (Hz)		
	1 st mode	2 nd mode	3 rd mode
Cracked	-12	+7	-27
Notched (no friction)	-13	-5	-80
Difference (%)	-0.28	-0.86	-2.73

The obtained characteristics of the cracked blade cannot be described with a SDOF linear model. The blade crack forms a two-degrees-of-freedom (2DOF) non-linear system for any form of blade vibration. The equivalent linear equation that satisfies the non-linear equation with accuracy ε takes the following form:

$$\frac{d^2 y}{dt^2} + 2h_\varepsilon(b) \frac{dy}{dt} + \alpha_\varepsilon^2(b)y = \varepsilon p \cos(\omega t) \quad (8)$$

where: ε – small parameter, p – amplitude of the exciting force, b – steady-state vibration amplitude, $\alpha_\varepsilon(b)$ – equivalent natural (free-vibration) frequency, $h_\varepsilon(b)$ – equivalent elementary damping coefficient.

The measured and analyzed parameters of the blade are described with the following relationships:

- vibration amplitude

$$b(\omega) = \frac{\varepsilon p}{\sqrt{(\alpha_\varepsilon^2(b) - \omega^2)^2 + 4h_\varepsilon^2(b)\omega^2}} \quad (9)$$

- resonance frequency

$$\omega = \sqrt{(\alpha_\varepsilon^2(b) - 2h_\varepsilon^2(b)) \pm d} \quad (10)$$

$$d = \sqrt{4h_\varepsilon^2(b)(h_\varepsilon^2(b) - \alpha_\varepsilon^2(b)) + \left(\frac{\varepsilon p}{b}\right)^2}$$

- vibration phase angle

$$\varphi(\omega) = \arctan \left[\frac{-2h_\varepsilon(b)\omega}{\alpha_\varepsilon^2(b) - \omega^2} \right] \quad (11)$$

4.3. Early fatigue identification

The LCF and HCF data analysis showed that blade modal properties could be used to observe the material strengthening phase [11,29,30]. Increase in

the 1st mode resonance frequency of approx 0.4% is a symptom of the initial resonance system quality factor growth (correlation with structural and magnetic anisotropy), Figure 6. This phase can be described with linear SDOF model. The orientation indicator of maximum cyclic material strengthening is $R_m/R_{e0.2}$ (like as for metal magnetic memory NDT according to ISO-15242).

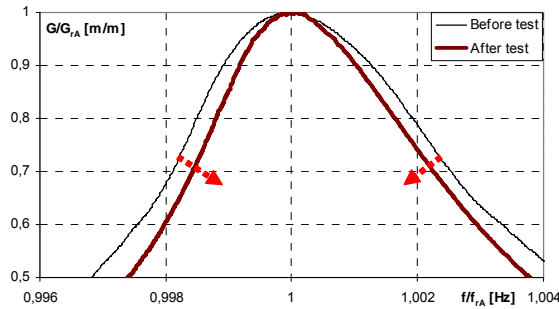


Fig. 6. Changes in modal parameters during material strengthening phase

The growing asymmetry of the resonance curve was observed only in the final fatigue phase; it preceded the 1st mode frequency decrease, Figure 7.

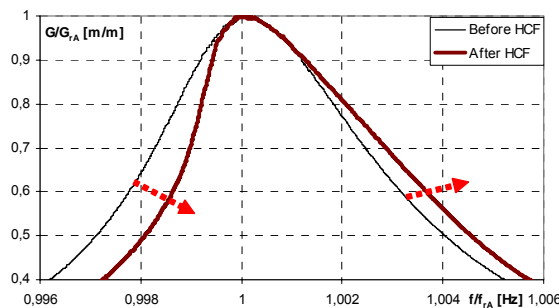


Fig. 7. Changes in modal parameters during material weakening phase ($\delta f_{rA} = -0.5$ Hz)

4.3. JCF phenomena

Influence of the cracked blade's resonant curve discontinuity on the propagation rate was investigated for blades made from titanium alloy. It was found that in the case of constant frequency input (HCF tests without fine tuning to current resonant frequency), characteristic curve sloping to right and resonant curve discontinuity helps stopping the crack propagation.

The speed rate of its development was conditioned by the load history of a blade. The asymmetry is a symptom of the material weakening phase [11,29,30]. The speed rate of the resonance curve asymmetry development, from the very first symptom of an open crack, is determined by the blade loading history.

Discontinuity of the resonant curve (blade pulse input discharge and load even for constant external load) is a source of very fast crack propagation

during frequency transient phase – the phenomenon is called **Jump Cycle Fatigue (JCF)**, Figure 8.

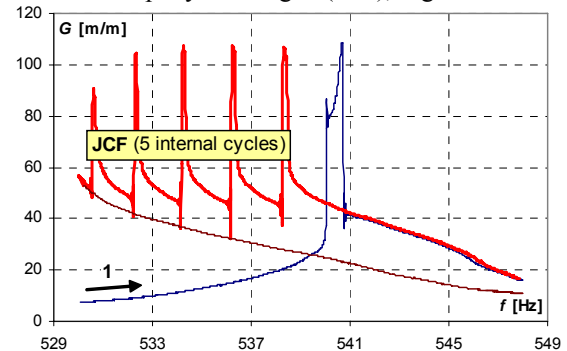


Fig.8. JCF phenomenon for a cracking blade with Ti5.8Al-3.7Mo (sine sweep 4 Hz/min with constant external load)

The JCF is a reason for the serial material tearing during the decrease in excitations frequency, observed in the unstable phase of cracking. Those observations are fundamental for the prognosis of crack propagation velocity and determination safe prognosis horizon for blade operation and fatigue reverse engineering - correct interpretation of fracture structure (answer on the question “How many load cycles took place during crack propagation?”). Arrest lines of fatigue strap map only a number of cycles for internal loads. Their values could be bigger several times than a number of cycles for external loads, which result from a flight mission profile.

5. THE METAL MAGNETIC MEMORY METHOD

Modal properties of compressor blade (K, C) are correlation with local and global magnetic properties of its material by grain-lattice and lattice-spin coupling (magneto-mechanical effects i.e. Villari effect, ΔE effect, stress magnetization and spontaneous magnetization of ferromagnetic in the Earth field) [12,31-33]. Zones RSC of local residual stress concentration, plastic, material anisotropy (mechanical and magnetic) and dislocation concentration are potential place of cracking nucleation and local magnetic anomaly [31].

The RSC are searched by passive observer - the metal magnetic memory method (MMM). Stress, strain (elastic and plastic) and dislocation density (sources of structural anisotropy) change material magnetization M and external magnetic field B in the vicinity of blade surface (magnetic permeability μ and electrical conductance ρ of polycrystalline material) [18,34]. The Earth's magnetic field and electro-magnetic noise are natural external source of magnetic field.

For small elastic deflection (strain) of the blade, the magneto-mechanical effects are described by reversible thermodynamic relation [35]:

$$\mu_0 \left(\frac{\partial \mathbf{M}}{\partial \boldsymbol{\sigma}} \right)_{\mathbf{H}} = \left(\frac{\partial \mathbf{B}}{\partial \boldsymbol{\sigma}} \right)_{\mathbf{H}} = \left(\frac{\partial \boldsymbol{\lambda}}{\partial \mathbf{H}} \right)_{\boldsymbol{\sigma}} \quad (12)$$

where, μ_0 - magnetic permeability of free space,

$\left(\frac{\partial \mathbf{M}}{\partial \boldsymbol{\sigma}} \right)_{\mathbf{H}}$, $\left(\frac{\partial \mathbf{B}}{\partial \boldsymbol{\sigma}} \right)_{\mathbf{H}}$ - reversible isofield magneto-

mechanical coefficients, $\left(\frac{\partial \boldsymbol{\lambda}}{\partial \mathbf{H}} \right)_{\boldsymbol{\sigma}}$ - reversible

isostress magnetostrictive coefficient. The magnetostrictive phenomena $\boldsymbol{\lambda} = [\lambda_{\parallel}, \lambda_{\perp}, \lambda_n]$ describes properties of material surface in parallel and perpendicular to load direction and material magnetic properties in orthogonal to surface.

The magneto-mechanical effects are partially irreversible for elastic strain and RSC (source of stress magnetization and local magnetic anomaly).

Potential possibilities of MMM were tested during active and passive experimental with used of compass (simple magnetometer), GM-04 magnetometer with Hall sensor, and IKN-1M-4 stress concentration recorder. Very good relation has been observed between the MMM results and blade node lines after LCF tests [18]. Local magnetic anomaly has been also observed near the close crack gap after HCF tests. Nevertheless, the most interesting phenomena is non-destructive detect of stress prehistory (a change of remanent magnetization), Figure 9.

On the base of former research absolutely, that exist the circumstances of use MMM to diagnosis the VHCF problems.

5.1. Magneto-mechanical damping

Applying a stress to a ferromagnetic blade causes a variation of magnetization due to the magneto-elastic coupling, which results in the so-called “ ΔE effect” (i.e. an apparent reduction of Young’s modulus below the purely elastic value found in the magnetically saturated state) and also in a related dissipation of mechanical during loading/ unloading or in case of vibration. The latter effect can give rise to a strong magneto-mechanical damping with stress-dependent and stress-independent components (a small change of K in Equation 5) [36].

Experiments show that ferromagnetic have a higher internal friction than other metals because of phenomena of an electro-magnetic nature resulting from the application of elastic fields. Considering five main contributions to the total energy of a ferromagnetic without an external field (exchange energy W_{ex} , magnetocrystalline anisotropy energy W_k , magneto-elastic (or magnetostrictive) energy W_{λ} , magnetostatic energy W_m , energy of magnetic domain walls W_w), four main mechanisms of magneto-mechanical damping may be defined [36]:

- magnetoelastic hysteresis damping, Q_h^{-1}

- macroddy-current damping, Q_a^{-1}
- microddy-current damping Q_u^{-1}
- damping at magnetic transformation Q_{PhT}^{-1}

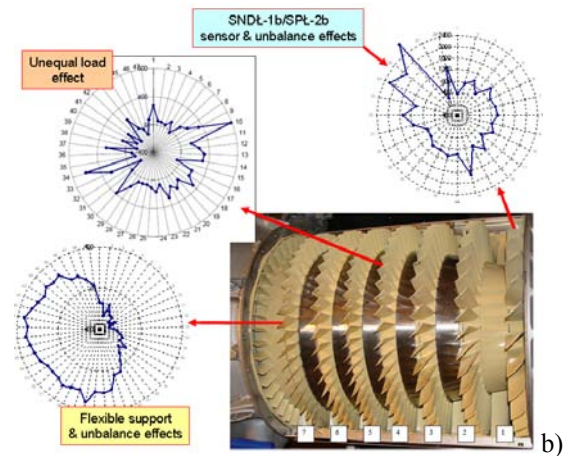
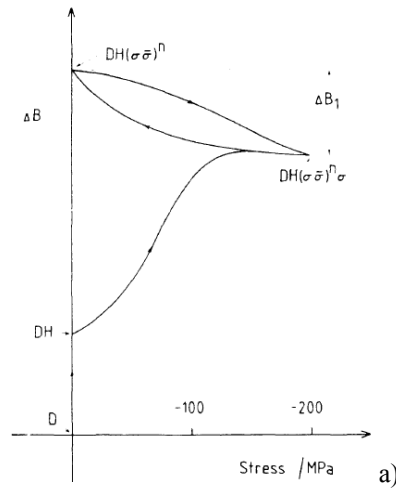


Fig. 9. Detect of stress prehistory: a) irreversible process of stress magnetization [34]; b) identification of blade fatigue risk [28]

Therefore, the total magneto-mechanical damping Q_m^{-1} in ferromagnetic blade can be considered as sum of these components:

$$Q_m^{-1}(\varepsilon, \omega, T) = Q_h^{-1}(\varepsilon, \omega, T) + Q_a^{-1}(\omega, T) + Q_u^{-1}(\omega, T) + Q_{Ph.T} \quad (13)$$

where contrary to Q_a^{-1} and Q_u^{-1} , the hysteretic contribution Q_h^{-1} depends on the strain amplitude.

The damping Q_m^{-1} is also dependent on the load frequency, material temperature, and initial conditions (micro- and macrostructure, magnetization, residual stress) – the Q_m^{-1} is nonlinear [37], so damping coefficient C in Equation 5 and the FEM model of damage blade is nonlinear too.

6. CONCLUSION

1. During 15 years of using the tip timing method in the Armed Forces of Poland, the following things have occurred:
 - The statistical mean time between fatigue break-offs of blades has been increased (nine times for calendar-based data, and five times on the hourly basis). Since 1991 no fatigue crack of any compressor blade in the SO-3 engines has been found;
 - The surge as a result of maladjustment of the fuel system and latent defects of subsystems has been eliminated (fatigue problems results from maintenance);
 - Five SO-3 engines have been taken out of service due to excessive errors in shapes of the blades.
2. The shape of cracked blade resonant curve is described by blade's material and conditions existing on the edge of the crack gap. The characteristic curve is sloped into left for the crack with material weakening. On the other hand, for the gap with material hardening, the curve is sloped into right. Asymmetry of resonant curve wasn't found on the blade with notched – a simple crack simulation model, often found in the literature.
3. The mode frequency of cracked blade depends on the condition of the crack edge. For the titanium blade with 12 mm crack and hardening stiffness characteristic, a vibration frequency of the first mode was considered as efficient under technical specification conditions!
4. Nonlinear properties of a crack blade are fundamental for the prognosis of the crack propagation rate and for the determining safe prognosis horizon. These modal symptoms of material damage are correlated with magnetic symptoms.
5. Diagnostic symptoms of the material weakening occur before:
 - the 1st mode frequency decrease by 3 Hz, the symptom of airfoil crack according to current technical and overhaul requirements;
 - an open crack, identified during the engine overhaul with a classical NDT method.
6. MMM method is developed in cooperation with The Faculty of Automotive and Construction Machinery Engineering (Warsaw University of Technology) during project "MONIT".

The study has been prepared under the research project no. ON 504000534 financially supported by the Ministry of Science and Higher Education in the years 2008–2010.

REFERENCES

- [1] US Patents 2575710 (1951), 3058339 (1962), 3467358 (1969), 3597963 (1971), 4153388 (1979), 4593566 (1986), 4827435 (1989),

- 5148711 (1992), 5479826 (1996), 6094989 (2000)
- [2] Witos M. (1994): *Diagnosing of technical condition of turbine engine compressor blades using non-contact vibration measuring method*. Dissertation, ITWL Warszawa (pol.)
- [3] Von Flotow A., Drumm M. J. (2002): *Engine Sensing Technology Hardware & Software to Monitor Engine Rotor Dynamics Using Blade Time-Of-Arrival and Tip Clearance*. Hood River, OR, USA, <http://www.hoodtech.com>
- [4] Washburn R. (2004): *Amplitude and Phase Variations Associated with Low Order Resonance Responses Subjected to Time Varying Excitation Sources*. Proc. of 9th National Turbine Engine High Cycle Fatigue Conference
- [5] Zielinski M., Ziller G. (2005): *Noncontact Crack Detection on Compressor Rotor Blades to Prevent Further Damage after HC-Failure*. RTO MP-AVT-121 Meeting Proceedings, NATO, paper 19, <http://www.mtu.de>
- [6] Witos, M., Szczepanik, R. (2005): *Turbine Engine Health/Maintenance Status Monitoring with Use of Phase-Discrete Method of Blade Vibration Monitoring*. RTO-MP-AVT - 121 Meeting Proceedings, NATO, paper 2
- [7] Duan F., Fang Z., Sun Y., Ye S. (2005): *Real-time Vibration Measurement Technique Based on Tip-timing for Rotating Blades*. Opto-Electronic Engineering, Vol. 30(1), pp. 29-31
- [8] Ayes B.W., Arnold S., Vining Ch., Howard R. (2005): *Application of Generation 4 Non-contact Stress Measurement System on HCF Demonstrator Engines*. Proc. of 10th National Turbine Engine High Cycle Fatigue (HCF) Conference. Dayton, USA
- [9] <http://www.agilismasurementsystems.com>
- [10] Brouckaert J.F. (editor) *Tip Timing and Tip Clearance Problems in Turbomachinery*. Lecture Series 3-2007, VKI Belgium, 2007
- [11] Witos M. (2008): *On the Modal Analysis of a Cracking Compressor Blade*. Research works of AFIT, Issue 23, pp. 21-36
- [12] Vlasov V.T., Dubov A.A. (2004): *Physical Bases of the Metal Magnetic Memory Method*. ZAO "Tisso" Publishing House, Moscow
- [13] Ding X., Li J., Li F., Pang X. (2008): *Magnetic Memory Inspection of High Pressure Manifolds*. 17th World Conference on Non-destructive Testing, 25-28 Oct 2008, Shanghai, China
- [14] Lisiecki J. (2004): *O metodzie magnetycznej pamięci materiału*. Prace Naukowe ITWL, Warszawa, Zeszyt 18, s. 51-84
- [15] Liu Q., Lin J., Chen M., Wang C., Wang G., Zhao F. Z., Geng Y., Zheng Ch. (2008): *A Study of Inspecting the Stress on Downhole Metal Casing in Oilfields with Magnetic Memory Method*. 17th World Conference on

- Nondestructive Testing, 25-28 Oct 2008, Shanghai, China
- [16] Radziszewski A. (2001): *Doświadczenia z kontroli urządzeń i ich oprzyrządowania w polskich przedsiębiorstwach z zastosowaniem metody magnetycznej pamięci metalu*. Materiały 30 KKBN, Szczyrk. Zeszyty Problemowe. Badania Nieniszczące, Nr 6 (2001), s. 165-170
- [17] Roskosz M. (2005): *Zastosowanie metody magnetycznej pamięci metalu do badań wirników sprężarek*. Problemy i innowacje w remontach energetycznych. PIRE 2005. VIII Konferencja naukowo-techniczna, Szklarska Poręba, s. 259-270.
- [18] Witoś M., Wiśnoch M. (2009): *Metoda magnetycznej pamięci metalu w diagnozowaniu techniki lotniczej*. XV Seminarium „Nieniszczące badania materiałów”, Zakopane, 10-13 marca 2009; <http://www.ndt-imb.com/portal>.
- [19] Shaniavski A.A. (2007): *Modeling of fatigue cracking of metals. Synergetics for aviation*. Publishing House of Scientific and Technical Literature “Monography”, Ufa (ros.).
- [20] Shaniavski A.A. (2003): *Tolerance Fatigue of Aircraft Components. Synergetics in engineering applications*. Publishing House of Scientific and Technical Literature “Monography”, Ufa (ros.).
- [21] Murakami Y., Nomoto T., Ueda T. (1999): *Factors Influencing the Mechanism of Super-long Fatigue Failure in Steels*. Fatigue and Fracture of Engineering Materials and Structures, Vol. 22, pp. 581-590.
- [22] Murakami Y., Takada Y., Toriyama T. (1998): *Super-long life tension-compression fatigue properties of quenched and tempered 0.46%C steel*. International Journal of Fatigue Vol. 16, pp. 661-667.
- [23] Sakai T. (2009): *Review and prospects for current studies on Very High Cycle Fatigue of metal materials for machine structural use*. Journal of Solid Mechanics and Materials Engineering, Vol. 3, No 3, pp. 425-439.
- [24] Witek L. (2009): *Experimental crack propagation analysis on the compressor blades working in high cycle fatigue condition*, [in] Fatigue of Aircraft Structures Monographic Series (editor Niepokólczycki A.), Institute of Aviation Scientific Publications, Warsaw, pp. 195-204.
- [25] <http://www.mtiinstruments.com>
- [26] www.vibrationresearch.com/software
- [27] De Silva C.W. (2007): *Vibration Damping, Control and Design*. Taylor & Francis
- [28] Witoś M. (2010): *Increasing the durability of turbine engine components through active diagnostics and control*. Research works of AFIT, Issue 29 (pol., in print).
- [29] Ostrovsky L.A., Johnson P.A. (2001): *Dynamic nonlinear elasticity in geomaterials*. Revista del Nuovo Cimento, Vol. 24, No 7, pp. 1 - 46, <http://www.lanl.gov/orgs/ees/ees11/geophysics/nonlinear/2001/nrc8730.pdf>
- [30] Buch A. (1964), Zagadnienia wytrzymałości zmęczeniowej, PWN, Warszawa.
- [31] Tae-Kyu Lee, J.W. Morris, Jr., Seungkyun Lee and J. Clarke: *Detection of fatigue damage prior to crack initiation with scanning SQUID microscopy*. Review of Progress in Quantitative Nondestructive Evaluation, Vol. 25.
- [32] Altherton D.L., Jiles D.C. (1986): *Effects of stress on magnetization*. NDT International, Vol. 19, No 1, pp. 15-19.
- [33] Birss R. R., Faunce C. A. (1971): *Stress-Induced Magnetization in Small Magnetic Fields*. Journal de Physique, Colloque C I, supplément au n° 2-3, Tome 32, Février-Mars, page C 1 – 686-688.
- [34] Robertson I.M. (1991): *Magneto-Elastic Behaviour of Steels for Naval Applications*, MRL Technical Report, MRL-TR-90-27, DSTO Materials Research Laboratory
- [35] Atherton D.L., Sudersena Rao, T., de Sa V., Schönbachler M. (1988): *Thermodynamic Correlation Tests Between Magnetostrictive and Magnetomechanical Effects in 2% Mn Pipeline Steel*. IEEE Transactions on Magnetics, Vol. 24, No 5, September, pp. 2177-2180.
- [36] Blanter M.S., Golovin I.S., Neuhäuser H., Sinning H.-R. (2007): *Internal Friction in Metallic Materials. A Handbook*. Springer-Verlag, Berlin.
- [37] Gui Y. S., Wirthmann A., Macking N., Hu C.-M. (2009): *Direct measurement of nonlinear ferromagnetic damping via the intrinsic foldover effect*. Phys. Rev. B 80, 060402(R).



Ph.D. Miroslaw WITOŚ, leader of SHM team (TTM, EMA and MMM methods) and innovation prospector, member of ESIS, DVM and GAMM. He has worked for AFIT since 1989. Work area: fatigue diagnostic, active control, expert system, transfer technology.



Major Mariusz ZIEJA gradu-ated from Military University of Technology in 2000. M.Sc. in Mechatronics spe-cialized in Aircraft Avionics. In 2008 achieved Ph.D. in Mechanical Engineering. He is engaged in development and implementation of IT systems to support aircraft maintenance, safety and reliability management.

EVALUATION OF ON-BOARD DIAGNOSTIC SYSTEMS IN CONTEMPORARY VEHICLES*

Sławomir WIERZBICKI

Faculty of Technical Sciences, University of Warmia and Mazury in Olsztyn
e-mail: slawekw@uwm.edu.pl

Summary

In line with legal regulations, contemporary vehicles have to be equipped with electronic on-board diagnostic systems that conform to EOBD requirements. Those solutions feature diagnostic monitors that support self-testing of most systems in a vehicle. Technological progress and the uniformization of vehicle solutions have enabled users to monitor the systems on-line and modify their operating characteristics with the use of system control software.

This article discusses the threats posed by the implementation of uniform systems that support communication between external devices and vehicle systems. The overviewed solutions could compromise operating safety and significantly increase engine emissions – the main criterion for evaluating the technical condition of contemporary engines.

Keywords: mechanical vehicle, mechatronic system, CAN networks, on-board diagnostics.

OCENA FUNKCJONOWANIA SYSTEMU DIAGNOSTYKI POKŁADOWEJ WSPÓLCZESNYCH POJAZDÓW SAMOCHODOWYCH

Streszczenie

Współczesne pojazdy samochodowe zgodnie z obowiązującymi przepisami obowiązkowo wyposażane są w elektroniczne systemy diagnostyki pokładowej zgodne z normą EOBD. Dzięki zastosowaniu tych rozwiązań pojawiły się nowe możliwości samodiagnostyki większości układów pojazdu poprzez monitory diagnostyczne zawarte w oprogramowaniu sterującym. Wraz z rozwojem i ujednoczeniem rozwiązań stosowanych w pojazdach pojawiły się również możliwości monitorowania on-line pracy poszczególnych układów, a także możliwości zmiany ich charakterystyk roboczych poprzez zmianę oprogramowania sterującego danym układem.

W niniejszym artykule przedstawiono zagrożenia wynikające z wprowadzenia ujednoczonych sposobów komunikacji zewnętrznych urządzeń z układami pojazdów, mogących wpływać zarówno na bezpieczeństwo eksploatacji jak i znaczny wzrost emisji spalin – główne kryterium oceny stanu technicznego współczesnych silników.

Słowa kluczowe: pojazd mechaniczny, układ mechatroniczny, sieć CAN, diagnostyka pokładowa.

1. INTRODUCTION

Contemporary vehicles are complex mechanical systems that are largely controlled by electronic (microprocessor) systems. The discussed systems, often referred to as mechatronic control systems, comprise:

- sensors which measure operating parameters (rotational speed, temperature, position) and transmit that information in the form of analog or digital electrical signals;
- controllers which process the received information based on the algorithms stored in memory and send control signals to actuators;
- actuators which analyze the received control signal to direct the activities of an actuating element, e.g. solenoid valve, servomotor or stepper motor.

In comparison with mechanical systems, electronically controlled systems deliver much greater control accuracy due to an absence of mechanical connections between measuring and actuating systems. Electronically controlled systems also analyze a greater number of control signals to produce output values. Closed-loop control systems are used to guarantee that actuating elements are controlled with a high degree of accuracy (Fig. 1) [5].

Microprocessor control in vehicles and machines creates extensive access to information processed by the controller. Such information is used to control a given system and regulate the activities of other systems. Data that are registered and processed by the controller are also used by other control systems to evaluate the technical condition of vehicle parts and generate information for the user [4, 5, 7, 8].

* The paper was supported by the Polish Ministry of Science and Higher Education as the research project no N N509 573039.

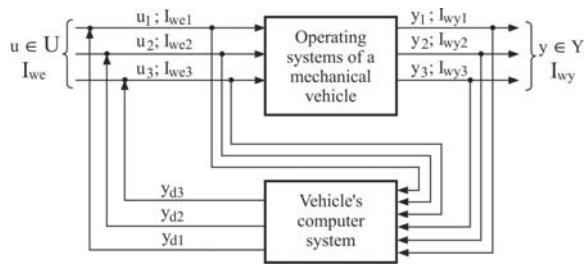


Fig. 1. System control in contemporary mechanical vehicles: $u \in U$ – set of input signals, I_{in} – input data, $y \in Y$ – set of output signals, I_{out} – output data, $y_i(I_{out})$ – task progress information, y_{di} – control signals

Contemporary vehicles are standard equipped with on-board diagnostic systems. The current market standard is EOBD (European On Board Diagnostics) which dictates the rules for communication between external diagnostic devices and vehicle controllers [4].

2. EOBD (OBD II) STANDARD

In the late 20th century, the rapid development of microprocessor controlled systems prompted the development of new standards for communication between control systems and diagnostic devices. The OBD II standard was developed in the US in 1996 to enable the use of several communication protocols between diagnostic devices and the vehicle. The European equivalent of OBD II is the EOBD (European On-Board Diagnostics) standard. It was introduced in Europe in 2000, and initially, it applied only to vehicles with petrol engines. In 2003, the standard became mandatory for diesel engines as well as vehicles powered by LPG [4, 7, 8].

The following stage of development of electronic control systems witnessed the implementation of the CAN (Controller Area Network) standard of communication with external diagnostic devices [2, 4, 8, 9]. An unquestioned advantage of the EOBD standard was that it introduced uniformity into communication with diagnostic devices as well as uniform norms for coding errors that affect the safety of vehicle users and the level of toxic pollutants released into ambient air [4]. The replacement of mechanical control systems with electronically controlled devices improved the vehicle's operating characteristics and enabled simple monitoring of basic working parameters, including operating temperature and voltage at battery terminal clamps (Fig. 2).



Fig. 2. Display window with information about engine temperature and battery voltage

Contemporary mechatronic systems rely on monitors that control the continuity of electric systems and values registered by various system components. Those solutions provide users with information about other events that affect driving safety, such as failure of the vehicle's lighting system (Fig. 3) [2, 4, 8, 9].



Fig. 3. Diagnostic message informing the user about rear lamp circuit failure

3. CONTROL SYSTEMS IN MECHANICAL VEHICLES

Microprocessor controllers are the backbone of every modern control system. The controller processes signals from sensors that measure input values, data transmitted by other systems as well as information about the outputs supplied by control and measuring devices. Based on the above data, the controller makes decisions to change working parameters.

Contemporary vehicles and machines are complex mechatronic systems which generally operate as part of a global electronic platform that monitors all electronically controlled systems in a vehicle. This solution supports dispersed control of all systems where every controller performs its functions independently and, if required, exchanges information with the controllers of other systems.

The vast majority of corporations manufacturing vehicles and machines (construction, road and farming equipment) operate their own platforms for

managing electronic control systems. Those platforms have uniform electronic system architecture which, subject to the vehicle's or machine's equipment standards, differs with regard to the number of applied modules, systems and their configurations. Most vehicles have uniform bus architecture which relies on CAN and other sub-networks. In this approach, sub-networks are often other CAN networks with different data transmission speeds, as well as other types of networks, such as LIN (Local Interconnect Network) which controls comfort and convenience applications in vehicles [2, 8, 9]. The configuration of an on-board computer system in a contemporary vehicle is illustrated in Figure 4.

A diagnostic connection port (DLC – Data Link Connector) is an important part of a vehicle's electronic bus system. In addition to diagnosing the vehicle's systems, DLC can modify the existing software if errors are detected during the operation of a given group of vehicles, and it can block selected functions (e.g. by limiting the engine's rotational speed when vehicles are transported from the manufacturing plant to the dealer's facility). In most cases, mechatronic systems have adaptive algorithms which respond to the wear of various elements and adapt the system to new requirements. Despite the obvious advantages that follow from

adapting the system to the technical condition of its constituent elements, this solution can also have negative consequences by concealing errors in the adaptation process [1, 3].

4. THREATS POSED BY ELECTRONIC CONTROL SYSTEMS

The introduction of uniform standards of communication between external devices and on-board microprocessor-based systems has created new, relatively simple options for monitoring the operation of control systems in vehicles. Selected diagnostic functions can be switched off by the on-board computer, such as DPF (Diesel Particulate Filter), a device designed to remove particulate matter from the exhaust gas of a diesel engine. When the filter is physically removed, the control unit switches the engine to emergency mode. Many service providers on the auto-motive market offer to disable the filter in the software that monitors engine operation. The above significantly increases pollutant emissions into ambient air, and the error is not recognized by the monitoring system. Other standard systems in a vehicle can be disabled in a similar manner, and the user may not even be aware of the above.

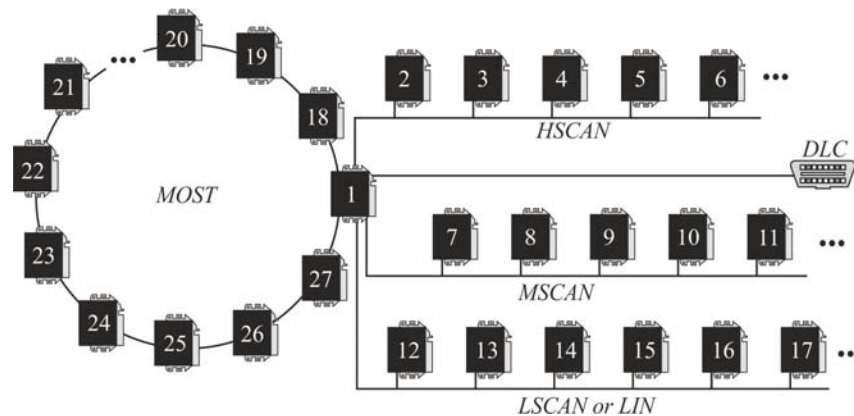


Fig. 4. Block diagram of a vehicle's network: 1 – main module/geteway, 2 – engine control module, 3 – ABS, 4 – transmission control module, 5 – yaw rate sensor which measures lateral and longitudinal acceleration, 6 – electro-hydraulic power steering, 7 – body control module, 8 – instrument panel cluster, 9 – parking assistance system module, 10 – sensing and diagnostic module for air bag control, 11 – underhood electrical center, 12 – passenger door module, 13 – sun roof module, 14 – auxiliary heating, 16 – driver door module, 17 – driver seat module, 18 – radio, 19 – CD/DVD, 20 – CD changer, 21 – phone, 22 – navigation GPS, 23 – display, 24 – tuner TV, 26 – control panel, 27 – USB port, *DLC* – Data Link Connector, *HSCAN* – High-Speed Controller Area Network, *MSCAN* – Mid-Speed Controller Area Network, *LSCAN* – Low-Speed Controller Area Network, *LIN* – Local Interconnect Network, *MOST* – network Media Oriented Systems Transport

Chiptuning is yet another popular manipulation of the engine's microprocessor controlled function. Control software is modified to change the system's working parameters, and this procedure is often performed to modify the engine's power characteristics and torque. The major systems of every vehicle, including the engine and the transmission system, operate based on fixed control algorithms, and the only differences result from changes in the value of control parameters in various memory areas. Any change of values registered in this area of controller memory modifies control values and changes the operating characteristics of the relevant system. Controller memory also features different value limiters which can be changed to boost a vehicle's performance or speed. Vehicle controllers are generally provided with tamper protection systems that rely on checksums, but tuning applications can be used to introduce the desired changes and prevent the system from spotting those modifications.

Communication interfaces and software available on the market provide users with virtually unlimited possibilities of configuring the operating parameters of their vehicles, in particular engine performance. Data describing engine performance and the correlations between engine parts are usually stored in the form of maps which are automatically identified by specialist software (Fig. 5) [6]. The data can be easily manipulated by editing a memory map or changing the values in the memory map table. The widespread availability of cheap and easy-to-use software for modifying controller operations can lead to structural damage of the vehicle and its components (Fig. 6). Alterations of the engine's control settings can also increase pollutant emissions into ambient air.

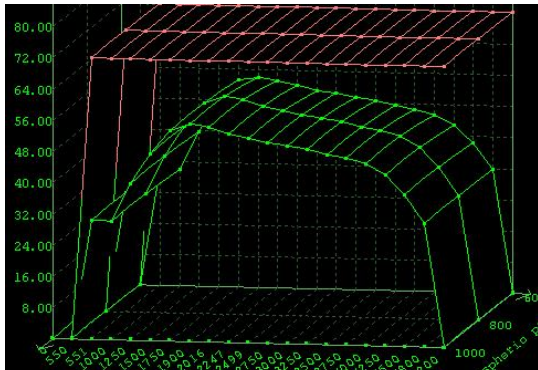


Fig. 5. A memory map stored in the controller to limit engine torque



Fig. 6. A piston damaged (burnt out) by an incorrect modification of the engine's control software

Some car workshops modify engine control software to "repair" errors that are reported during vehicle operation. This practice is popularly applied to fix a common error in older cars with diesel engines. Many users find that a warm diesel engine is difficult to start, whereas no such problems are reported when the engine is cold. The above results from the wear of the starter (high internal resistance) or low battery voltage. In diesel engines, the injected fuel dose is determined based on a memory map stored in controller memory (Table 1). As shown in Table 1, at engine temperatures higher than 20°C and rotational speed below 200 rpm, the required fuel dose is 0. Therefore, the engine cannot be started if the required rotational speed is not achieved. The presented data indicate that for an engine to be started at higher temperatures, higher rotational speed is initially required, which is difficult to achieve with a damaged starter. When the values in the marked area of the memory map are modified, fuel can be injected at lower rotational speed, thus facilitating engine start-up.

Table 1
Memory map describing the fuel injection dose subject to the engine's temperature and rotational speed

		Engine temperature [°C]								
		-30	-10	0	15	20	40	70	85	100
engine speed [rpm]	0	49	45	33	0	0	0	0	0	0
	200	49	45	33	29	0	0	0	0	0
	250	49	45	33	29	27	21	0	0	0
	280	49	45	33	29	27	24	22	21	19
	756	49	44	33	29	27	24	22	21	19
	1008	48	43	32	27	25	24	22	21	19
	1260	44	39	29	23	22	23	17	16	19
	1554	41	36	22	18	16	19	10	9	6

It should be noted that the described relationship contradicts the general rule for combustion engines. Mechanically controlled engines are always easier to start when warm. Therefore, the introduction of electronic control systems could lead to an incorrect diagnosis of errors when the condition-symptom method is used.

The characteristics of an electronically controlled system can also be changed by modifying sensor parameters. As a result of the above, the control system is "fooled" by falsified input settings. System modification leads to changes in output values and, consequently, working parameters.

System parameters can also be changed with the use of tuning boxes which are ready-made solutions available on the market. When connected to the control system, they can boost engine power (PowerBox) or lower fuel consumption (Ecobox). In older-generation systems, the signal transmitted to the controller was reinforced or weakened relative to the signal emitted by the sensor. In advanced control systems, when the set range of signal values is exceeded, the system operates outside of the programmed range, and the error is detected by diagnostic monitors of the respective system. The latest tuning boxes are programmable, and the signal produced based on the sensor-generated signal can be freely modified. The characteristics of a programmable box is presented in Figure 7. The use of a box with similar characteristics eliminates the danger that extreme signal values will be exceeded. The introduced changes cannot be easily identified by the control system, and they can modify operating parameters at average load values. Fuel pressure is increased when a box component is inserted in a common rail engine between the fuel pressure regulator in the fuel rail and the controller. At constant injection pulse values, increased fuel system pressure results in higher engine power.

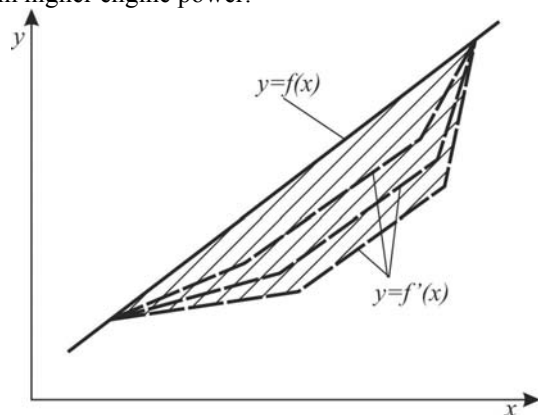


Fig. 7. Characteristics of a programmable box: $y=f(x)$ – original characteristics of signal y relative to parameter x , $y=f'(x)$ – programmable functions, shaded area is the programmable area of changes

5. CONCLUSIONS

Contemporary vehicle control systems feature advanced on-board diagnostic capabilities that monitor the functioning of the vehicle's major systems. Following the standardization of control systems and protocols for communication with external devices, those systems can be easily modified or even deactivated. The resulting changes may not be identified by on-board or external diagnostic systems. Under current law, most manipulations of control system settings cannot be detected during periodic vehicle inspections.

Changes in the operation of car systems may be difficult to identify because they require comprehensive tests covering the entire vehicle. The latest tuning solutions can both activate and deactivate a vehicle's control systems with the use of a remote control unit. Selected solutions feature engine control systems with two independent control algorithms for economy and high-speed driving. In many cases, only one engine control program is modified, which makes it even more difficult to identify the changes.

The solutions for modifying mechatronic systems are increasingly advanced, and workshops performing periodic car inspections are practically unable to diagnose the introduced alterations. According to the suppliers, tune-up applications that modify vehicle and engine operating parameters can be easily installed even in brand-new cars without the danger of voiding the manufacturer's warranty, provided that the device is removed prior to a visit in the dealer's service station.

LITERATURA

1. DĄBROWSKI Z., MADEJ H.: *Masking mechanical damages in the modern control systems of combustion engines*. Journal of KONES Powertrain and Transport. Vol. 13. No. 3/2006.
2. FREI M.: *Samochodowe magistrale danych w praktyce warsztatowej*. WKŁ, Warszawa, 2011.
3. MADEJ H.: *Diagnozowanie uszkodzeń mechanicznych w silnikach spalinowych maskowanych przez elektroniczne urządzenia sterujące*. ITE, Radom 2009.
4. MERKISZ J., MAZUREK S.: *Pokładowe systemy diagnostyczne pojazdów samochodowych*. WKŁ, Warszawa, 2007.
5. NIZIŃSKI S., WIERZBICKI S.: *Zintegrowany system informatyczny sterowania pojazdów*. Diagnostyka, nr 30 t.2/2004. s. 47–52.
6. PRAJWOWSKI K.: *Possibilities of changes of parameters of the dryer to engine Fiat 1.3 JTD*

- performances*. Journal of KONES Powertrain and Transport. Vol. 18. No. 4/2011, s. 389-396.
7. ROKOSCH U.: *Układy oczyszczania spalin i pokładowe systemy diagnostyczne samochodów OBD*. WKŁ, Warszawa 2006.
 8. ŚMIEJA M., PIĘTAK A., IMIOLEK M., WIERZBICKI S.: *Wykorzystanie sieci komunikacyjnych w aspekcie rozwoju nowoczesnych systemów diagnostycznych pojazdów mechanicznych*. Biuletyn Wojskowej Akademii Technicznej. Warszawa, vol. 1(661)/2011. s. 231-242.
 9. ZIMMERMANN W, SCHMIDGALL R.: *Magistrale danych w pojazdach. Protokoły i standardy*. WKiŁ, Warszawa 2008.



Dr inż. **Sławomir WIERZBICKI** –

pracuje obecnie na stanowisku adiunkta w Katedrze Mechatroniki, UWM w Olsztynie.

W pracy zajmuje się zagadnieniami zasilania współczesnych silników spalinowych o zapłonie samoczynnym oraz systemami elektronicznymi nadzorującymi eksploatację i diagnostykę pojazdów i maszyn roboczych. Jest autorem kilkunastu publikacji z tych zagadnień.

Jest członkiem Polskiego Towarzystwa Diagnostyki Technicznej, Polskiego Towarzystwa Naukowego Silników Spalinowych oraz Polskiego Naukowo-Technicznego Towarzystwa Eksploatacji. Od 2004 roku pełni funkcję sekretarza czasopisma „Diagnostyka”.

DIAGNOSTICS GAS TURBINE ROTORS IN NON STATIONARY STATES

Andrzej GRZĄDZIELA

Wydział mechaniczno – Elektryczny, Akademia Marynarki Wojennej
Ul. Śmidowicza 69, 81-103 Gdynia, Fax. 058 626 26 48, e-mail: a_grzadziena@amw.gdynia.pl

Summary

Vibration tests of marine gas turbine engines are performed as research of on-line and off-line types. On-line Systems generally monitored one or two vibration symptoms, which assess the limited and/or the critical values of parameters and they, potentially, can warn and/or shutdown engines. Off-line Systems are usually used for vibration analysis during non-steady state of work. The paper presents comparison of different methods of analysis of vibration symptoms measured under run-up and shut-down processes of marine gas turbine engines. Results of tests were recorded on gas turbine engine DR76 type of the COGAG type propulsion system. Main goal of the research was qualified on helpfulness and unambiguous result, from synchronous measurement, order tracking and auto tracking. All vibration symptoms were chosen from the methodology of the diagnosing gas turbine engines operated in the Polish Navy, called Base Diagnosing System. Second purpose of the paper was the estimation of the possibility of usage those analysis methods of gas turbine engines for on-line monitoring systems.

Keywords: dynamics, gas turbines, rotor vibration, run-up and shutdown processes

DIAGNOZOWANIE UKŁADÓW WIRNIKOWYCH SILNIKÓW TURBINOWYCH W STANACH NIEUSTALONYCH

Streszczenie

Badania drganiowe okrętowych turbinowych silników spalinowych są realizowane według procedur typu on-line i off-line. Systemy monitorują najczęściej jeden lub dwa parametry drganiowe, których przekroczenie skutkuje wywołaniem sygnałów alarmowych lub zatrzymaniem silnika. Systemy off-line są zwykle dedykowane dla analiz w stanach nieustalonych. Referat przedstawia porównanie różnych metod diagnozowania realizowanych podczas procesu rozruchu oraz wybiegu silnika turbinowego. Wyniki badań są efektem testów na silnikach DR 76 użytkowanych w kombinowanym układzie napędowym COGAG. Podstawowym celem badań była ocena przydatności metod pomiaru i analizy z wykorzystaniem synchronizmu sygnałów, śledzenia rzędów i autośledzenia. Kolejnym celem badań była ocena możliwości zastosowania proponowanych metod w badaniach typu on-line.

Słowa kluczowe: dynamika, drgania wirnika, proces rozruchu i wybiegu

1. INTRODUCTION

Exploitation of marine propulsion systems is a complex issue due to the specific characteristics of the marine environment and the need to maintain a high level of readiness for service and reliability of ships. The use of diagnostic procedures off-line or on-line allows you to use them according to their current condition. This is particularly important in the case of turbine engine, hourly plan and annual plan of technical services is the main usage criteria. This strategy of exploitation makes scheduling maintenance, logistics and security simpler and easier to implement, but also contributes to a significant increase in costs due to the need for replacement of components (often more technically efficient). Furthermore, operating such a exploitation policy makes it impossible for the early detection of

other primary causes of faults that occur between appointing terminals.

Diagnostics of gas turbine engines includes a wide range of parameters, controls and maintenance procedures [1]. One of them is the control of unacceptable balance of rotors. Identification of different unbalanced states, determining its value and the accurate placements of corrective masses is commonly known. Such procedures are carried out on Polish ships for over 20 years. Prepared and used test equipment ensures the implementation of diagnostic tests on four types of turbine engines in service. In the case of naval propulsion diagnostic procedures these are limited for several reasons. The most important of these is the need to maintain a constant readiness to start the engine, associated with the tactical requirements. In addition, due to the fact that the engines are foreign

construction, there is a lack of information on the structural parameters of the engine, reducing warranty, no spare parts readily available, etc. The use of vibration diagnostics, makes the use of the engine more rational; from a technical point of view, especially towards vitality of service, which in effect will not withdraw, even a technically efficient ship, from service. Measurements and analysis of vibration parameters of marine gas turbine engines can be divided into:

- off-line (measurements performed in free-run mode, periodically);
- an on-line (real-time monitoring).

Both methods have their advantages and disadvantages. Off-line Systems are usually offered as a very simple analyzers - data collectors. Measurement path is determined in the collector interface, with preset measuring settings, so that the measurement could be performed by an average technical staff, whose main task is a precise procedure. The analysis of measurement results is carried out off the ship, sending the results to the coast laboratory. Currently, there is not many off-line data collectors, who would engage in that precise diagnostic evaluation. The main advantage of such devices is their price. It should be emphasized that the data collectors are useful mainly to assess the go-state of vibrations of turbine engines.

On-line diagnosis of vibrations provides continuous surveillance of the technical condition of gas turbine engines, including registration, analysis, forecasting and alarming. It allows you to recognize the basic signs of changes in the technical condition with the possibility of analyzing the trend of selected symptoms. On-line vibration systems usually work as part of a complex and symptomatic diagnosis of marine propulsion systems. Proper diagnosis of such structures, for example, turbine engine, depends on various issues, including how the measurement and processing of vibration signals was taken. Important in the further analysis is the fact that internal combustion engines in gas turbine propulsion ships do not run at a constant speed with compressor and turbine rotors.

This is the main reason for synchronizing the processing of selected displacements (of the signals) i.e. the rotational frequency of one or both of the engine rotors [2,3]. This method allows you to identify the most common groups of rotor systems, which allows you to identify their failure. Damages to operating gas turbine engines can be categorized as follows:

- damage or crushing of first-stage compressors' blades or power turbine blades (rare);
- the appearance of unbalance, originating from heating or salinity;
- cracks sealing systems and leakage of lubricating oil to the inside of the drum rotor;
- lack of alignment between the gas-dynamic gas generator and power turbine;

- thermal damage to the combustion chambers – torsion of power turbine rotor;
- damage to the auxiliary engine mechanism.

Some failures can be resolved in the recorded spectra as a change in vibration frequency of rotating engine components, hence the introduction of a synchronous sampling of the transient engine operation, e.g. in the boot process or in the run.

The occurrence of non-stationary effects, typical for residual unbalance may be due to small, incremental damage whose symptoms may be poorly recognized in the early stages of development. The results of the identification of such phenomena is exemplified in the article comparing the various methods of synchronous signal processing method such as PLD or Order Tracking [7]. The presented method for identification of defects can be introduced into the turbine engine monitoring systems as a tool for early identification of unbalance.

2. THE AIM AND TEST METHODS

Monitoring of vibration signals from rotating machinery is a well-known diagnostic procedure, known throughout the world [2,5,7]. Most of rotating machinery and marine gas turbine combustion engines are designed as a supercritical machines, hence, in steady states, are diagnostically limited. Therefore it was decided to analyze the dynamics of rotors of gas turbine engines, using a method of off-line measurements of the unknown states. It was expected that the results would yield information on the following areas: unbalance of rotors, lack of concentricity of the rotors, changes in their vibration frequency and changes in the speed of rotor system critical.

Marine gas turbine combustion engines mounted on a DR76 type of propulsion system for ships COGAG class Tarantula Polish Navy were studied using this method. Longitudinal cross section of rotor system is shown in Figure 1.

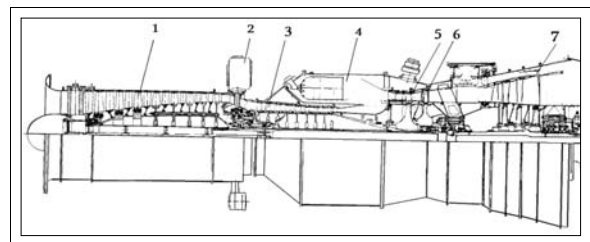


Fig. 1. Cross section of a gas turbine engine system of the type DR76 (1 - low-pressure compressor (LPC), 2 - drives, 3 - high-pressure compressor (HPC), 4 - combustion chamber, 5 - high pressure turbine (HPT), 6 - low-pressure turbine (LPT), 7 - power turbine (PT))

The study included analysis of the vibration parameters during start-up and run of rotors. Comparison of the results of modeling of dynamic

loads using FEM (Final Elements Methods) and measurements of on the real object makes it possible to take correct decisions and give the proper diagnosis.

3. MODEL OF THE UNBALANCED ROTOR

Application of computer simulation to diagnose the condition of turbine engine rotors should be used already during the process of calculation and design, which it is currently implemented. The problem begins when the manufacturer does not provide this kind of know-how in the technical specification for the user. Such a situation arises in the case of exported warships equipped with turbine engines. While placing the engine, rotating parts are assembled with great care. Main objective is to reduce unbalance in rotors. But even the best procedures are not able to prevent factors, such as the inadequacy of heat treatment or the difference of thermal expansion of materials which may cause slight unbalance in rotor, mentioned as residual. Problems in the dynamics of Marine Gas Turbine Engines (MGTE) are associated with the following elements of the engine: rotors, bearings, bearing brackets (bearing struts), engine block, the type of construction, the terms of hydro-meteorological and during sea trials and the aerodynamic parameters inside the engine. Proper and stable work of MGTE engine is mainly connected with these parameters. Loss of energy in rotating machinery is manifested in the form of loss of torque, a decrease in rotor speed, exhaust temperature increase or intensity in vibrations. Vibration energy dissipation is related to: unbalancing of rotors, oversize tolerated shaft misalignment, abrade of blade tips with the inner roller, wear of axis and radial bearings, asymmetry of elasticity and damping asymmetry of the rotor and the gas-dynamic processes anomaly. Emission of vibration yields a lot of information, including the ability to diagnose the technical condition of rotors. Vibration measurement, identification, classification, mathematical analysis, including the use of trend function, give information on the actual technical state and allow the prediction of the wear process in the future.

In the identification an important factor is to compare the results of modeling with the results of the measurements. Each rigid body has six degrees of freedom, whereas the deformable objects have an unlimited number of degrees of freedom. Rotating machinery such as MGTE have a number of degrees of freedom equal to the sum of all degrees of free parts of the engine, minus the number of rigid nodes connecting these elements. Each part of the engine can be described by physical characteristics such as stiffness and damping, obtained from vibration measurements the actual object or model or the modeling of the geometry and properties of materials (the use of rigidly connected structures). The use of a certain type of rigid object model

allows the use of the motion ordinary differential equations. Deformable objects require the use of partial differential equations. This second assumption is much more complicated, but can help to achieve to the actual object, especially when it's in a wide range of engine speeds. This was the reason for the choice of the second type of model turbine engine. Diagram of diagnosis using the MGTE model shown in Figure 2.

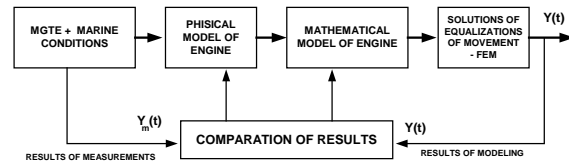


Fig. 2. Scheme of diagnostics model MGTE

Residual unbalance may appear in all sections of the rotor, however, two vectors of unbalance, at both ends of the shaft, may represent the replacement model. These vectors vary in values and phase shifts. Such an FE model allows for dynamic response to unbalance which in effect allows you to compare modeling results with the reports of vibration measurement. The most sensitive point in the unbalance of GT rotor, with respect to vibrations, is the measuring point on the front of the generator exhaust bracket bearing the vertical direction. This is the effect of the minimum thermal expansion of the rigid support used for measurement of radial vibrations at this point. The model is linear so it is clear that response is directly proportional to the value of unbalance. The rotor is loaded dynamically and statically from various sources [4]. Identification of the sources and their calculations of the loads were a major problem during the modeling and evaluation of the actual object's vibration. Damage in the objects such as blades, have an impact on changes in the moments of inertia of rotating parts. This results in a shift of the main axis of inertia, which is not parallel to the axis of rotation. It is the main source of unbalance in the form of vibrations of rotor. Implementation of the mathematical model is difficult, mainly due to the problems of determining the stiffness and damping of supports and bearings at different temperatures - Figure 3.

Shape of the axis deflection is defined as discrete sets:

- Set of static deflections – u_s ;
- Set of dynamic deflections – u_d .

Both sets depend on actual technical state of rotor and geometry, which can change through cracks and wanes of engine parts.

$$\mathbf{u}(\omega t) = \mathbf{u}_s + \mathbf{u}_d(\omega t) \quad (1)$$

This equation is a discrete set of points of axis movement of the rotor. Taking into account the damping and stiffness of the support bearings, we

can demand that they are functions of temporary positions, namely:

$$k_{ik} = f(u) \quad c_{ik} = f(u) \quad (2)$$

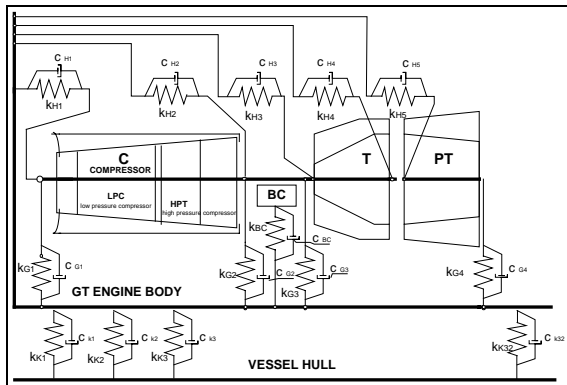


Fig. 3. Axi – symmetric lumped mass inertia model of the MGTE, where: LPC – low pressure compressor, HPT – high pressure compressor, T – turbines (low & high pressure), PT – power turbine, BC – burning chambers, k – stiffness, c – dumping.

For the simplification it is assumed that, for a constant speed, these values are constant. Using FEM modeling can provide a three-dimensional discrete model. Rotors MGTE, in the circular symmetry, have been described by one-dimensional, two-beam bar having a symmetrical six degrees of freedom. All parts of the model have geometric and physical properties of the elements. Discrete model of traffic parameters have been obtained by solving the equation:

$$\mathbf{K}\mathbf{u} + \mathbf{C}\dot{\mathbf{u}} + \mathbf{M}\ddot{\mathbf{u}} = \mathbf{F}(t) \quad (3)$$

where: \mathbf{K} – matrix of structure's stiffness

\mathbf{C} – matrix of structure's damping

\mathbf{M} – matrix of structure's inertia

\mathbf{F} – vector of forces

$\mathbf{u}, \dot{\mathbf{u}}, \ddot{\mathbf{u}}$ – displacement and their

derivatives

(velocity and acceleration)

This can be solved as a linear problem, but in MGTE rotor must allow for changes in stiffness and damping, which are functions of motion parameters. In this case equation (3) should be expressed as:

$$\mathbf{K}(\mathbf{u}, \dot{\mathbf{u}})\mathbf{u} + \mathbf{C}(\mathbf{u}, \dot{\mathbf{u}})\dot{\mathbf{u}} + \mathbf{M}\ddot{\mathbf{u}} = \mathbf{F}(t) \quad (4)$$

Equation (4) indicates that the rotor motion should be described as a nonlinear dynamic problem, and therefore should expect more than one harmonic in both measured and modeled spectrum [8].

4. NON – STEADY STATES VIBRATION SIGNALS ANALYSIS

To obtain the measurements of the real object Bruel & Kjaer 3560B analyzer was used. Namely, it was used during the collection and processing of measurement data using the PULSE(v.12). Two transducers (accelerometers ICP) have been fitted to the steel girders, situated on the flanges, on the front and on central pillar of the LPC. The fixing cantilevers are characterized by vibration resonance frequency value differing from harmonic frequencies due to rotation speed of the given rotors. Measurements were made perpendicular to the axis of rotation of the rotor. Such a choice was made on the basis of theoretical analysis of unbalance and as a result of analysis of the results of preliminary research on the subject.

Common assessment of the unbalance of rotors was developed through the concept of dimensionless coefficients of diagnosis. Using theoretical analysis of dynamic interactions, as well as using the results of initial diagnostic tests, the following symptoms were selected as the most sensitive to changes in balancing rotors [2]:

- First harmonic of amplitude of the corresponding velocity of the rotor,
- Second harmonic of amplitude of the corresponding velocity of the rotor,
- S 1 - the ratio of the average amplitude of vibration corresponding rotor speed (and harmonic) and the second harmonic of the corresponding rotor,
- S 2 ratio of the average amplitude of vibration corresponding rotor speed (and harmonics) corresponding and the third harmonic of the rotor.

These symptoms can confirm the theoretical assumption of nonlinear rotor dynamics.

5. VIBRATION ANALYSIS OF THE RUN-UP PROCESS

The first test was to analyze the process of starting the engine. The characteristic changes in LPC rotor speed is shown in Figure 4. Synchronous signal measured by a tachometer connected with the auxiliary drive gear box where the transmission ratio averaged on $i=0,125$, so the LPC rotor was 8 times greater (in speed) than that shown in Figure 4. The main objective of the analysis of synchronous oscillations in the boot process was to determine the dynamics of the disorder. The impact of "other" signals is shown in Figure 5.

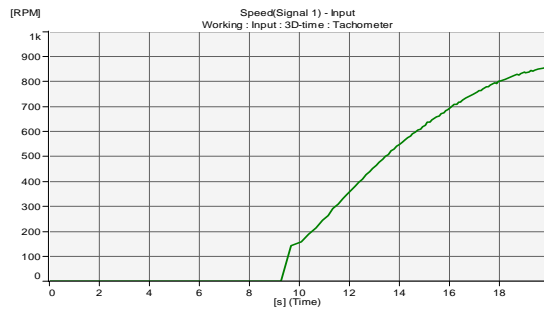


Fig. 4: Rotors LPC rotational speed characteristics during run-up process

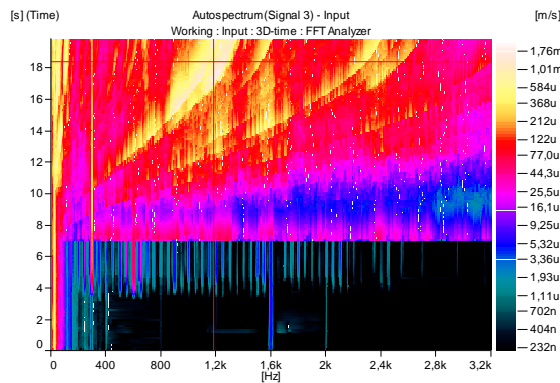


Fig. 5. Synchronous spectra of the velocity of vibration during run-up process with using the band – pass filter of 0,1Hz – 3,2 kHz range

The boot process started at the point $t=7$ seconds (see Figure 5), so all recorded vibration signals recorded from the start point contained the signals coming from other sources, i.e. non-rotating motor or frequency of its vibrations or a combination thereof. This allows to identify the main "other" signals, such as: $f_1 = 305$ Hz, $f_2 = 600$ Hz, $f_3 = 1.6$ kHz, and $f_4 = 2$ kHz, which are associated with sources outside the engine. The highest signal during the boot process is the rotor speed and harmonic vibrations, but in Figure 5 it is not clearly visible due to the lack of a synchronous signal tracking.

6. VIBRATION ANALYSIS OF THE SHUT-DOWN PROCESS

Next test was associated with the analysis of vibration parameters and related to the process runs the motor rotor. Figure 6 shows autospectrum of the velocity measured over the middle LPC bearing using the order tracking procedure. Changes of parameters are presented in the domain of time function, in contrast to the boot process, where the dominant energy range of vibration signal was 1/2 harmonic - seen as a 4th order. The pressure drop of the lubricating oil in the bearing caused an increase in values ranging from displacement and slope between the HPC and LPC rotor (rotating shafts each other, while the shaft rotates within the LPC HPC shaft - see Figure 1) and the typical dominance of the subharmonics.

The increase in stiffness of the bearing system confirms the existence of the harmonic "right-hand branches" at the point where t (time) is equal to 4 seconds for the following rows: 4, 8 and 12, which is associated with a pressure drop of lubricating oil in the bearings.

Analysis of the dynamics of the turbine engine rotor in transient states of a system PULSE should be applied in both processes, ie start-up and run. The start-up process helpsto recognize the "other" signals, but the definition of dynamic functions is very difficult due to the significant acceleration of the rotors. Identifying characteristics of rotor system dynamics is much more recognizable in the process runs through the analysis of orders - Figure 7 and 8.

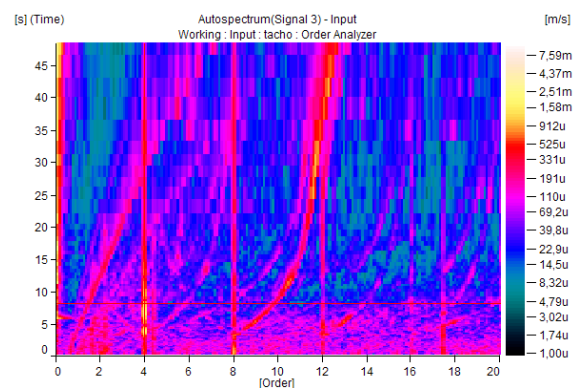


Fig. 6. Autospectrum of velocity of vibration in the shut-down process with the use of order tracking procedure, in the domain of time function

Analysis of the first harmonic (8th order) allows to observe changes in dynamics as trends. Application of the rotational speed function as a field of analysis is the most important factor in the study of the use of the Order Tracking procedure. This allows you to detect changes in the natural frequency, ignoring interference from the signals originating from the thermodynamics processes of turbine engines.

Subharmonics signal analysis is very useful in the diagnosis of rotating machinery. Autospectrum of 1 / 2 subharmonic's velocity range (considered in the LPC rotor) indicates the individual characteristics of particular rotors. The nature of changes in order values in the rotor speed can be thought of as an individual fingerprint of each rotor.

All changes to the technical condition of rotor system, such as changes in stiffness and damping parameters of alignment, or unbalance result in changes in characteristics of subharmonics - Figures 7 and 8.

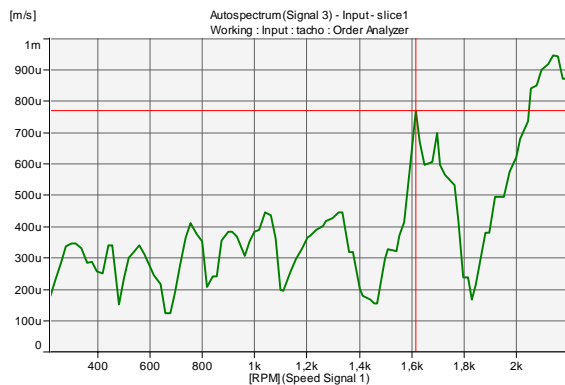


Figure 7. Autospectrum of 8 order (I harmonic) of velocity of vibration in the shut-down process of LPC rotor stoppage

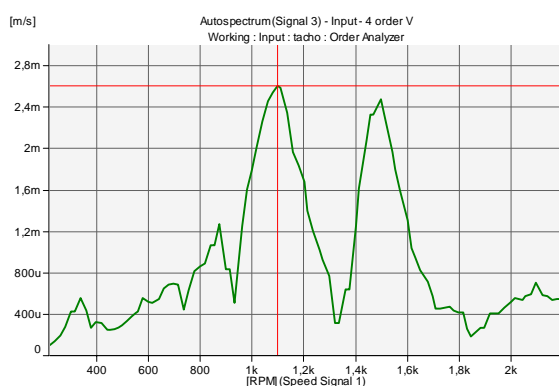


Fig. 8. Autospectrum of 4 order (subharmonic) of velocity of vibration in the shut-down process of LPC rotor stoppage

7. CONCLUSIONS

All statistical analysis performed on the available population of engines clearly show that the selected parameters analyzed in the non-stationary processes are the basis for predicting changes in the technical condition of rotor system. Implementation of this research turns out to be a credible verification of the technology. Conclusions presented below have been incorporated into operational diagnostics of marine gas turbine engines:

- Synchronous measurement of vibration signals during the boot and run processes enables us to recognize symptoms of damage, including the formation of resonance and changes in natural frequencies and unbalanced rotors
- symptoms of S1 and S2 do not have sufficient sensitivity for use in transient states due to the instability of the processes and the need for averaging the results,
- application of auto tracking and monitoring the turbine engine rotor systems can identify a wide range of typical damages, confirmed by the vibroacoustic diagnostics.

Application of the proposed methods of analysis allows for the rational management of engine life time even in the developed processes of consumption. The analysis of test results obtained gives the following conclusions:

- the approach to the assess the technical condition of gas turbine engines rotor system allows to quickly detect changes in the permitted unbalance and the maintained database enables easier identification of the studied group of engines
- studies on trends in chosen parameters make it possible to reliably detect changes in the value of sensitive operational parameters during the operation of the engine and to evaluate its capabilities.

REFERENCES

- [1] Charchalis A. Grzadzila A: Diagnosing of naval gas turbine rotors with the use of vibroacoustic parameters. The 2001 International Congress and Exhibition on Noise Control Engineering. The Hague, The Netherands 2001, pp. 268
- [2] Downham E., Woods R.: The rationale of monitoring vibration on rotating machinery, ASME Vibration Conference, Paper 71 - Vib - 96, Sept. 8 - 10, 1971
- [3] Grzadzila A.: Vibroacoustic method of shafting coaxiality assessment of COGAG propulsion system of a vessel, „Polish Maritime Researches”, 1999, No 3, pp. 29–30.
- [4] Grzadzila A: Diagnosing of naval gas turbine rotors with the use of vibroacoustics parameters, „Polish Maritime Researches”, 2000, No 3, Gdańsk 2000, pp. 14–17.
- [5] Grzadzila A.: Vibration analysis of unbalancing of marine gas turbines rotors, „Mechanika”, 2004, t. 23, z. 2, pp. 187–194.
- [6] Pedersen T. F., Gade S., Harlufsen H., Konstantin-Hansen H.: Order tracking in Vibroacoustic Measurements: A Novel Approach Eliminating the Tacho Probe, „Technical Review”, 2006, No 1, Brüel & Kjær, pp. 15–28.
- [7] Krzyworzeka P., Adamczyk J., Cioch W., Jamro E.: Monitoring of nonstationary states in rotation machinery, Biblioteka Problemów Eksploatacji, Wydawnictwo ITeE, Radom 2007.
- [8] Rządowski R.: Dynamics of steam and gas turbines, IFFM Publishers, Gdańsk, 2009.



Andrzej GRZĄDZIELA, Ph. D is a Dean of the Mechanical Electrical Faculty of the Polish Naval Academy. Vibroacoustics, technical diagnostics and ships propulsion construction are his professional area. He is a V-ce President of the Polish Association of the Technical Diagnostics.

SELECTION OF MEASURING EQUIPMENT IN ASSEMBLY PROCESS - ANALYSIS OF SELECTED ELEMENTS

Eliza JARYSZ-KAMIŃSKA

West Pomeranian University of Technology, Szczecin, Institute of Manufacturing Engineering,
Al. Piastów 19, 71-310 Szczecin, ejarysz@zut.edu.pl

Summary

The paper presents function of selection of measuring equipment - *DWP* function. Analysis of the individual elements of described the function can be used for isolation the most important measurement components of the selection of measuring equipment for selected measurement processes. The paper shows one chosen element of function of selection of measuring equipment – metrological characteristics. Those characteristics are shown on the example of chosen measuring equipment which is used in the alignment deviation measurements carried out during the assembly of elements of the ships propulsion system.

Keywords: measuring equipment, metrological characteristics, ships propulsion system.

DOBÓR WYPOSAŻENIA POMIAROWEGO W PROCESACH MONTAŻOWYCH - ANALIZA WYBRANYCH ELEMENTÓW

Streszczenie

W artykule przedstawiono funkcję doboru wyposażenia pomiarowego - funkcja *DWP*. Analiza poszczególnych elementów przedstawionej funkcji może służyć wyodrębnieniu najistotniejszych składników doboru wyposażenia pomiarowego dla wybranych zadań pomiarowych. W artykule zobrazowano jeden z elementów funkcji doboru wyposażenia pomiarowego - właściwości metrologiczne. Charakterystyki te przedstawiono na przykładzie wyposażenia pomiarowego wykorzystywanego w trakcie pomiarów odchyłki współosiowości realizowanych w trakcie montażu elementów okrętowego układu napędowego.

Słowa kluczowe: wyposażenie pomiarowe, właściwości metrologiczne, okrętowy układ napędowy.

1. INTRODUCTION

The selection of measuring equipment includes in its scope activities both associated with choosing the method of realization of measurement process and also the need to define the characteristics of the required equipment to assemble the ships propulsion system.

Appropriate analysis of criteria gives the opportunity to select the measuring equipment which may allow to provide the service of measurement and gives the results of measurement with required accuracy and reliability. Measuring equipment which is used affects the quality of the entire production process and thereby on competitiveness and customer confidence to the company.

2. CRITERIA OF THE SELECTION OF MEASURING INSTRUMENTS

In all types of measurements the proper selection of measuring instruments plays an important role. The selection is decided by the

criteria for both technical and metrological, which are linked to the characteristics of measuring instruments and devices. The analysis of subsequent criteria of selection of measuring equipment allows to distinguish from many measuring equipment those which are the best for the realized measurement process.

In mechanical engineering criteria for rational selection of measuring instrument are [1]:

- kind of measured dimension,
- means of determining and fixing the measured item,
- means to receive information about the measurand,
- the possibility to develop a performance result of a measurement,
- the possibility of a direct transfer the measurement's results to the data analysis system,
- value of a measurand,
- optimal uncertainty of measurement.

When selection the measuring instruments is taken into account the required accuracy of the product, batch size, degree of mechanization and

automatization, measurement and economic characteristics of the measuring tool must be kept in mind. The following elements are required to determine [2]:

- accuracy class of the product based on the tolerances specified in the standards or technical conditions,
- precision of measuring equipment necessary to make a product within the specified tolerances,
- the type and accuracy of measuring equipment used in process of control tools as well as direct control of the product,
- mean of connection control tools with state's etalons.

Other significant factors influencing the choice of the same technical equipment proposals are general factors, such as [3], [4]:

- availability of additional equipment,
- compatibility,
- ease of service and preparation of work,
- safety,
- technical maturity,
- exploitation development.

3. SELECTION OF MEASURING EQUIPMENT

Selection of measuring equipment for the measurement process and the selection of its properties in accordance with the requirements is provided through a well-organized measurement management system. The scope of this system, which can differentiate the supervision of measuring equipment can be divided into three phases [5], [6]:

1. Planning, in which needs are defined in terms of access, the use of measurement systems, requirements, properties, time and place and quantity of the necessary equipment, and with this range of purchases and the necessary training. Information necessary for planning are derived from all areas of production.
2. The management of measuring equipment, which includes the disposition and management of data related to the equipment, evaluation and data analysis of metrological confirmation system, as well as documenting the activities of its control.
3. Control of the characteristics include an evaluation of purchased equipment and systematic monitoring of its metrological characteristics. The scope of these activities is checking equipment purchased or repaired for fulfilling the established requirements.

The issue of selection of the measuring equipment can be presented in general form as function. It illustrates how many factors affect the choice of measuring equipment.

$$DWP = f[(W_1...W_i), (U_1...U_j), (S_1...S_k), (P_1...P_l), (C_1...C_m), (K_1...K_n), (K_{j_1}...K_{j_o}), (Z_1...Z_p), (I_1...I_r)] \quad (1)$$

where:

- DWP – (pol. Dobór Wyposażenia Pomiarowego) selection of measuring equipment,
- W - metrological characteristics of measuring instruments such as the accuracy of the measuring range,
- U - functional characteristics of measuring equipment such as ease of use, reliability, durability, maintainability,
- S - characteristics of equipment and measurement systems and software for analyzing the results (uncertainty, reproducibility, repeatability),
- P - structural characteristics of the propulsion system (technical specifications, dimensions, specify the test section and areas of measurement process),
- C – labour consumption,
- K - the cost of measurement, including direct measurement of total costs and maintenance costs of the equipment,
- K_j - the cost of quality: the cost of providing and quality assessment,
- Z - personnel management (training, motivation, experience, skills),
- I - Infrastructure - buildings, facilities, handling equipment.

The presented function does not deplete the possibilities of the analyzed criteria in the selection process of measuring equipment. Factors which occur in formula (1) are components of both technical and economical. In this case, the determination of optimal ratios which are the best in a specific sense of the processes is very difficult. These indicators can be both described as number and descriptive, can be presented both quantitatively and qualitatively. This makes it impossible to make an exact mathematical notation of *DWP* function and thereby to achieve the value of measurand of the function (1), which is the criteria of its optimality.

4. ANALYSIS OF THE SELECTION OF MEASURING EQUIPMENT DURING THE ASSEMBLY OF SHIPS PROPULSION SYSTEM

When analyzing the selection of measuring equipment in every industry it should be aware that if there is a need to purchase equipment, particular attention should be paid to the selection of an appropriate manufacturing process of measuring equipment. The prevailing factor here is - the question of functionality and versatility of measurement tools. It is necessary to plan the use of tools on the basis of realized technological processes. Consideration should be given to the knowledge of the exploitation of ships propulsion system during normal operation, the types of couplings and examine the foundations and connections, mounting screws and other working conditions. (1)

The next step is the cost analysis, which will determine the rationality of taking expenses. Depending on the adopted selection criteria the decision taken must be economically justified. The number of objects on which these measurements will be carried out depends on the form of business. Purchase of expensive equipment would not be profitable for the production of small series of large units, where there is a significant time-consuming process, while the cost of purchase for repairs purpose will be recovered in a short time, due to the large number of watercrafts using the services of a repair shipyard.

A selection of measuring equipment, its characteristics, range, accuracy, durability in the conditions of production, the analysis of quantity and place where the equipment is placed is essential for the well-functioning management systems. These elements support the surveillance and control mechanisms and thus to ensure the high quality of products. Particularly in small enterprises during the selection of equipment the attention should be paid to its versatility, as well as flexibility used for the periodic inspection of software, defined as the ability to customize to the specific requirements of industry standards.

Properly decisions regarding the selection of the measuring equipment must be based on appropriate supporting systems. These decisions are made under the basis of analysis of many variants of solutions which can be used thanks to constant development of measuring techniques but using them involves different consequences. To enter into this decision-making process a large number of criteria must be selected, one introduce an enormous amount of data (factors expressed by quantitatively and qualitatively), which increases the workload analysis. It is necessary to develop systematic procedures, modern techniques for making decisions on the measuring equipment used for measuring tasks in the assembly of ships propulsion systems. It should be noted to carefully select criteria. In this paper limited number of criteria was taken in consideration (*DWP* function (1)). The social or ecological criteria were omitted in undertaken

analysis. Adoption of such criteria directly affects the use of chosen equipment. The rest of this article will present considerations for the metrological characteristics of measuring instruments used during the assembly of ships propulsion system.

5. COMPARISON OF THE METROLOGICAL INSTRUMENTS USED FOR MEASURING IN THE SHAFTS ASSEMBLY PROCESS

During preparation of the technological processes, it is necessary to plan the use of particular equipment in consecutive stages during the control measurements.

In accordance with standards PN-EN ISO/IEC 17025:2005 (5.5) [7], equipment and its software used for testing shall be capable of achieving the accuracy required and shall comply with specifications relevant to the tests concerned. Each item of equipment and its software used for testing significant to the result shall be uniquely identified. The equipment can be selected at the stage of planning the measurement operation but it is very important that the whole measurement process be consider when selecting measuring equipment to satisfy requirements [8]. The correctness and reliability of the measurement is determined by many factors [7]: human factors, accommodation and environmental condition, test method or metrological characteristic [8] of a measuring equipment as required for the intended use (for example accuracy, stability and range).

To illustrate the selected components of *DWP* function (1), taking in consideration mentioned metrological properties of measuring instruments that can be used while measuring the deviation of aligned elements of the shaft, were set together.

The tables presents a comparison of selected metrological characteristics for machine tools: gap gauge, dial gauge, and measuring method using piano wire (Tab. 1) and also optical and laser instruments (Tab. 2). The statements contained in the tables use the same evaluation criteria.

Tab. 1. Overview of the metrological characteristics of selected metrological instruments used during the measurement done by conventional methods in the assembly process of the propulsion system

Characteristics	Conventional methods		
	Gap gauge and Knife edge rule	Dial gauge	Piano wire
Range of indication	0,05-1 mm	10 mm	Depends on used measuring instrument
Accuracy of measurement	0,1 mm	0,02 mm	Depends on used measuring instrument, construction of element and value of a measurand
Scale interval	0,05 mm 0,1 mm	0,01 mm	Depends on used measurement instrument: e.g.: inside micrometer 0,01 mm
Measured part of shaft line	Point of measurement	Point of measurement	Depends on construction
Error of measurement	1 ¹	1 ¹	1 ¹
Method of measurement	Point method	Radial-axial method, double radial method	Point method
Operator's experience	Long experience	Long experience	Long experience
Operator's training	Long term	Short term	Long term
Ability to save the data files	No	No	No
Number of measuring points	4 + control position between pair of shafts	4 * number of sections depending on the construction (between the shafts, shaft and gearbox)	3 sections * 4 positions + 10 measuring points on the foundation of elements of propulsion system ²
Results analysis	Point done by operator	Point done by operator	Point done by operator
Maintenance	Required	Required	Maintenance of used measuring instrument
Type of power supply	None	None	None
Accessories	None	Grip, fixing bridge	Stand, view fifers
Additional software	None	None	None
Problems	Surface Shape error, measurement environment	Deflection of fixing grip, grip construction, hysteresis of sensor, parallax error, measurement environment	Sag and tension, setup of stands, measurement environment

¹ Error values can be determined for the particular case of measurement in the measurement of statistical methods.

Example: The value of permissible error for dial gauge for the entire range is 20 μm [PN 68/M53260 Warsztatowe środki pomiarowe. Czujniki zębate zegarowe]. The permissible error for the inside micrometers is $(3 + V + L/50) \mu\text{m}$, where L in mm a V-number of extensions [data sheets for Mitutoyo analog inside micrometers series 139].

² Depending on the design of the item being measured, the table shows the number of measurement points during the measurement of single shaft of a Con-ro vessel.

Tab. 2. Summary of selected characteristics of optical and laser instruments

Characteristics	Optical instrument	Laser instrument
Range of indication	Depends on kind and type of instrument	Unlimited with the possibility of extending depending on the kind and type of equipment; for example measuring distance for laser measurement systems company's Easy-Laser D505 is 20m., D650 Linebore is 40 m., maximum distance between sensor and laser for Rotaling Prüftechnik Ultra is 10 m.
Accuracy of measurement	Depends on used measurement equipment and kind of a measurand,	0,001 mm
Measurand	Any size	Reliable to 30 m (in view of laser beam diffusion)
Operator's experience	Long experience	Long experience is not required
Operator's training	Directly on instrument	Training is organize by the equipment manufacturers, software indicates the steps of measurement
Stability of instrument	Stability of the optical system during the measurement	Stability of laser beam is depends of environment condition
Ability to safe the data files	Only in a few models	Directly in the equipment
Method of measurement	Point method	Multipoint method or the method of measurement in continuous operation
Number of measuring points	Preset by the operator depending on the size measured	Preset by the operator within 0-99, in case Static method (Optaling, Rotaling Ultra) measured at 45 degrees in 3 to 8 points
Results analysis	Perform by operator	Perform direct by the instrument
Maintenance	Required	Required
Instrument stability	Stable, long term used glass elements	Stable, resistant to environment condition depending on the class of protection
Type of power supply	Own power supply – buttry, off-site power	Own power supply – buttry, off-site power
Accessories	E.g. measurement roller for autocollimator are performed independently	Included, opportunity to buy additional mounting arms or rods
Additional software	No	Possibility to increase the number of modules
Problems	Environment condition effect	Environment condition effect

Properties shown in the statement of chosen metrological characteristics included in Tab. 1 and Tab. 2 refer to the chosen example, measuring systems used in talk over the conditions. They can provide the database for the selection of the measurement systems used during the assembly process.

Above mentioned metrological characteristics of measuring equipment (Tab. 1, Tab. 2) when taking into account such criteria as structural characteristics of propulsion system (*P*), quality characteristics of equipment (*S*) allow to make comparative analysis and to make the selection of measuring equipment. Such analysis can be treated as initial stage of

planning. In this paper economical aspects (K , K_j) in shipyard's real production conditions (availability of resources) are not mentioned so that it is not possible to make the practical implementation of evaluation and selection of measuring equipment (*DWP* function).

That is the reason why in the paper the factor W is chosen as the factor which determines the planning of measuring supplies in measurement management system.

On the example of Con-ro Vessel type B 201-II which shaft line length is 56 meters it is necessary, when taking into account data from (Tab. 2), to exclude laser instrument when determining the theoretical shaft line and use optical instrument or piano wire instead.

There is a possibility to obtain greater grade of accuracy of measurement when using optical or laser instrument but the use of conventional methods allow to obtain ample enough range of accuracy in technical conditions while assembling the shaft line. It is recommended to use laser instruments due to the necessity to make additional elements for dial gauge, piano wire and optical instruments to measure the alignment deviation of flanges of propulsion system elements. The use of laser instruments enable to reduce the setup time. The measurement precision, the possibility of its direct recording and repeatability of the measurement results are the advantages of using laser instruments and such things cannot be achieved by using conventional methods (Tab. 1). Laser instruments enable also sighting through the elements of propulsion system and controlling horizontal and vertical correction in real time and such features are not possible when using dial gauge.

6. CONCLUSIONS

Evaluation of the usability of measuring instruments for all types of applications is a natural necessity to ensure the proper conduct of the measurement process. Based on evaluation of the measurement system, and hence the efficiency of measuring equipment, a lot of decisions is taken under the control of the next stages of the assembly process of the ships propulsion system.

A well-organized control over a measuring equipment, most of all its selection will bring a lot of benefits for company including: the ability of measurement systems to provide reliable results, minimal risk of errors during measurement and misinterpretation of results, reduction of measurement costs, standardize procedures and instructions for the selection of measuring instruments.

The analysis of the selected criteria indicates the possibility of selection of measuring equipment which can allow to execute the measurement service giving the measurement results of the measurements with the required accuracy and reliability.

BIBLIOGRAPHY

- [1] Jakubiec W., Malinowski J.: *Metrologia wielkości geometrycznych*, Warszawa, Wydawnictwa Naukowo-Techniczne, 2004.
- [2] Gliwiński J.: *Legalizacja narzędzi do pomiarów długości i kąta*, Warszawa, Wydawnictwa normalizacyjne Alfa, 1984.
- [3] Muhlemann A. P., Oakland J. S., Lockyer K. G.: *Zarządzanie: produkcja i usługi*, Warszawa, Wydawnictwo Naukowe PWN, 2001,
- [4] Weiss J., *Dobór wyposażenia technicznego*, www.zie.pg.gda.pl/~jcz/dobor_wyp_tech.doc, marzec 2003.
- [5] Iglantowicz T.: *Nadzór nad wyposażeniem pomiarowo-kontrolnym w technikach wytwarzania*, Metrologia w systemach jakości-3. VI Sympozjum Klubu Polskie Forum ISO 9000, Kielce, Politechnika Świętokrzyska, 2000.
- [6] Jarysz-Kamińska E.: *Nadzór nad wyposażeniem pomiarowym jako element systemu zarządzania jakością w procesach wytwarzania*, XII Krajowa III Międzynarodowa Konferencja Naukowa Metrologia w Technikach Wytwarzania, Politechnika Białostocka, Augustów 19-21 września 2007.
- [7] PN-EN ISO/IEC 17025:2005 General requirements for the competence of testing and calibration laboratories.
- [8] PN-EN ISO 10012:2004 Measurement management systems - Requirements for measurement processes and measuring equipment.

Ph.D. **Eliza JARYSZ-KAMIŃSKA** is an assistant in Institute of Manufacturing Engineering on Faculty



of Mechanical Engineering and Mechatronics in West Pomeranian University of Technology in Szczecin. In her scientific work she deals with estimate of shaft misalignment ships propulsion system evaluation.

WIND TURBINES' ROLLING ELEMENT BEARINGS FAULT DETECTION ENHANCEMENT USING MINIMUM ENTROPY DECONVOLUTION

Tomasz BARSZCZ*, Nader SAWALHI**

**AGH University of Science and Technology, Department of Robotics and Mechatronics,
Al. Mickiewicza 30, 30-059 Krakow, Poland, tbarszcz@agh.edu.pl*

*** Prince Mohammad Bin Fahd University (PMU), Mechanical Engineering Department
AlKhobar 31952, Saudi Arabia*

Summary

Minimum Entropy Deconvolution (MED) has been recently introduced to the machine condition monitoring field to enhance fault detection in rolling element bearings and gears. MED proved to be an excellent aid to the extraction of these impulses and diagnosing their origin, i.e. the defective component of the bearing. In this paper, MED was applied for fault detection and diagnosis in rolling element bearings in wind turbines.

MED parameter selection as well as its combination with pre-whitening is discussed. Two main cases are presented to illustrate the benefits of the MED technique. The first was taken from a fan bladed test rig. The second case was taken from a wind turbine with an inner race fault. The usage of the MED technique has shown a strong enhancement for both fault detection and diagnosis. The paper contributes to the knowledge of fault detection of rolling elements bearings through providing an insight into the usage of MED in rolling element bearings diagnostic by providing a guide for the user to select optimum parameters for the MED filter and illustrating these on new interesting cases both from a lab environment and an actual case.

Keywords: rolling bearing, fault detection, Minimum Entropy Deconvolution (MED), wind turbine.

POPRAWA WYKRYWANIA USZKODZEŃ ŁOŻYSK TOCZNYCH W TURBINACH WIATROWYCH PRZY UŻYCIU METODY MINIMUM ENTROPY DECONVOLUTION

Streszczenie

Metoda Minimum Entropy Deconvolution (MED) została niedawno wprowadzona do diagnostyki w celu poprawy wykrywania uszkodzeń łożysk tocznych i przekładni. MED okazała się bardzo pomocna w ekstrakcji impulsów pochodzących od tych uszkodzeń i określania miejsca ich pochodzenia (np. uszkodzonego elementu łożyska). W niniejszym artykule MED zastosowano do wykrywania uszkodzeń łożysk tocznych w turbinach wiatrowych.

W artykule opisano zagadnienie selekcji parametrów metody MED oraz metody „wybielania sygnału” (ang. pre-whitening). Korzyści płynące z zastosowania metody przedstawiono na dwóch przypadkach. Pierwszym jest stanowisko laboratoryjne, a drugim – turbina wiatrowa z uszkodzoną bieżnią wewnętrzną łożyska generatora. Zastosowanie metody MED pozwoliło na znaczącą poprawę zarówno wykrycia, jak i lokalizacji uszkodzenia. Najistotniejszymi częściami niniejszego artykułu są: opis metody MED, wskazówki dotyczące optymalnego dostrojenia metody oraz interesujące przypadki zarówno laboratoryjne, jak i rzeczywiste.

Słowa kluczowe: łożysko toczne, wykrywanie uszkodzeń, Minimum Entropy Deconvolution (MED), turbina wiatrowa.

1. INTRODUCTION

Rolling element bearings (REBs) are components, which transfer the load through elements in rolling contact. The REB consists of: inner race, outer race, balls (or in general, rolling elements) and a cage, which holds the rolling elements in a given relative position. Rolling element bearings are key components in modern machinery. Detection of their faults is very important, as it prevents any further deterioration to other components which

may lead to catastrophic failure. One of the most important and more and more popular machines using REBs are wind turbines.

Figure 1 shows the gearbox and the main bearing of a 1.5 MW turbine. The typical wind turbine drivetrain consists of a main shaft, planetary gearbox, two stage parallel gearbox and a generator. Depending on the location in a wind turbine drivetrain, the replacement of a bearing can cost between 2500 to 32000 EUR, while the replacement of a gearbox may cost anything

between 75000 to 240000 EUR [1]. These operations depend very much on the accessibility to the wind turbine, which in turn depends on weather conditions, especially wind speed. This aspect is even more important for the offshore wind parks. Bearing spalls, subject to the machine speed and load, usually propagate slowly, thus giving the analyst enough time for monitoring and maintenance scheduling before any catastrophic failure. Therefore, a huge body of research in the area of bearing diagnostics concentrated on the early detection of the bearing faults to enable providing enough lead time for maintenance purposes [2]. The knowledge about the technical status of the REB and its fault development and propagation are being employed to develop a reliable prediction of the remaining useful life of the rolling elements bearings in what is known as bearing prognostics [3], which is becoming an important aspect of the new trend in monitoring the health of rotating machines. Cempel proposed a set of methods for machinery components lifetime prediction and calculation of limit values [4].

As has been shown by many authors [e.g. 5, 6], the envelope spectrum is a very efficient diagnostic tool for REB faults, as the information about the fault is extracted from the spacing between impulses and not by the excited frequencies. The process of obtaining the envelope spectrum is often referred to as the signal demodulation. There are several methods to properly select the frequency band to perform the demodulation. An informative source for rolling element bearing diagnostics can be recalled in [2].



Fig. 1. The view of the 1.5 MW wind turbine gearbox (front) and the main bearing (behind).

To illustrate the content of a measured vibration signal with a defective rolling element bearing, a simple model of the generation process is presented in figure 2. The symbol “*h” represents the convolution of the combined vibration signal (deterministic signals, bearing defective signal and noise) with the transfer path between the vibration source and the sensor location. In reality, the mechanism is far more complex, as it involves a number of vibration sources which may be added or convolved in rather different forms.

For a clear diagnosis of the bearing fault a number of techniques have been proposed to separate deterministic components from bearing component. techniques such as discrete random separation (DRS) [7, 8], self adaptive noise cancellation (SANC) [6] and time synchronous averaging (TSA) [9], which benefits from the slippage phenomena has been proposed with good results. This technique was applied to wind turbines diagnostics by Barszcz [10]. A number of papers proposed methods to improve the signal to noise ratio of the REB fault component, by selecting a frequency range in which the energy of the signal components is relatively stronger. Different criteria for so called optimum frequency band (OFB) were proposed. A very successful approach (*kurtogram*), based on maximizing the kurtosis of the band filtered signal was proposed by Antoni and Randall [11]. Recently, Barszcz and Jabłoński [12] proposed the criterion of kurtosis of the envelope spectrum (*protrugram*), which is more robust to random impulsive impacts.

Another problem with detection of small impulses induced by REB faults is the transfer path between the faulty component (e.g. inner race) and the vibration sensor. Impacts, which are initially sharp after travelling the distance between the bearing and the sensor may be very distorted. The method was originally proposed by Sawalhi et al [13] with the application to a test rig. This paper provides a means for removing the effect of the transfer path *h through inverse filtration. The aim is to design an inverse filter to remove/minimize the effect of the transfer path filter. The base to optimize this filter is to minimize the entropy of the signal, or in other words to maximize the impulsiveness (kurtosis) of the signal. This filter will then be used to deconvolve (as opposed to convolve) the signal, thus recovering the defective bearing fault signal (impulses) in a rather clear way. The filter used to do so is referred to as minimum entropy deconvolution (MED).

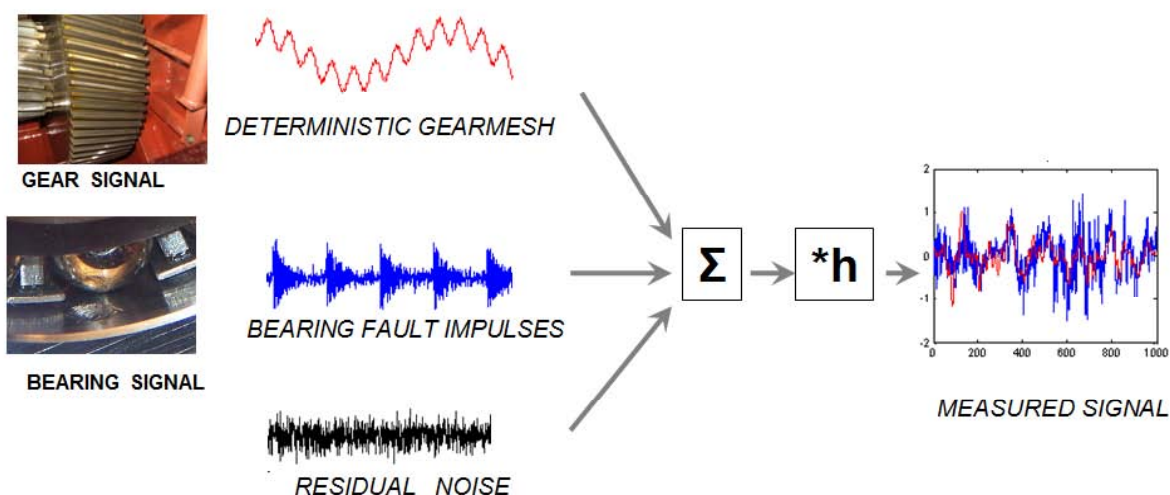


Fig. 2. Model of the generation of the vibration signal from a machine with gears and bearings.

2. MINIMUM ENTROPY DECONVOLUTION TECHNIQUE

The Minimum Entropy Deconvolution technique (MED) is a type of system identification method that was originally proposed by Wiggins [14]. Its main original use was to aid the extraction of reflectivity information in seismic data in order to identify and locate layers of subterranean minerals. MED has shown its effectiveness in deconvolving the impulse excitations from a mixture of response signals [15, 16]. In the machine condition monitoring field, it was used initially by Endo and Randall [17] to enhance the impulses arising from spalls and cracks in gears. It was then adopted by Sawalhi et al. [13] to enhance the detection of spalls in rolling element bearings in high speed machines.

Figure 3 illustrates the deconvolution process involved in the MED filtering when used to enhance the detection of bearing faults. In order to gain the full benefit from using the MED technique

for rolling element bearings, it is recommended that the signal is first order tracked. After the order tracking the synchronously averaged part (deterministic component) should be removed. Another recommended pre-processing step is to pre-whiten [13] the residual signal (i.e. total signal minus the synchronous average part). Pre-whitening can be achieved by using an autoregressive model (AR) [18]. As the main aim is to have a relatively flat spectrum, there is not usually a great emphasis on the selection of the order of the AR process.

The proposed algorithm has been implemented in this study by using the Objective Function Method (OFM) given in [19]. This method is an iterative optimization process, which is designed to maximize the kurtosis of the MED output (thus minimizing the entropy). The OFM achieves this by changing the values of the coefficients in the MED filter. The optimization process finishes when the values of the coefficients converge within the specified tolerance.

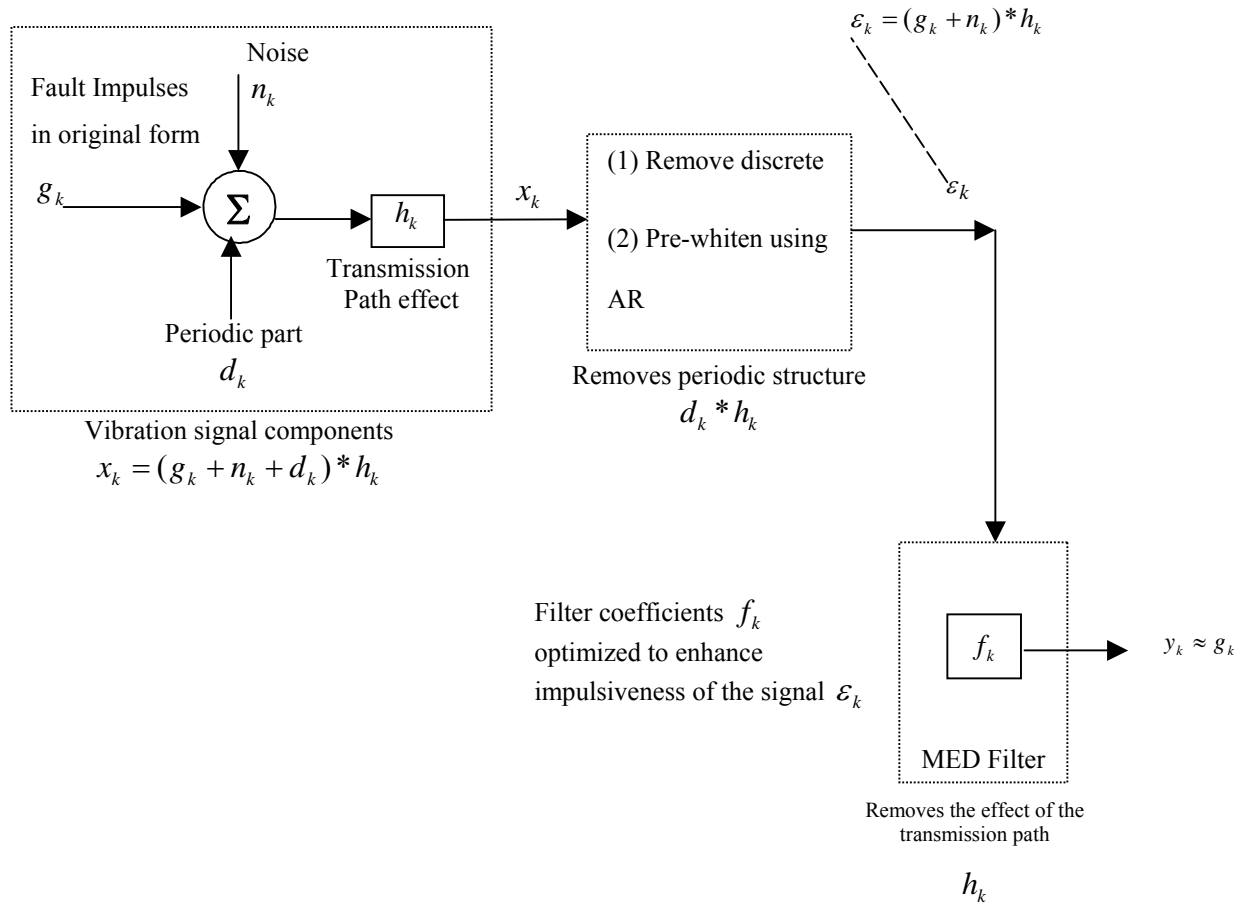


Fig. 3. The proposed inverse filtering (deconvolution) process to enhance the detection of bearing faults using the MED technique

3. CASE STUDY ON A WIND TURBINE REB

MED has been attempted on a signal taken from a wind turbine with extended inner race spalls. The turbine was of the GE 1.5sl type from one of German wind parks. This is a 1500 kW turbine with the doubly fed generator and pitch control [20]. The turbine has had a bearing fault on the generator shaft in its inner race as seen in figure 4.

The raw acceleration time domain signal, the results of the different processing stages, and their corresponding envelope spectra and selection criteria are shown in figures 5 and 6 and 7 respectively.



Fig. 4. Spalled inner race of a wind turbine

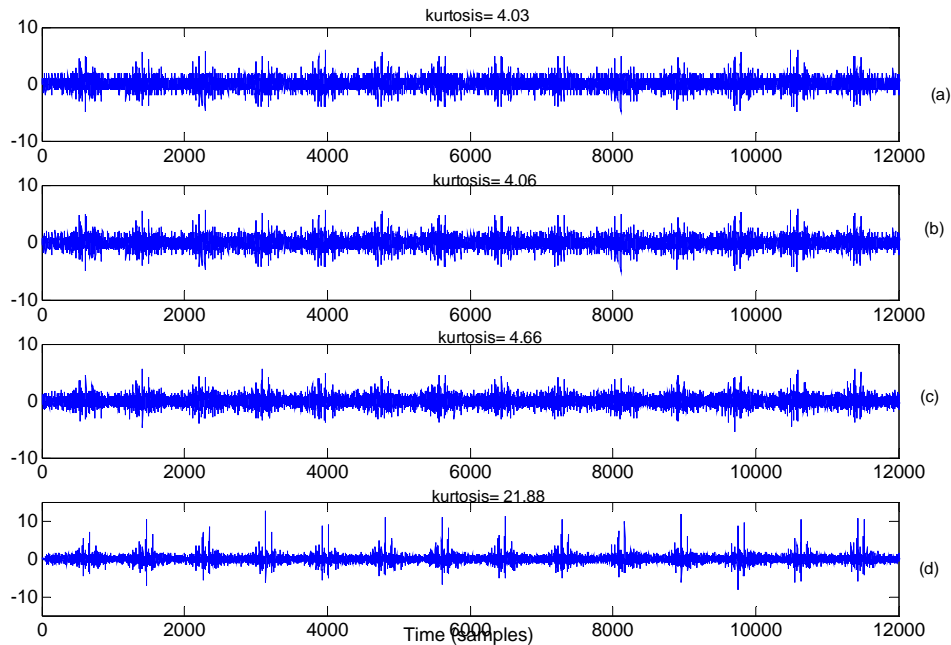


Fig. 5. vibration signals (acceleration) for the extended inner race fault (a) raw measured signal (b) After the removal of synchronous average (c) signal b Pre-whitened (d) signal c after using the MED

As can be seen from figure 5, the application of the MED has significantly increased the kurtosis of the vibration signal. While the kurtosis of the raw signal was just 4.03, it reached 21.88 after application of the obtained inverse filter. These results can be also clearly observed in figure 6, which presents the envelope spectra of signals from the figure 5. In the envelope spectra it is observed that MED not only causes the increased clarity of the BPFI harmonics, but also discloses the presence of strong modulation by the rotational speed of the shaft. The harmonic spacing in figure 6 equals 283.87 Hz, which was found equal to the repetition

period of the BPFI (ball pass frequency inner ring). The sidebands were spaced at 30.11 Hz, which is the rotational speed of the generator shaft during the measurement session.

Finally the dependency between AR and MED algorithms parameters were plotted (see figure 7). The trend observed earlier in the experimental research can be clearly seen here. A low AR order model has been used (AR (1)) and a filter length of 4096 was used (although 1024 or 2048 would also give enough good results).

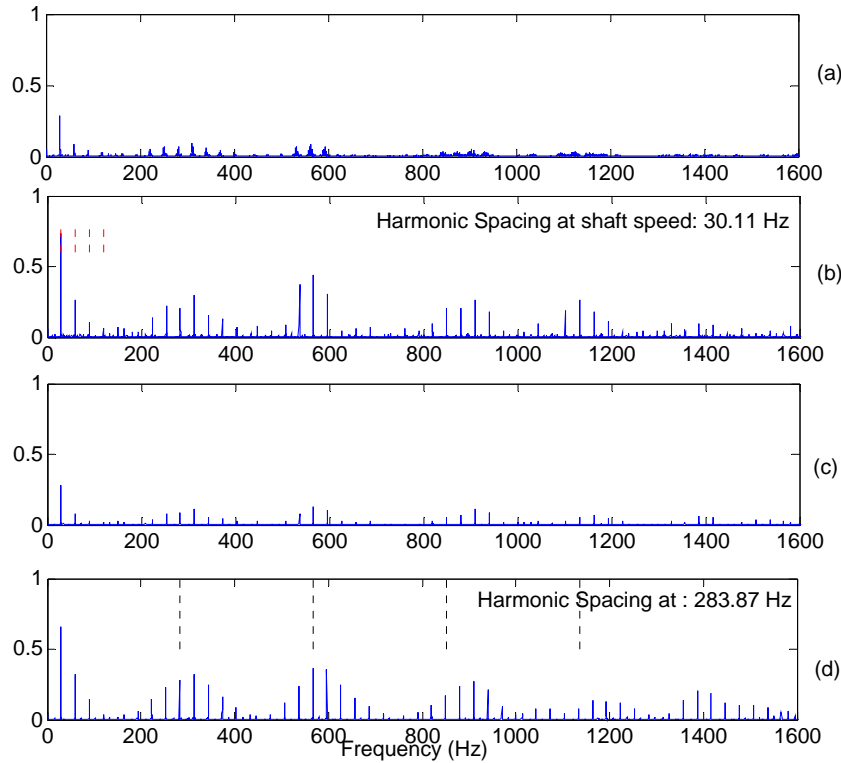


Fig. 6. Envelope spectra (band pass from 1000 to 10000 Hz): (a) raw (b) residual after subtracting the synchronous average (c) signal b pre-whitened (d) the MED result

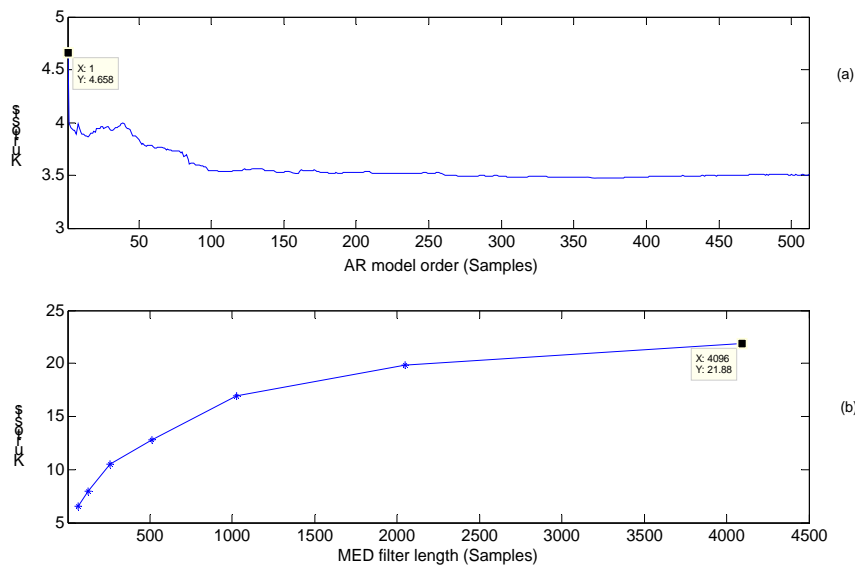


Fig. 7. Wind turbine data: AR and MED parameter selection (a) AR model order selection based on maximizing the kurtosis (B) MED filter length selection based on the kurtosis of the filtered signal

4. SUMMARY AND CONCLUSIONS

This paper presents further development of the minimum entropy deconvolution (MED) method to aid extracting faults in rolling element bearings. The MED technique was applied to signals with defective bearings taken from an experimental test rig and a wind turbine. The synchronously averaged signal (containing deterministic components) was

subtracted from the total signal to get a residual signal, which contains fault impulses. The residual signal was then pre-whitened to further aid the enhancement of the impulses by minimizing the variation between adjacent frequencies. The MED was then applied with the aim of removing the effect of the transfer path (deconvolution) and enhances the clarity of the impulses and then the detection and diagnoses of the bearing fault. It is

shown that MED significantly increase the peakedness of the vibration signals and the clarity of the impulses. This has been illustrated in both the time domain signals and further observed on the envelope spectra. In particular, the modulations at the shaft speed in the case of inner race faults were dramatically enhanced and observed with the introduction of the MED technique. The selection of the filter length for the MED and the model order for pre-whitening are based on maximizing the kurtosis of the signal, which in effect means more clarity in the impulses and a better detection and analyses of the fault. It is observed that for pre-whitening purposes a low model order is usually required to achieve a high kurtosis. For the MED filter, it is observed that the longer the filter the highest the kurtosis value (associated with a long tail). The variation between the kurtosis values above a filter length of 1024 samples is not dramatic, but the computational burden is. So a filter length between 1024 and 4096 samples would be suitable. Filters with length above 4096 samples will slightly increase the kurtosis, but will require a huge memory.

5. ACKNOWLEDGMENTS

The authors would like to express their gratitude to the company SeaCom GmbH (Herne, Germany) for access to the wind turbine data.

6. REFERENCES

- [1] Gajetzki, M. (2006): *SeaCom – Digital Measurement and Communication Systems*, SeaCom, Herne.
- [2] Randall R. B., Antoni J. (2011). *Rolling element bearing diagnostics--A tutorial*, Mechanical Systems and Signal Processing, 25: 485-520
- [3] Heng A., Zhang S., Tan A. C. C., Mathew J. (2009): *Rotating machinery prognostics: State of the art, challenges and opportunities*, Mechanical Systems and Signal Processing, 23: 724 – 739
- [4] Cempel C. (2008). *Decomposition of symptom observation matrix and grey forecasting in vibration condition monitoring of machines*. International Journal of Applied Mathematics and Computer Science, 18: 569 – 579
- [5] Klein, U. (2003): *Schwingungsdiagnostische Beurteilung von Maschinen und Anlagen (Vibrodiagnostic assessment of machines and devices)* [in German], Stahleisen Verlag, Duesseldorf 2003.
- [6] Ho, D., Randall, R.B. (2000): *Optimisation of bearing diagnostic techniques using simulated and actual bearing fault signals*, Mechanical Systems and Signal Processing 14: 763–788.
- [7] Antoni, J., Randall, R.B. (2004): *Unsupervised noise cancellation for vibration signals: Part I - evaluation of adaptive algorithms*. Mechanical Systems and Signal Processing, 18: 89–10.
- [8] Antoni, J., Randall, R.B. (2004): *Unsupervised noise cancellation for vibration signals: Part II - a novel frequency domain algorithm*. Mechanical Systems and Signal Processing, 18: 103–117.
- [9] Braun S. (2010): *The synchronous (time domain) average revisited*, The 24th International Conference on Noise and Vibration engineering (ISMA2010), Leuven (Belgium), 20 to 22 September 2010.
- [10] Barszcz, T. (2009): *Decomposition of vibration signals into deterministic and nondeterministic components and its capabilities for fault detection and identification*. International Journal of Applied Mathematics and Computer Science, 19: 327-335
- [11] Antoni, J., Randall, R.B. (2006): *The spectral kurtosis: application to the vibratory surveillance and diagnostics of rotating machines*. Mechanical Systems and Signal Processing, 20: 308-331.
- [12] Barszcz, T., Jabłoński, A. (2011): *A novel method for the optimal band selection for vibration signal demodulation and comparison with the Kurtogram*. Mechanical Systems and Signal Processing, 20: 308-331.
- [13] Sawalhi, N., Randall, R.B., Endo, H. (2007): *The enhancement of fault detection and diagnosis in rolling element bearings using minimum entropy deconvolution combined with spectral kurtosis*, Mechanical Systems and Signal Processing, 21: 2616-2633.
- [14] Wiggins, R. A. (1978): *Minimum entropy deconvolution*. Geophysical Exploration, 16: 21-35.
- [15] Nandi, A. K., Mampel, D., Roscher, B. (1997): *Blind deconvolution of ultrasonic signals in non-destructive testing applications*. IEEE Trans of Signal Processing, 45: 1382-1390.
- [16] Boumahdi, M., Lacoume, J. (1995): *Blind identification using the Kurtosis: Results of field data processing*. IEEE Trans of Signal Processing, 0-7803-2431-5/95, pp. 1960-1983.
- [17] Endo, H., Randall, R.B. (2007): *Application of a minimum entropy deconvolution filter to enhance Autoregressive model based gear tooth fault detection technique*. Mechanical Systems and Signal Processing, 21: 906-919.
- [18] Wang, W., Wong, A. K. (2002): *Autoregressive model-based gear fault diagnosis*. Transaction of ASME, Journal of Vibration and Acoustics, 124: 172- 179.
- [19] Lee J. Y., Nandi A. K. (1999): *Extraction of impacting signals using blind de-convolution*. Journal of Sound and Vibration 232: 945 – 962
- [20] Hau, E. (2006): *Wind Turbines. Fundamentals, Technologies, Applications, Economics*. 2nd Edition, Springer Verlag, Berlin Heisenberg.

3D MODEL OF ANODIC OXIDE COATING MODIFIED WITH CARBON PARTICLES

Grzegorz SŁUŻALEK, Henryk WISTUBA, Marek KUBICA

Wydział Informatyki i Nauki o Materiałach, Katedra Materiałoznawstwa
41-200 Sosnowiec; ul. Śnieżna 2, sluzalek@us.edu.pl, mkubica@us.edu.pl

Summary

In this paper shown three-dimensional model of composite hard anodic layer modified by carbon particles. Modifications were carried by vacuum sublimation by a graphite electrode. The modified layer is characterized by improved tribological properties (friction coefficient) compared to the unmodified layer. Test conditions and values of the coefficients of friction are presented for the combination of pin-on-disc pair in T-01M tester. The 3D model was made in parametric CAD program Solid Edge v19 pl, which allows to explain the decrease in the coefficient of friction.

Keywords: anodic oxide coating, carbon particles, 3D model, CAD, pin-on-disc.

MODEL 3D WARSTWY TLENKOWEJ MODYFIKOWANEJ CZĄSTKAMI GRAFITU

Streszczenie

W pracy przedstawiono trójwymiarowy model kompozytywnej warstwy ceramiczno-grafitowej powstałej w wyniku modyfikowania anodowej powłoki twardej. Modyfikacje przeprowadzono w procesie napyłania próżniowego. Warstwa modyfikowana charakteryzuje się lepszymi właściwościami tribologicznymi (współczynnik tarcia) w porównaniu do warstwy niemodyfikowanej. Warunki badań oraz wartości współczynników tarcia zestawiono dla skojarzenia trzpień-tarcza testera T-01M. Model 3D warstwy wykonano w parametrycznym programie CAD Solid Edge v19, który pozawala na wyjaśnienie zmniejszenia się współczynnika tarcia.

Słowa kluczowe: anodowa warstwa tlenkowa, model 3D, CAD, trzpień-tarcza, cząsteczki grafitu.

1. OXIDE CERAMIC LAYER

The object of the researchers was an oxide ceramic layer formed by using the duplex method which is obtaining the layer consists of anodic oxidation on aluminium. Al_2O_3 coatings were performed on the alloy EN-AW-5251 (disc) through hard anodizing in a three-component electrolyte of a constant temperature of 313 K and current intensity of $3 A/dm^2$ and the time was 60 minutes. The examination was performed by using the transmission electron microscope (JOEL's JEM 2010 ARP) revealed a columnar-fibrous structure of Al_2O_3 coatings. The aluminium oxide fibres are oriented in parallel to the direction of coating growth as the effect of the electric field present in the electrochemical process (fig. 1). Oxide fibres are arranged in parallel to one another (fig. 2).

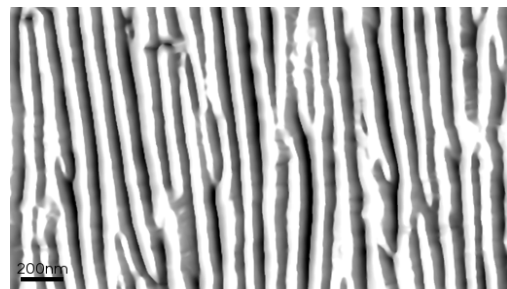


Fig. 1. Interactive 3D surface



Fig. 2. The columns 3D model of AOC created in Solid Edge.

2. COMPUTER IMAGE ANALYSIS

In the computer image analysis (CIA) of the ceramic-graphite oxide layer obtained using duplex method the following parameters were taken into account: the shape coefficient, average diameter and distance between fibres. The results along with the standard deviation are collated in Table 1. In the CIA was used specialist software for image processing and measuring namely: Metilo and ImageJ applications.

Table 1. Parameters of measuring interfaces

Object of the analyses	Parameter	Value
Straight ceramic fibre	Shape coefficient	0.142 ± 0.002
Straight ceramic fibre	Average diameter	$83 \pm 1.8 \text{ nm}$
Ceramic fibre	Distance between the fibres	$45 \pm 5 \text{ nm}$

Based on the results from the computer image analysis, a 3D coating model was proposed which has not been present so far in the literature regarding the subject discussed. The following types of the oxide coating modification were used by vacuum sublimation by a graphite electrode. A Joel IEE-4B vacuum sprayer was used for this purpose.

3. TRIBOLOGY

Tribological tests were performed by using T-01M tester (Fig. 3). The sample (pin) was made of PEEK/BG which is coupling with a counter-surface (disc) which has a composite of graphite oxide (fig. 4). There were reductions in the coefficient of friction-modified layer deposition (0.1737 ± 0.00083) compared to the unmodified layer of the friction coefficient (0.2133 ± 0.00832). In explanation of this phenomenon may help a 2D and 3D models of the graphite ceramic composite layer.

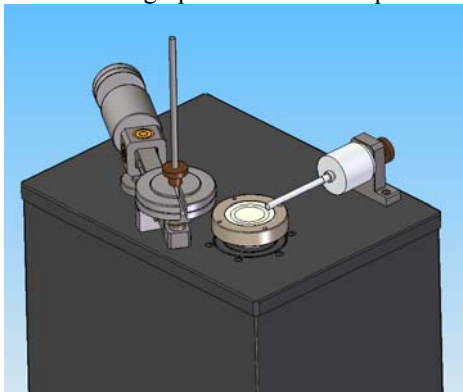


Fig. 3. Solid Edge 3D model of T-01M tester

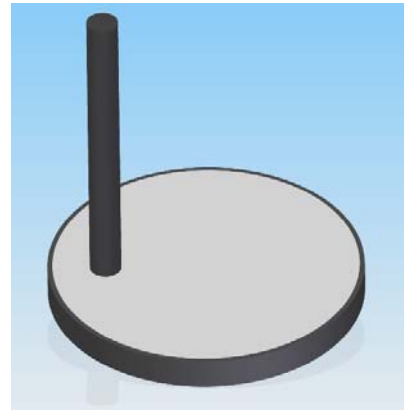


Fig. 4. Solid Edge 3D model of pin-on-disc couple

4. COMPUTER MODELS

The 2D and 3D models were made in a parametric program, Solid Edge v19 pl. The process of vacuum sublimation on a hard anode graphite layer, leading to a reduction in pore size and even to close them in case of pores less than $10\mu\text{m}$. The tribological process is characterized by wear and exposure covered or graphite-filled pores. The pores in which were placed on graphite trays act as grease, consequently leading to lower friction coefficient. The vacuum sublimation process probably caused covering the amorphous carbon surfaces and the oxide layer and internal diameter of the pores which have a diameter greater than 5nm . In the case of pores which diameter is less than 5nm , there is possibility of closing and sealing.

2D and 3D models of layer was shown on figure 5 and 6.

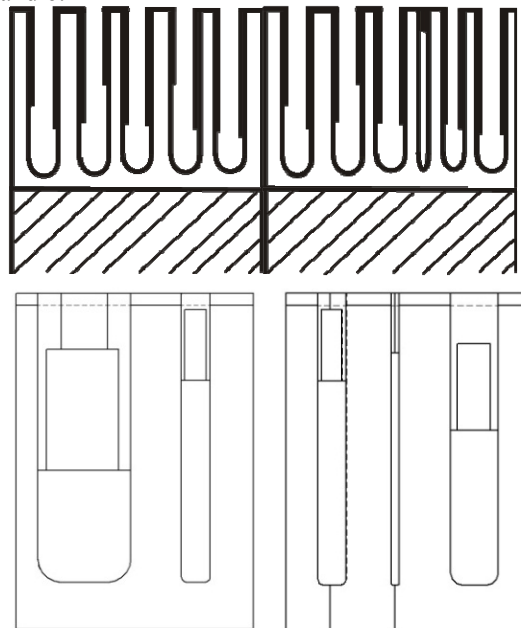


Fig. 5. Two dimensional models of anodic layer

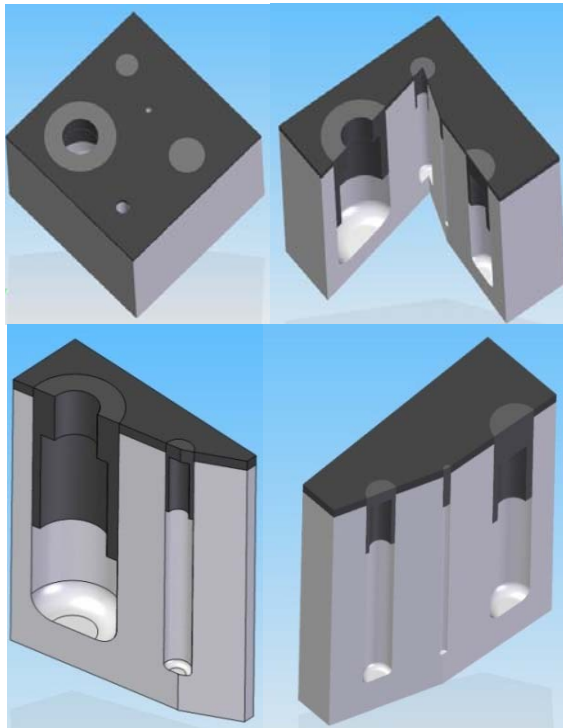


Fig. 6. Three dimensional models of anodic layer.

Stages of uncovering (abrasion) of next layers was shown on figure 7 and 8 in different angles.

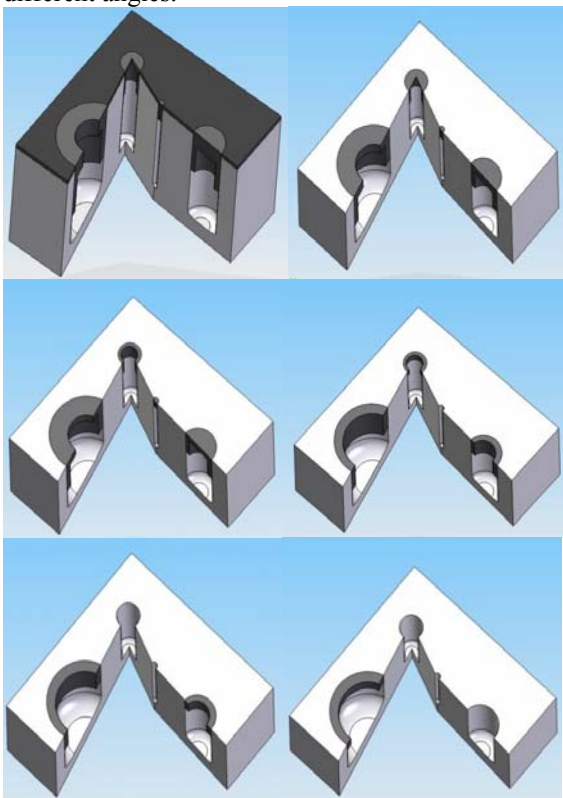


Fig. 7. Stages of uncovering (abrasion) of next layers

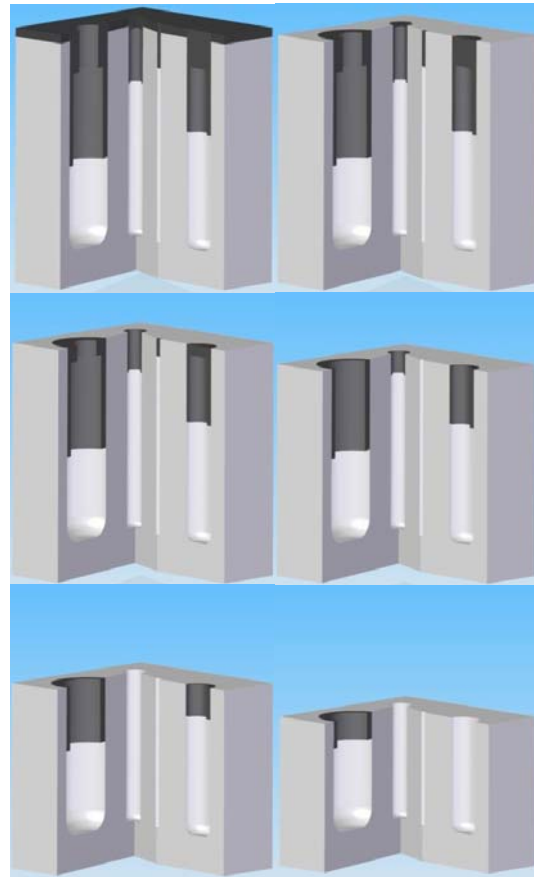


Fig. 8. Stages of uncovering (abrasion) of next layers

SUMMARY

Anodic oxide layer modified by the vacuum sublimation of carbon is characterizing of low values friction coefficient. Introduced graphite into the pores of acts as a lubricant, causing a permanent reduction in the coefficient of friction.

By means of CIA the ceramic-graphite layer composite is determined by average diameters of oxide fibres, average distances between the fibres and their shape coefficient.

Based on a qualitative CIA, of a 3D model of the ceramic-graphite duplex layer modified by vacuum sublimation was proposed.

AWARDS

Silver medal at the International Fair of Innovation and Economic Research Intarg Katowice 2011- University of Silesia awarded a „Method for producing composite coatings on aluminum and it is alloys, whose authors are PhD Grzegorz Służalek and PhD Henryk Wistuba.



Fig. 9. Silver medal at the International Fair of Innovation and Economic Research Intarg Katowice 2011

REFERENCES

- [1] Władysław Skoneczny, Marek Kubica: „Komputerowa analiza właściwości tribologicznych wybranych materiałów polimerowych w skojarzeniu ślizgowym z warstwą Al_2O_3 przy użyciu metody elementów skończonych”. Materiały Polimerowe. Politechnika częstochowska, Częstochowa 2010 r.
- [2] Grzegorz Służalek, Marek Kubica, Henryk Bąkowski: „Rozkład naprężeń i odkształceń wybranych węzłów tarcia w badaniu warstwy typu duplex”. Mechanik 2010r. nr 1.
- [3] Marek Kubica, Grzegorz Służalek, Mariusz Wrazidło: „Trójwymiarowy, animowany model Testera T-11 wykorzystywanego do badań tribologicznych węzłów tarcia trzpień-tarcza i kulka-tarcza”. Mechanik 2011r. nr 2.
- [5] G. Służalek, H. Wistuba: „Sposób wytwarzania powłok kompozytowych na aluminium i jego stopach”. Zgłoszenie patentowe P 390876 2010 r.
- [6] H. Wistuba, G. Służalek: „Sposób wytwarzania powłok kompozytowych na aluminium i jego stopach”. Zgłoszenie patentowe P 390877 2010 r.



Grzegorz SŁUŻALEK Ph.D. is an assistant professor in Department of Materials Science of University of Silesia. His scientific interests focus on CAx, FEA, nanomaterials, tribology.



Henryk WISTUBA Ph.D. Is senior research in Interdepartamental Laboratory of Structural Research University of Silesia His scientific interests focus on nanomaterials, tribology.



Marek KUBICA, M.Sc. of Computer Science and Technology, PhD student in the Faculty of Computer and Materials Science at University of Silesia. His scientific interests are oxide layers, computer image analysis, modeling, computer simulations and FEA.

APPLICATION OF EVOLUTION OF SINGULAR VALUES IN MULTISYMPTOM DIAGNOSTICS OF MACHINES

Maciej TABASZEWSKI, Czesław CEMPEL

Instytut Mechaniki Stosowanej, Politechniki Poznańskiej
Ul. Piotrowo 3, 60-965 Poznań
fax. 61 665 2307, email Maciej.Tabaszewski@put.poznan.pl

Summary

The paper presents a possibility of observation of singular values evolving in time as quantities carrying diagnostic information. To prove the usefulness of singular values for this purpose many numerical simulations have been conducted. It has been proved that when observing changes of singular values obtained from SVD during the lifetime of a machine, the appearance of reversal points must be taken into account. The appearance of such points may prove that the symptom values change abruptly (*eg. structure cracking*). The appearance of such an abrupt change can easily be overlooked because of variable working parameters of the machine, which influence the values of measured symptoms and generalized symptoms after SVD. Singular values are almost insensitive to changes of working parameters, so it is easier to pick out such changes in their evolution than directly in symptoms. The paper also presents an example of application of the proposed method for real diagnostic data obtained from ball bearings.

Keywords: vibroacoustic diagnostics of machines, SVD, singular values.

ZASTOSOWANIE EWOLUCJI WARTOŚCI SZCZEGÓLNYCH W WIELOSYMPTOMOWEJ DIAGNOSTYCE MASZYN

Streszczenie

W pracy przedstawiono możliwość obserwacji wartości szczególnych ewoluujących w czasie jako wielkości niosących informację diagnostyczną. Aby wykazać przydatność wartości szczególnych w tym zakresie dokonano wielu symulacji numerycznych. Wykazano w nich, że obserwując zmiany wartości szczególnych uzyskanych z rozkładu SVD w czasie życia maszyny, należy zwrócić uwagę na występowanie punktów zwrotnych. Występowanie tych punktów może świadczyć o skokowej zmianie wartości symptomów (*np. pęknięcia struktury*). Fakt wystąpienia takiego skoku może zostać łatwo przeoczony ze względu na zmienne parametry robocze maszyny, które z kolei wpływają na wartości mierzonych symptomów a także symptomów uogólnionych po rozkładzie SVD. Wartości szczególne są prawie nie wrażliwe na zmiany parametrów roboczych, tak więc łatwiej wychwycić tego typu skoki w ich ewolucji niż bezpośrednio w symptomie. W pracy przedstawiono także przykład zastosowania proponowanej metody dla rzeczywistych danych diagnostycznych pochodzących z łożysk tocznych.

Słowa kluczowe: diagnostyka wibroakustyczna maszyn, rozkład SVD, wartości szczególne.

1. WPROWADZENIE

Diagnostyka techniczna maszyn jest podstawowym narzędziem w strategii utrzymania ruchu uwarunkowanej stanem technicznym. Często, w praktycznych zastosowaniach, dokonuje się diagnozy stanu lub jego prognozy bazując na pojedynczej mierze sygnału diagnostycznego. Gdy miara ta jest współzmiennicza z cechami stanu możemy ją nazwać symptomem. W przypadku gdy stan techniczny daje się określić wykorzystując jeden symptom proces diagnozy lub prognozy jest oczywisty i sprowadza się do badania relacji wartości aktualnej lub przyszłej (*prognoza*) symptomu z jego

wartością prewencyjnego alarmu, co pozwala uniknąć awarii jak i uszkodzeń następczych.

W przypadku jednoczesnej rejestracji wielu symptomów, co w wielu przypadkach złożonych maszyn jest konieczne, istnieje wiele innych metod określenia stanu bieżącego lub przyszłego. Można tutaj stosować wszelkiego rodzaju metody klasyfikacji opartej o przykłady uczące [1][2][3], modele sieci neuronowych (*np. [4]*), zasadę pesymistycznej oceny (przekroczenie przez którykolwiek z symptomów jego wartości granicznej wywołuje alarm) itp. Ostania z przytoczonych możliwości szczególnie spełnia swe zadanie, gdy posiadamy wiele symptomów selektywnie wrażliwych na poszczególne uszkodzenia.

Inne podejście do problemu diagnostyki wielosymptomowej zostało zaproponowane przez Cempla. Pierwotnie wykorzystywano do tego celu rozkład PCA [5], a następnie SVD [6][7][8][9]. W tym podejściu problem wielowymiarowej prognozy czy diagnozy można sprowadzić do problemu o mniejszym wymiarze poprzez zastosowanie kombinacji liniowej odpowiednich pierwotnych wartości symptomów z wykorzystaniem wag zawartych w odpowiednich wektorach szczególnych. Zgodnie z tym powstanie wtedy nowa macierz obserwacji przy czym ilość uwzględnionych nowych symptomów zależy od przyjętej za istotną liczby wartości szczególnych. W ten sposób możemy zmniejszyć rozmiar pierwotnej macierzy obserwacji zastępując pierwotne kolumny symptomów odpowiednimi kombinacjami liniowymi. Podstawy tej metody przedstawiono w kolejnym rozdziale. Następnie przedstawione zostaną wyniki dotyczące próby zastosowania ewolucji samych wartości szczególnych jako miar niosących informację diagnostyczną. Pierwsze próby z udziałem ewolucji wartości szczególnych były podjęte w [10] i dotyczyły symptomów maszyn pracujących w ruchu ciągłym przy zmiennym obciążeniu. Uzyskane wyniki były zadziwiające ze względu na niewrażliwość wartości szczególnych na obciążenie. W związku z tym postanowiono bliżej przebadać problem na symulowanych symptomach oraz innych obserwacjach symptomów.

2. WYKORZYSTANIE ROZKŁADU SVD W DIAGNOSTYCE WIELOSYMPTOMOWEJ

Podstawą omawianej metody jest symptomowa macierz obserwacji **SOM** (ang. *Symptom Observation Matrix*) - patrz np. praca [8]. Opisane podejście umożliwia wydobywanie informacji o rozwijających się uszkodzeniach w oparciu o sukcesywnie dopisywane do macierzy wierszowych wektorów symptomów. Dyskretne odczyty tego wektora są realizowane z krokiem $\Delta\theta$ czasu życia maszyny θ ($0 < \theta < \theta_p$ gdzie θ_p jest czasem prewencyjnego wyłączenia) i tworzą opisywaną macierz **SOM** o p wierszach. Ostatnia dostępna informacja odnosi się do chwili $p\Delta\theta$.

Sposób powstawania macierzy **SOM** zilustrowano na rysunku 1.

Kolejne realizacje pomiarów

$$\begin{array}{l} \text{Czas} \quad \theta_1 \\ \text{życia} \quad \theta_2 \\ \text{obiektu} \quad \theta_p \end{array} \quad \begin{array}{l} \downarrow \\ \downarrow \\ \downarrow \end{array} \quad \begin{array}{l} \mathbf{v}_1 = [L_1(\theta_1) \dots L_n(\theta_1) S_1(\theta_1) \dots S_m(\theta_1)] \\ \mathbf{v}_2 = [L_1(\theta_2) \dots L_n(\theta_2) S_1(\theta_2) \dots S_m(\theta_2)] \\ \mathbf{v}_p = [L_1(\theta_p) \dots L_n(\theta_p) S_1(\theta_p) \dots S_m(\theta_p)] \end{array}$$

Dostępnych p realizacji

$$\mathbf{SOM} \quad \begin{bmatrix} \theta_1 & L_{11} & \dots & L_{1n} & S_{11} & \dots & S_{1m} \\ \theta_2 & L_{21} & \dots & L_{2n} & S_{21} & \dots & S_{2m} \\ \dots & \dots & \dots & \dots & \dots & \dots & \dots \\ \theta_p & L_{p1} & \dots & L_{pn} & S_{p1} & \dots & S_{pm} \end{bmatrix}_{pxr}$$

Rys. 1. Dynamiczne tworzenie macierzy **SOM** poprzez dodawanie kolejnych wektorów obserwacji

Jak wynika z rys.1 macierz **SOM** może być rozumiana szerzej niż tylko macierz symptomów związanych z cechami stanu. Zgodnie z ideą zaproponowaną wyżej, elementami macierzy **SOM** mogą także elementy wektora logistycznego **L** związanego np. z wartościami parametrów pracy obiektu (np. *prędkość obrotowa, obciążenie, kąt ustawienia kierownicy w wentylatorze itp.*), a w szczególnym przypadku także miara eksploatacyjna (np. czas θ). Uwzględnienie wektora logistycznego (np. *parametrów sterowania*) **L** jest niekiedy istotne z punktu widzenia kompletności informacji w macierzy **SOM**, gdyż wiadomo, że wartości tych parametrów wpływają na obserwowane wartości symptomów. Tak więc, jeżeli wspomniane parametry ulegają zmianie obserwowane symptomy można wyrazić jako:

$$S = f(\xi(\theta), \mathbf{L}) \quad (1)$$

gdzie: **L** – wektor logistyczny, $\xi(\theta)$ - cechy stanu ulegające zmianie na skutek zużycia (np. wartość luzów, sztywność elementu konstrukcji itp.) zależne od czasu życia θ .

W przypadku gdy elementy wektora **L** podlegają zmianom w trakcie eksploatacji obiektu, a nie zostanie to uwzględnione w macierzy **SOM**, obserwowane zachowanie symptomów może być niewytłumaczalne. W przypadku obiektów, które nie podlegają sterowaniu lub wpływ zmian parametrów sterowania na obserwowane symptomy jest nieistotny, macierz **SOM** upraszcza się znacznie. Założenie o braku istotnego wpływu na wartości symptomów wymaga, aby obserwacji podlegały tylko „wyspecjalizowane” wielkości uzyskane np. na zasadzie selekcji częstotliwościowej.

Niestety często pełna informacja o wektorze **L** nie jest dostępna w systemie diagnostycznym a zmiany parametrów roboczych silnie kształtują zachowanie

symptomów. Nasuwa się więc pytanie czy mimo braku możliwości bezpośredniego uwzględnienia \mathbf{L} w macierzy obserwacji można w prosty sposób wyeliminować wpływ tych zmian na wartości symptomu a jednocześnie wyselekcjonować użyteczną informację diagnostyczną. Próba rozwiązanie tego problemu zostanie przedstawiona w rozdziale 3.

W pracy [8] zostało wykazane, iż maksimum informacji diagnostycznej możemy z macierzy \mathbf{SOM} uzyskać, jeśli wszystkie odczyty wstępnie wycentrować i znormalizować do wartości początkowej $S_m(0) = S_{0m}$ danego symptomu. Otrzymamy w ten sposób bezwymiarową symptomową macierz obserwacji:

$$\mathbf{O}^{(pr)} = [S_{nm}], \quad S_{nm} = \frac{S'_{nm}}{S_{0m}} - 1, \quad (2)$$

gdzie wartości z „*prim*” symbolizują pierwotne wymiarowe wartości mierzonych symptomów.

Do bezwymiarowej macierzy obserwacji zastosujemy procedurę rozkładu względem wartości szczególnych SVD, [11][12]. Łatwo wywnioskować, że możemy uzyskać tylko $u \leq r$ niezależnych informacji o rozwijających się uszkodzeniach F_t . Taki rozkład SVD możemy prowadzić po wykonaniu każdej obserwacji [8]: $n = 1, 2, \dots, p$, i w ten sposób śledzić ewolucję uszkodzeń $F_t(\theta_n)$ w obiekcie. Jedno uszkodzenie F_t może opisywać para wielkości po rozkładzie SVD, mianowicie [8][9]: SD_t oraz wartości szczególne σ_t . Pierwszy to uogólniony symptom uszkodzenia, który można nazwać nawet dyskryminantą i można ją otrzymać jako iloczyn prawostronny macierzy obserwacji i wektora \mathbf{v}_t [8][9]:

$$\mathbf{SD}_t = \mathbf{O}^{(pr)} \cdot \mathbf{v}_t = \sigma_t \cdot \mathbf{u}_t. \quad (3)$$

Teoretycznie dla danego czasu życia θ zaawansowanie uszkodzenia F_t może być odzwierciedlone przez wartość szczególną σ_t , natomiast chwilowa jego ewolucja przez dyskryminantę \mathbf{SD}_t [8][9].

Podobne rozumowanie można zastosować do ewolucji wielkości sumarycznych otrzymanych z SVD, a więc do sumy wszystkich dyskryminant \mathbf{SD}_t i sumy wszystkich wartości szczególnych σ_t , co może obrazować całościowe zaawansowanie zużycia w obiekcie, jak niżej:

$$\begin{aligned} SD(\theta) &= \sum_{i=1}^z |SD_i(\theta)| = \sum_{i=1}^z |\sigma_i(\theta) \cdot u_i(\theta)| \\ &\sim \sum_{i=1}^z |F_i(\theta)| = P(\theta) \\ DS(\theta) &= \sum_{i=1}^z |\sigma_i(\theta)| \sim \sum_{i=1}^z |F(\theta)_i| = F(\theta). \end{aligned} \quad (4)$$

Na podstawie (3) możemy zapisać, że pierwszy, najważniejszy uogólniony symptom uszkodzeń ma postać:

$$SD_{1j}(\theta) = \sum_i S_{ji}(\theta) v_{i1} \quad (5)$$

Zastosowanie skumulowanych symptomów zastępczych \mathbf{SD} , które stanowią liniową kombinację pierwotnych symptomów z odpowiednimi wagami wymaga niestety pewnych dodatkowych zabiegów. Aby móc wnioskować o stanie lub prognozować zmianę stanu wykorzystując tego typu symptomy konieczne jest wyznaczenie ich wartości granicznych. Ponieważ wartości takie nie istnieją, a warunkach przemysłowych nie można liczyć na przeprowadzenie diagnostycznego eksperymentu czynnego, pozostaje wykorzystać tutaj teorię niezawodności symptomowej [7].

3. WYKORZYSTANIE WARTOŚCI SZCZEGÓLNYCH DO DETEKCJI USZKODZEŃ

Wielokrotnie prezentowano już wyniki dotyczące wykorzystania symptomów uogólnionych \mathbf{SD} w diagnostyce wielosymptomowej [8][9]. Natomiast pozostaje pytanie czy istnieje możliwość wykorzystania informacji zawartej w samych wartościach szczególnych σ_t rozkładu SVD? Wartości szczególne zawierają w sobie informację o zmienności danych. Ponieważ z reguły w fazie przyspieszonego zużycia symptomy diagnostyczne gwałtownie zmieniają swój zasób informacji takie zmiany powinny być widoczne także w wartościach szczególnych. Należy zaznaczyć także, że wielu przypadkach mamy jednak do czynienia z multiplikatywnym wpływem parametrów roboczych na wartości obserwowanych symptomów [13]. W końcowej fazie eksploatacji przed awarią, przy dużych wartościach symptomów diagnostycznych, wpływ na nie parametrów roboczych będzie wyraźniejszy, a co za tym idzie, powinna zwiększyć się wariancja. Pierwsze próby wykorzystania wartości szczególnych wykonano w [10], gdzie okazało się, że są one jednak niewrażliwe na zmiany obciążenia.

Aby sprawdzić przydatność diagnostyczną wartości szczególnych dokonano szeregu symulacji. Przeprowadzone symulacje numeryczne w warunkach sterylnych, przy minimalizacji wpływu nieznanymi czynników (*które musiałby być uznane za losowe*), miały za zadanie wypracować sposób interpretacji informacji zawartej w wartościach szczególnych i skojarzyć ją ze zmianami wartości symptomów. W tym celu skupiono się na symptomach drganiowych i zrealizowano oprogramowanie pozwalające na generowanie sygnałów drganiowych charakterystycznych dla różnych zjawisk i uszkodzeń generowanych w maszynie wirnikowej z wałem ułożyskowanych w dwóch łożyskowych kulkowych. Dodatkowo do

procedur wprowadzono możliwość uwzględnienia szumu addytywnego, oraz zmian obciążenia. W ten sposób uzyskano możliwość symulacji rzeczywistych pomiarów, łącznie z wykorzystaniem symptomów definiowanych w określonych pasmach częstotliwości¹. Symulacja taka pozwalała na uaktywnienie w danym momencie określonego typu uszkodzenia, przy czym model rozwoju symptomu z nim związanego miał charakter wykładniczy z arbitralnie narzuconymi parametrami. Zaproponowana metoda symulacji dawała przede wszystkim możliwość łatwego definiowania symptomów wyselekcjonowanych częstotliwościowo jak i dawała pełną kontrolę czynników wpływających na model. Zakładano przy tym, że jeśli powstające uszkodzenie zmienia w jakiś sposób zachowanie symptomu w rzeczywistości i wpływa to na wartości szczególne to także podobne jakościowo zmiany powinny być widoczne w przeprowadzonych symulacjach.

Symulacji dokonywano uwzględniając uszkodzenia rozwijające się od pewnej określonej chwili czasowej. Symulowano przypadki rozwoju jednego uszkodzenia, dwóch niezależnych uszkodzeń oraz braku uszkodzeń (*symptomy przez cały okres analizy wykazywały w przybliżeniu stałe wartości*). Rozpatrywano zarówno symptomy, które są selektywnie czułe na określone uszkodzenia (*filtracja wąsko pasmowa*), symptomy o charakterze ogólnym, które mogą zawierać jednocześnie informację o wielu uszkodzeniach (*w szerokim paśmie częstotliwości*), jak i ich kombinacje. Założono, że pierwsze z uszkodzeń objawia się w paśmie częstotliwości obrotowej wirnika, natomiast drugie w paśmie wokół drugiej harmonicznej. Sama interpretacja fizyczna nie była uznana tutaj za najważniejszą, choć symptomy można skójarzyć z rosnącym niewyrównoważeniem i np. pękaniem wału. W przypadku symptomów uogólnionych przyjęto miary takie jak: wartość skuteczna, szczytowa, średnia, współczynniki szczytu, luzu i impulsowości. Natomiast w przypadku symptomów selektywnych rozpatrywano wartość skuteczną, szczytową i średnią w różnych pasmach tak, aby w każdej symulacji występowała ta sama liczba miar (*eliminacja ewentualnego wpływu liczby rozpatrywanych symptomów na wyniki symulacji*). Dodatkowo w części symulacji uwzględniano dwustanową zmianę obciążenia. Dokonywano także zmian w sposobie pojawiania się uszkodzeń. Rozpatrywano tutaj dwa zasadnicze przypadki. W pierwszym z nich uszkodzenie rozwijało się monotonicznie, w drugim, najpierw następował jego skokowy wzrost (*np. pęknięcie*) i następnie monotoniczny rozwój. Tabela 1 przedstawia ogólne zestawienie zrealizowanych symulacji.

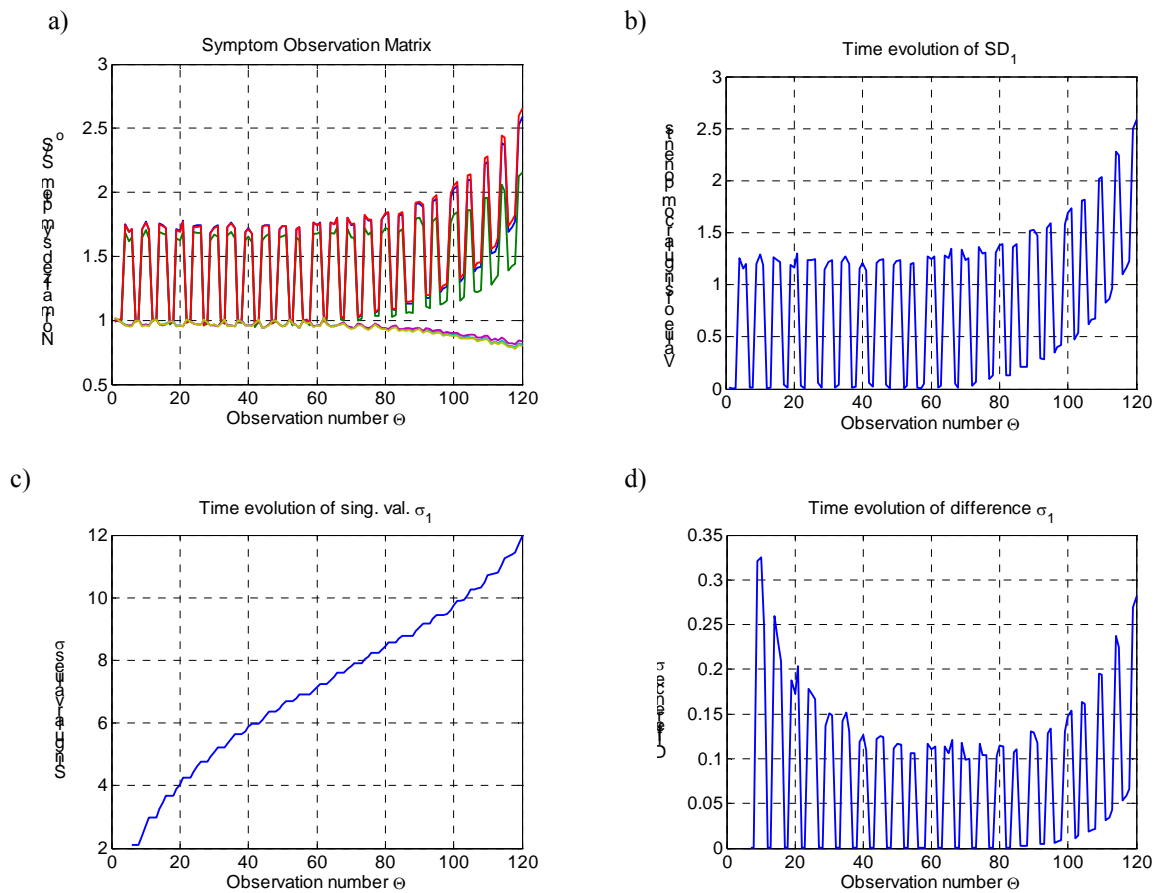
Tabela 1. Ogólny zakres zrealizowanych symulacji

Liczba niezależnych uszkodzeń	Symptomy	Zmiana obciążenia	Sposób symulacji uszkodzenia
Bez, 1 lub 2	Ogólne lub selektywne	Bez lub dwustanowa	Gwałtowne (skokowe) pojawienie się i monotoniczny wzrost lub tylko monotoniczny wzrost

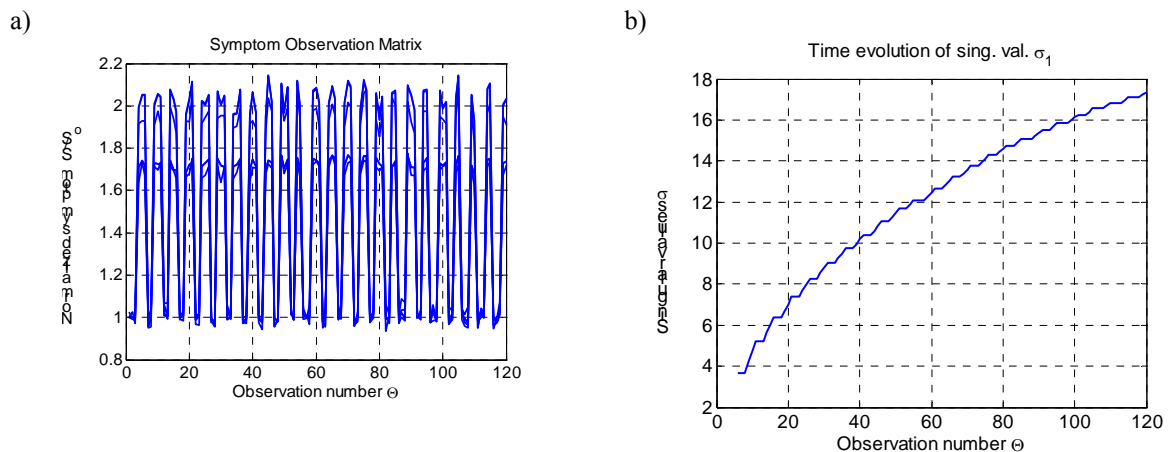
Przykładowe wyniki symulacji przedstawiono na rysunku 2. Na rysunku 2a widoczna jest ewolucja symulowanych wartości symptomu. Dodatkowo bardzo istotny jest tutaj wpływ zmian obciążenia. Choć wartości SD_1 mogą być dobrym symptomem uogólnionym to jak widać, są bardzo czułe także na zmiany obciążenia (rys. 2b). Tej cechy nie ma już ewolucja wartości szczególnej σ_1 , a przynajmniej wspomniany wpływ nie jest tak istotny, aby utrudniał modelowanie takiego przebiegu (rys. 2c). Co ciekawe po obliczeniu przyrostów kolejnych wartości σ_1 widoczny jest wyraźnie wpływ cyklicznych zmian obciążenia (rys. 2d). Można, więc powiedzieć, że przynajmniej σ_1 ma pewne właściwości kumulacyjne w stosunku wartości symptomu. Wynika stąd też, że sam przebieg wartości σ_1 umożliwia wygładzenie fluktuacji symptomu pozostawiając tylko ogólny trend, co mogłoby pozwolić na wykorzystanie σ jako nowego uogólnionego symptomu diagnostycznego.

Kolejne wyniki zarysowanej uprzednio symulacji zostały przedstawione na rysunkach 3a i 3b. Na rysunku 3 zaprezentowano dla porównania przypadek, w którym nie rozwija się żadne uszkodzenie a występują jedynie zmiany obciążenia. Porównując rysunki 3b i 2c można dojść do wniosku, że charakter zmiany są różne, jednak sama wartość σ_1 nie nadaje się bezpośrednio do oceny stanu technicznego. Jest to spowodowane faktem, że wzrost σ_1 wynika także z przyrostu liczby wierszy w macierzy **SOM** (*zwiększenie liczby obserwacji*) a nie tylko ze zmiany wartości symptomu. Jest to pewien ujemny aspekt symulacji, bowiem w normalnej diagnostyce eksploatacyjnej nie robimy pustych odczytów jeden po drugim, ale po określonym czasie $\Delta\theta$ co jest równoznaczne ze wzrostem zużycia eksploatacyjnego obiektu.

¹ W ten sposób wszystkie symptomy były liczone z symulowanego sygnału a nie symulowane niezależnie. Dodatkowo symulacja pozwoliła na uwzględnienie takich czynników jak charakterystyka filtra i brak doskonałej selekcji częstotliwościowej.



Rys. 2. Przykładowy wynik symulacji dla jednego rozwijającego się uszkodzenia i zmiennych parametrów obciążenia



Rys. 3. Przykładowy wynik symulacji dla przypadku braku rozwoju uszkodzenia

Można więc powiedzieć, że trend wartości szczególnej zawiera informację także o zaawansowaniu miary eksploatacji. Niemniej jednak dobrze że symulacja wykazała taką właściwość ewolucji wartości szczególnych σ_i . Na dodatek nie ma żadnego związku pomiędzy osiąganymi wartościami symptomów a wartościami szczególnymi. Stąd też ewentualne wykorzystanie wartości szczególnych jako źródła informacji musi

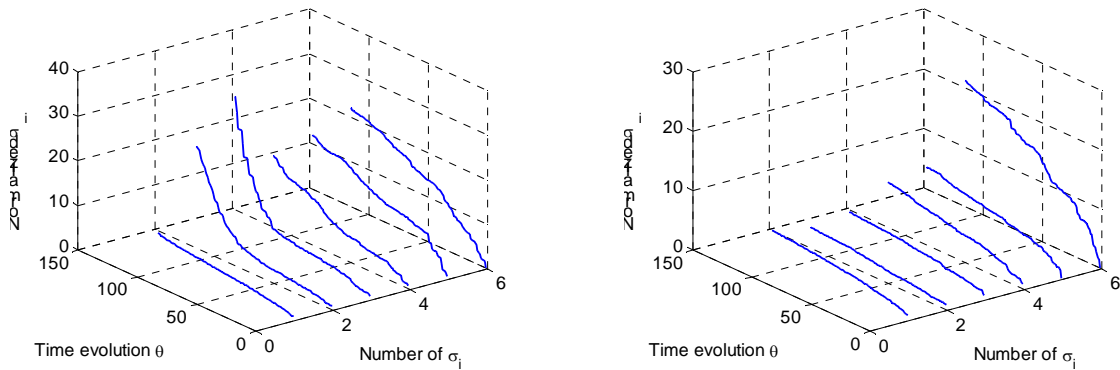
być oparte o inną ideę niż badanie relacji z wartościami granicznymi. Podobny wniosek możemy wyciągnąć z analizy, innych niż pierwsza, wartości szczególnych. Dodatkowo wrażliwość poszczególnych wartości szczególnych jest bardzo różna co ukazano na rysunku 4 obrazującym ich zmiany po normalizacji do wartości początkowej.

Innym ważnym spostrzeżeniem jest fakt, że na wartości osiągnięte przez σ silnie wpływa dobór

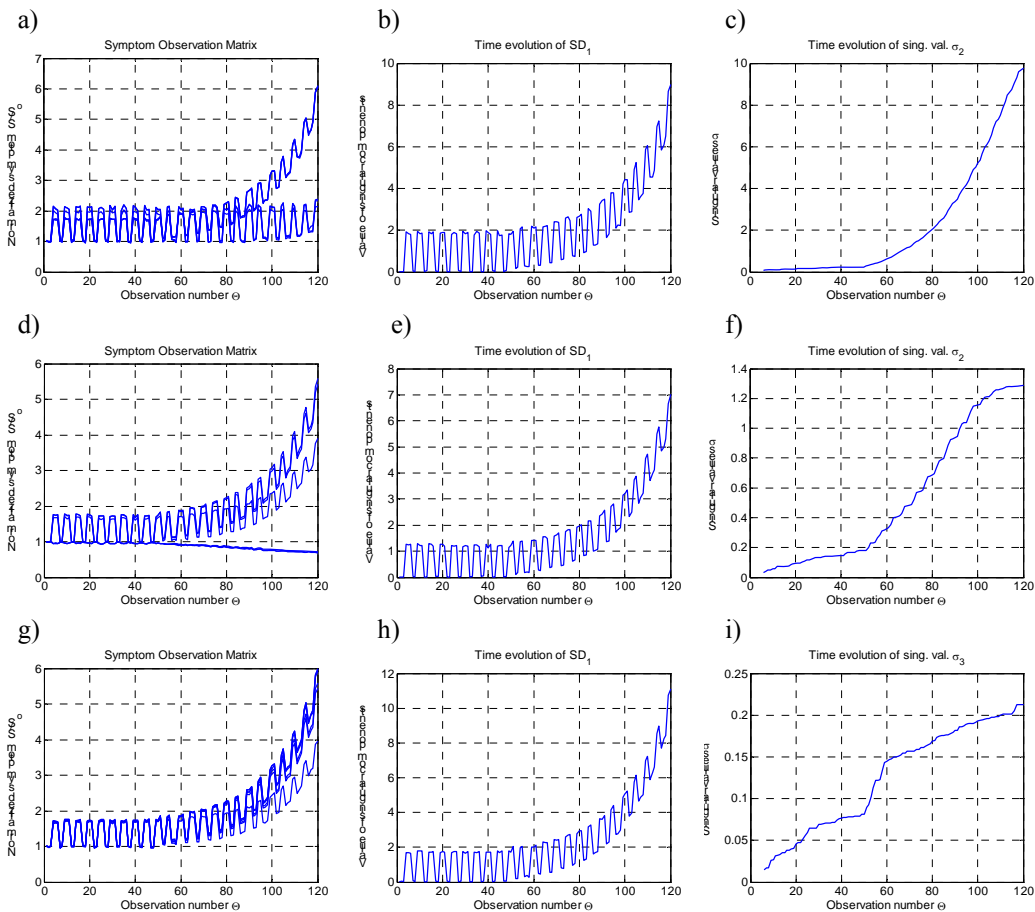
symptomów (liczba symptomów zawierających tą samą/podobną informację diagnostyczną). Wszystkie te czynniki powodują, że wykorzystanie ewolucji wartości szczególnych jako pewnego symptomu nie jest łatwe.

Sytuacja zmienia się, gdy rozpatrujemy przypadki, w których następuje skokowe zainicjowanie jakiegoś uszkodzenia a następnie jego monotoniczny rozwój. Przykład takiej symulacji przedstawiono na rysunku 5.

W przypadku obserwacji samych trendów pierwotnych symptomów, w przypadkach zmian obciążenia, taki gwałtowny wzrost może zostać niezauważony. W pierwszej kolumnie rysunku 5 przedstawiono symulowane symptomy diagnostyczne. W pierwszym wierszu mają one charakter wąskopasmowy, w drugim szerokopasmowy, w trzecim są kombinacją jednych



Rys. 4. Ewolucja kolejnych normalizowanych wartości szczególnych dla symptomów z rysunków 2a i 3a



Rys. 5. Porównanie możliwości wykrycia uszkodzenia pojawiającego się skokowo

i drugih. W każdym z wymienionych przypadków, w obecności zmian obciążenia fakt wystąpienia nagłego uszkodzenia (w symulacji taki skok wystąpił przy pomiarze nr 50) może zostać przeoczony. Natomiast może on być związany np. z nagłym pęknięciem, oderwaniem masy itp., które dalej będzie się rozwijać. Fakt ten może zostać także przeoczony w przypadku obserwacji wektorów \mathbf{SD} (kolumna 2 rysunku 5).

Skokowe zmiany widać natomiast w wartościach szczególnych objawiając się jako punkty zwrotne trendu (kolumna trzecia). Niestety pewną niedogodnością jest to, że zmiany są wyraźnie w różnych przebiegach wartości szczególnych: niekiedy w σ_2 , σ_4 a niekiedy w σ_3 lub innych. Ostatecznie zależy to od wykorzystanych symptomów. W przypadku przeprowadzonych symulacji zawsze występuje jednak jakaś wartość szczególna, w której omawiany skok symptomu jest znacznie łatwiej zidentyfikować niż w samym symptomie. Podobne informacje można odczytać w przypadku wystąpienia wielu uszkodzeń (rysunek 6). Jak wynika z rysunku 6 który dotyczy symulacji z dwoma niezależnie rozwijającymi się uszkodzeniami zainicjowanymi skokowo przy pomiarze nr 50 i nr 80, w σ_1 pojawiają się dwa punkty zwrotne. W σ_2 pojawiła się tylko informacja o drugim uszkodzeniu a w σ_5 przede wszystkim o pierwszym. I tak jak od tej pory są one zdecydowanie wyraźniej widoczne niż w pierwotnych symptomach.

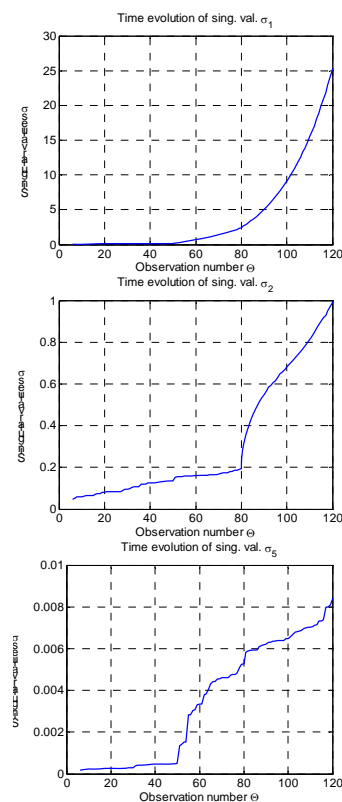
Z podsumowania wykrytych powyżej właściwości pojawia się możliwość diagnostycznego zastosowania ewolucji wartości szczególnych do detekcji gwałtownych zmian wartości symptomów, które na skutek zmian parametrów roboczych, mogą być mało widoczne bezpośrednio w obserwowanych miarach.

Takie gwałtowne skoki symptomu mogą wskazywać na nagłe pojawienie się określonych uszkodzeń. Należy zwrócić uwagę, że zakładamy, że po gwałtownej inicjalizacji uszkodzenia następuje w miarę monotoniczna zmiana symptomu (*nie licząc wpływu zmian obciążenia*). W przypadku dużych fluktuacji losowych obserwowanych symptomów taki sposób detekcji może być utrudniony i wywoływać fałszywe alarmy.

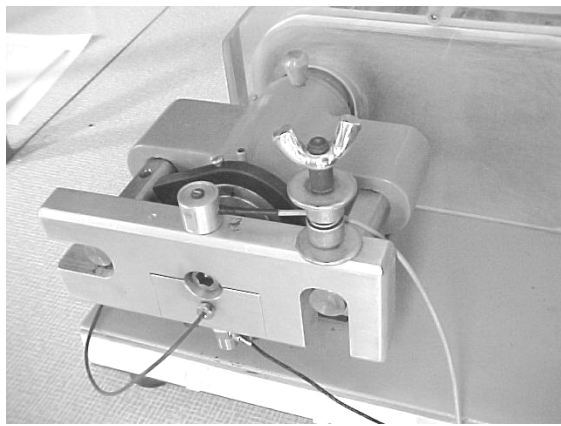
W celu wykorzystania proponowanej metody należy dokonać analizy zmian wszystkich wartości szczególnych, gdyż to, w której z nich pojawi się informacja diagnostyczna zależy od doboru symptomów. Wtedy pojawienie się punktów zwrotnych w krzywych ewolucji wartości szczególnych może być podpowiedzią o nagłym wystąpieniu uszkodzenia i skłaniać do zastosowania stosownych metod diagnozowania.

4. PRÓBA WYKORZYSTANIA WARTOŚCI SZCZEGÓLNYCH DO RZECZYWISTYCH DANYCH DIAGNOSTYCZNYCH

Aby zweryfikować możliwość zastosowania wartości szczególnych w zakresie przedstawionym wcześniej wykorzystano dane diagnostyczne pochodzące z eksperymentu przyspieszonego zużycia małowabarytowych łożysk tocznych. Podczas omawianego eksperymentu łożyska były nadmiernie obciążone oraz dodatkowo źle zmontowane (*ściśnięte nadmierne w obudowie w jednym kierunku*). Na rysunku 7 przedstawiono zdjęcie suportu stanowiska testowego, wraz z zamontowanym łożyskiem. Podczas eksperymentu w pewnej grupie badanych łożysk stosowano dodatkowo zmienne obciążenie w kierunku radialnym. Podczas eksperymentu dokonywano rejestracji sygnałów przyspieszeń drań, emisji akustycznej, temperatury łożyska oraz mocy pobieranej przez silnik. Z dostępnych sygnałów wyznaczono kilkanaście symptomów.



Rys. 6. Punkty zwrotne w ewolucji wartości szczególnych przy skokowej inicjalizacji symulowanych uszkodzeń

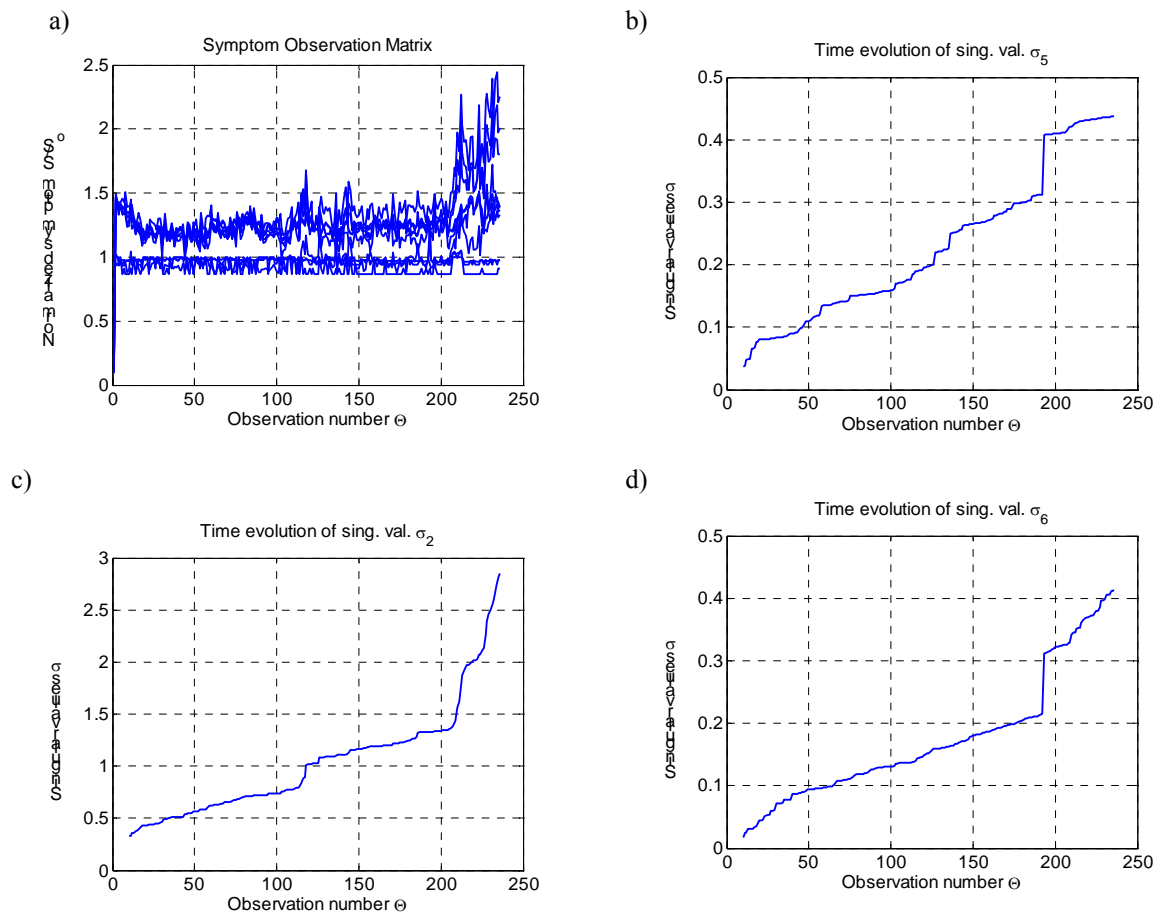


Rys. 7. Widok ogólny głowicy pomiarowej

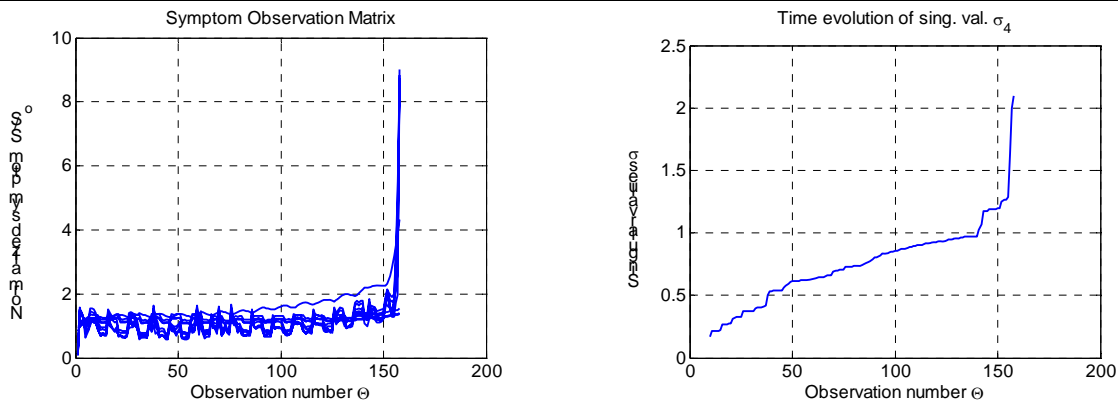
Na rysunku 8a przedstawiono przykładowe rejestracje dziesięciu symptomów dla przypadku braku zmian obciążenia łożyska. Z analizy symptomów wynika, że faza przyspieszonego

zużycia rozpoczęła się po ok. 200 pomiarze. Odpowiedni skok widać zresztą w przebiegu związanym z σ_2 (rys. 8c). Natomiast w przypadku σ_5 i σ_6 odpowiednie punkty zwrotne widoczne są przed tą chwilą (rys. 8b i 8d). Interesujące jest to, że bardzo niewielkim skokiem zareagował w tym czasie tylko jeden z symptomów, co można było przeoczyć analizując tylko symptomy.

Kolejny przykład na rysunku 9 ukazuje przykładowy wynik eksperymentu dla przypadku zmiennego obciążenia. W ewolucji σ_4 po 140 pomiarze widać wyraźny skok. Mógłby on zostać przeoczony, gdyby analiza opierała się tylko na obserwacji wartości symptomu (*ich reakcja była nieznaczna*). W tym momencie odnotowano także krótki dźwięk wskazujący na pęknięcie pierścienia zewnętrznego łożyska. Wyraźnie widać to tylko we wspomnianej wartości szczególnej.



Rys. 8. Przykładowe analizy dotyczące eksperymentu przyspieszonego zużycia łożysk tocznych



Rys. 9. Przykładowe analizy dotyczące eksperymentu przyspieszonego zużycia łożysk tocznych dla przypadku zmiennego obciążenia z pęknięciem pierścienia dla $N=140$

5. PODSUMOWANIE

Podsumowując można stwierdzić, że obserwacja wartości szczególnych może być podpowiedzią o skokowym wystąpieniu uszkodzenia. Potwierdzają to symulacje jak i przeprowadzone eksperymenty. Warto dokonywać obserwacji wartości szczególnych w poszukiwaniu punktów zwrotnych, które mogą informować o tego rodzaju gwałtownych zmianach, które z kolei mogą zostać niezauważone w obserwacjach samych symptomów czy **SD**. Ma to szczególne znaczenie w przypadkach zmian obciążenia, które mogą zamaskować takie zjawiska. Niestety wnioskowanie w oparciu o wartości szczególne nie jest łatwe. Po pierwsze nie ma reguły, w której z nich pojawi się przydatna informacja. Przeważnie najbardziej czytelne są zmiany w różnych od pierwszej wartości szczególnej. Z drugiej strony czasami wspomniane skoki (*choć niewielkie*) pojawiają się przypadkowo lub przynajmniej w wynikach przeprowadzonego eksperymentu nie ma dowodów na skojarzenie ich z jakimiś uszkodzeniami. Wydaje się jednak, że informacja zawarta w wartościach szczególnych może być praktycznie wykorzystana do zwrócenia uwagi eksperta diagnostyki i do uruchomienia innych procedur diagnostycznych.

Praca naukowa została sfinansowana częściowo ze środków na naukę w latach 2009 – 2012 jako projekt badawczy 1751/B/T02/2009/37.

LITERATURA

- Korbicz J., Kościelny J. M., Kowalczyk Z., Cholewa W. (red.), *Diagnostyka procesów. Modele. Metody sztucznej inteligencji. Zastosowania*, Warszawa, WNT 2002.
- Tabaszewski M., *Prognozowanie w wielosymptomowej diagnostyce maszyn*, Rozprawy nr 446, Wydawnictwo Politechniki Poznańskiej, Poznań 2010, s. 153
- Kornacki J., Ćwik J., *Statystyczne systemy uczące się*, Warszawa, WNT 2005.
- Tabaszewski M.; *Wielosymptomowa, prognoza stanu i czasu do awarii z wykorzystaniem sieci neuronowych*, Diagnostyka 2 (42)/2007, s. 43-48.
- Tumer I. Y., Huff E. M., *Principal component analysis of tri-axial vibration data from helicopter transmission*, 56th Meeting of the Society of Machine Failure Prevention Technology, 2002.
- Cempel C., *Innovative developments in systems condition monitoring*, Keynote Lecture, Proceedings of DAMAS'99, Dublin 1999.
- Natke H. G., Cempel C., *Model Aided Diagnosis of Mechanical Systems*, Springer Verlag, Berlin, 1997, p248.
- Cempel C., *Multidimensional Condition Monitoring of Mechanical Systems in Operation*, Mechanical Systems and Signal Processing, 2003, 17(6), 1291 – 1303.
- Cempel C., Tabaszewski M., *Multidimensional condition monitoring of the machines in non-stationary operation*, Mechanical Systems and Signal Processing, Vol. 21, 2007, pp 1233-1247.
- Cempel C., *The evolution of generalized fault symptoms and fault intensities as indicators of observation redundancy and coming system breakdown*, Mechanical Systems and Signal Processing, 25 (2011), p3116-3124.
- Kielbasinski A., Schwetlik H., *Numeric Linear Algebra*, WNT Press Warsaw, 1992, p502.
- Golub G. H., VanLoan Ch. F., *Matrix Computation*, III-rd edit, J Hopkins Univ. Press, Baltimore, 1996, p694.
- Gałka T., Tabaszewski M.; *An application of statistical symptoms in machine condition diagnostics*; Mechanical Systems and Signal Processing, vol 25, No. 1, (2011), str. 253-265



Dorota KOZANECKA

**Diagnostyka
mechatronicznego
układu wirującego
maszyny**

ITE, Radom, 2010

System aktywnych, sterowanych cyfrowo łożysk magnetycznych stanowi interesującą alternatywę w konstrukcjach nowoczesnych maszyn przepływowych, których zadaniem jest realizacja procesów technologicznych związanych ze spełnieniem szczególnych wymagań eksploatacyjnych.

Pewność ruchu, bezpieczeństwo i niezawodność maszyny jest krytycznym warunkiem zastosowania niekonwencjonalnego, magnetycznego systemu łożyskowego w praktyce przemysłowej i dlatego efektywna diagnostyka tego systemu jest zagadnieniem kluczowym tej technologii.

W monografii przedstawiono podstawy teoretyczne, koncepcję i procedury specjalistycznego oprogramowania przy wykorzystaniu zaawansowanych technologii informatycznych, dla unikatowego systemu diagnostycznego układu wirującego z aktywnym łożyskiem magnetycznym.

Architektura systemu (rozdział 3) została opracowana według, prezentowanej w literaturze, filozofii „mechatronicznej, inteligentnej maszyny”, zgodnie z którą zbudowano wielopoziomą platformę diagnostyczną dla obiektów, jakimi są układy wirujące maszyn z aktywnym łożyskiem magnetycznym. Tego typu obiekty mechatroniczne realizować mogą koncepcję sterowania drganiami wirującego wału po-przez zastosowanie technologii aktywnego zarządzania maszyną, którego celem jest zwiększenie niezawodności i optymalizacja warunków ich eksploatacji.

Specyfika wybranego obiektu mechatronicznego stawia specjalne wymagania związane z budową systemu diagnostycznego, który nadzoruje jednocześnie funkcjonowanie aktywnego łożyska magnetycznego. Wiąże z to faktem, że źródłem mierzonych sygnałów dla systemu diagnostycznego są czujniki pomiarowe zainstalowane w łożysku, co stanowi integralną część systemu aktywnej kontroli drgań wału.

Zaprezentowana w monografii koncepcja wielopoziomowej platformy diagnostycznej umożliwi precyzyjną diagnostykę mechatronicznego obiektu na trzech poziomach zarządzania:

- Poziom „0” - badań modelowych (rozdział 4);
- Poziom „I” - uruchamiania i próbnych rozruchów (rozdział 5);
- Poziom „II” - w czasie normalnej eksploatacji (rozdział 6).

Unikatowy system diagnostyczny dynamiki linii wału maszyny podpartej w aktywnych łożyskach magnetycznych bazuje na uzyskiwanych *on-line* informacjach zawartych w sygnałach pomiarowych w różnych fazach pracy systemu łożyskowego (zawieszenie wirnika, rozruch, nominalne warunki pracy, wybieg), w obecności różnych zakłóceń z możliwością jego aplikacji dla różnej konfiguracji stanowisk badawczych. Zastosowane metody analizy i formy prezentacji uzyskiwanych wyników pozwalają na ich odniesienie do parametrów charakterystyk dynamicznych dla maszyn klasycznie ułożyskowanych (np. położenie równowagi statycznej, trajektoria czopa, portret fazowy, charakterystyki Bodego, *FFT*).

Oprogramowanie systemu diagnostycznego jest złożone z warstw programowych, dla których podstawowym założeniem jest komunikacja i wymiana danych między komputerem nadrzędnym i układem pomiarowo – sterującym łożyska.

Finalnym efektem działania systemu jest diagnostyka mechatronicznego układu wirującego z pomocniczym, aktywnym łożyskiem magnetycznym, realizowana na poszczególnych poziomach zarządzania, zarówno na etapie projektowania, uruchamiania, jak również w czasie eksploatacji maszyny.

Obszar zainteresowania czasopisma to:

- ogólna teoria diagnostyki technicznej
- eksperymentalne badania diagnostyczne procesów i obiektów technicznych;
- modele analityczne, symptomowe, symulacyjne obiektów technicznych;
- algorytmy, metody i urządzenia diagnozowania, prognozowania i genezowania stanów obiektów technicznych;
- metody detekcji, lokalizacji i identyfikacji uszkodzeń obiektów technicznych;
- sztuczna inteligencja w diagnostyce: sieci neuronowe, systemy rozmyte, algorytmy genetyczne, systemy ekspertowe;
- diagnostyka energetyczna systemów technicznych;
- diagnostyka systemów mechatronicznych i antropotechnicznych;
- diagnostyka procesów przemysłowych;
- diagnostyczne systemy utrzymania ruchu maszyn;
- ekonomiczne aspekty zastosowania diagnostyki technicznej;
- analiza i przetwarzanie sygnałów.

Wszystkie opublikowane artykuły uzyskały pozytywne recenzje wykonane przez niezależnych recenzentów.

Topics discussed in the journal:

- General theory of the technical diagnostics,
- Experimental diagnostic research of processes, objects and systems,
- Analytical, symptom and simulation models of technical objects,
- Algorithms, methods and devices for diagnosing, prognosis and genesis of condition of technical objects,
- Methods for detection, localization and identification of damages of technical objects,
- Artificial intelligence in diagnostics, neural nets, fuzzy systems, genetic algorithms, expert systems,
- Power energy diagnostics of technical systems,
- Diagnostics of mechatronic and antropotechnic systems,
- Diagnostics of industrial processes,
- Diagnostic systems of machine maintenance,
- Economic aspects of technical diagnostics,
- Analysis and signal processing.

All the published papers were reviewed positively by the independent reviewers.

Redaktorzy działowi:

dr hab. inż. Tomasz BARSZCZ
prof. dr hab. inż. Wojciech CHOLEWA
prof. dr hab. Wojciech MOCZULSKI
prof. dr hab. inż. Stanisław RADKOWSKI
prof. dr hab. inż. Wiesław TRĄMPCZYŃSKI
prof. dr hab. inż. Tadeusz UHL

Kopia wszystkich artykułów opublikowanych w tym numerze dostępna jest na stronie www.diagnostyka.net.pl

Druk:

Centrum Graficzne „GRYF”, ul. Pieniężnego 13/2, 10-003 Olsztyn, tel. / fax: 89-527-24-30

Oprawa:

Zakład Poligraficzny, UWM Olsztyn, ul. Heweliusza 3, 10-724 Olsztyn
tel. 89-523-45-06, fax: 89-523-47-37

Cena 25 zł (w tym 5% VAT)

A Symposium on

**VIBRATION AND STRUCTURAL ACOUSTICS
MEASUREMENT AND ANALYSIS**

Promoted by

César M. A. Vasques
INEGI-Instituto de Engenharia Mecânica e Gestão Industrial, Universidade do Porto
Campus da FEUP, Dr. Roberto Frias 400, 4200465 Porto, Portugal
Tel: +351-22 957 87 10
E-mail: cmav@fe.up.pt

In Conjunction with

**15TH INTERNATIONAL CONFERENCE ON
EXPERIMENTAL MECHANICS (ICEM15)**
Faculty of Engineering, University of Porto
PORTO, PORTUGAL
July 22-27, 2012
(<http://paginas.fe.up.pt/clmieem15>)

Wszystkie opublikowane w czasopiśmie artykuły uzyskały pozytywne recenzje, wykonane przez niezależnych recenzentów.

Redakcja zastrzega sobie prawo korekty nadesłanych artykułów.

Kolejność umieszczenia prac w czasopiśmie zależy od terminu ich nadesłania i otrzymania ostatecznej, pozytywnej recenzji.

Wytyczne do publikowania w DIAGNOSTYCE można znaleźć na stronie internetowej:

<http://www.diagnostyka.net.pl>

Redakcja informuje, że istnieje możliwość zamieszczania w DIAGNOSTYCE ogłoszeń i reklam.

Jednocześnie prosimy czytelników o nadsyłanie uwag i propozycji dotyczących formy i treści naszego czasopisma.

Zachęcamy również wszystkich do czynnego udziału w jego kształtowaniu poprzez nadsyłanie własnych opracowań związanych z problematyką diagnostyki technicznej. Zwracamy się z prośbą o nadsyłanie informacji o wydanych własnych pracach nt. diagnostyki technicznej oraz innych pracach wartych przeczytania, dostępnych zarówno w kraju jak i zagranicą.